Organisation for Economic Co-operation and Development

ENV/CBC/MONO(2022)27

Unclassified

English - Or. English

1 September 2022

ENVIRONMENT DIRECTORATE
CHEMICALS AND BIOTECHNOLOGY COMMITTEE

Case Study on the use of Integrated Approaches for Testing and Assessment for developmental neurotoxicity hazard characterisation of acetamiprid

Series on Testing and Assessment
No. 365

JT03501674

OECD Environment, Health and Safety Publications

SERIES ON TESTING AND ASSESSMENT

NO. 365

Case Study on the use of Integrated Approaches for Testing and Assessment for developmental neurotoxicity hazard characterisation of acetamiprid

IOMC

INTER-ORGANIZATION PROGRAMME FOR THE SOUND MANAGEMENT OF CHEMICALS

A cooperative agreement among FAO, ILO, UNDP, UNEP, UNIDO, UNITAR, WHO, World Bank and OECD

Environment Directorate

ORGANISATION FOR ECONOMIC COOPERATION AND DEVELOPMENT

Paris 2022

About the OECD

The Organisation for Economic Co-operation and Development (OECD) is an intergovernmental organisation in which representatives of 38 industrialised countries in North and South America, Europe and the Asia and Pacific region, as well as the European Commission, meet to co-ordinate and harmonise policies, discuss issues of mutual concern, and work together to respond to international problems. Most of the OECD's work is carried out by more than 200 specialised committees and working groups composed of member country delegates. Observers from several countries with special status at the OECD, and from interested international organisations, attend many of the OECD's workshops and other meetings. Committees and working groups are served by the OECD Secretariat, located in Paris, France, which is organised into directorates and divisions.

The Environment, Health and Safety Division publishes free-of-charge documents in twelve different series: **Testing and Assessment**; **Good Laboratory Practice and Compliance Monitoring**; **Pesticides**; **Biocides**; **Risk Management**; **Harmonisation of Regulatory Oversight in Biotechnology**; **Safety of Novel Foods and Feeds; Chemical Accidents; Pollutant Release and Transfer Registers; Emission Scenario Documents; Safety of Manufactured Nanomaterials;** and **Adverse Outcome Pathways.** More information about the Environment, Health and Safety Programme and EHS publications is available on the OECD's World Wide Web site (www.oecd.org/chemicalsafety/).

This publication was developed in the IOMC context. The contents do not necessarily reflect the views or stated policies of individual IOMC Participating Organizations.

The Inter-Organisation Programme for the Sound Management of Chemicals (IOMC) was established in 1995 following recommendations made by the 1992 UN Conference on Environment and Development to strengthen co-operation and increase international co-ordination in the field of chemical safety. The Participating Organisations are FAO, ILO, UNDP, UNEP, UNIDO, UNITAR, WHO, World Bank and OECD. The purpose of the IOMC is to promote co-ordination of the policies and activities pursued by the Participating Organisations, jointly or separately, to achieve the sound management of chemicals in relation to human health and the environment.

This publication is available electronically, at no charge.

- **Also published in the Series on Testing and Assessment: link**

For this and many other Environment, Health and Safety publications, consult the OECD's World Wide Web site (www.oecd.org/chemicalsafety/)

or contact:

OECD Environment Directorate,
Environment, Health and Safety Division
2 rue André-Pascal
75775 Paris Cedex 16
France

E-mail: ehscont@oecd.org

Foreword

OECD member countries have been making efforts to expand the use of alternative methods in assessing chemicals. The OECD has been developing guidance documents and tools for the use of alternative methods such as (Q)SAR, chemical categories and Adverse Outcome Pathways (AOPs) as a part of Integrated Approaches for Testing and Assessment (IATA). There is a need for the investigation of the practical applicability of these methods/tools for different aspects of regulatory decision-making, and to build upon case studies and assessment experience across jurisdictions.

The objective of the IATA Case Studies Project is to increase experience with the use of IATA by developing case studies, which constitute examples of predictions that are fit for regulatory use. The aim is to create common understanding of using novel methodologies and the generation of considerations/guidance stemming from these case studies.

This case study was developed by EU ToxRisk for illustrating practical use of IATA and submitted to the 2021 review cycle of the IATA Case Studies Project.

The case study was reviewed by the project team, and endorsed at the 6th meeting of the Working Party on Hazard Assessment in June 2022.

The case study is illustrative examples, and their publication as OECD monographs does not translate into direct acceptance of the methodologies for regulatory purposes across OECD countries. In addition, the cases study should not be interpreted as official regulatory decisions made by the authoring member countries.

This document is published under the responsibility of the Chemicals and Biotechnology Committee of the OECD.

Acknowledgements

The authors of this Case Study were

Ylva Johansson[1)]*, Jonathan Blum[2)]*, Rebecca von Hellfeld[3,9)], Thomas Braunbeck[3)], María Hinojosa[1)], Melinda Zana[4)], Andras Dinnyes[4)], Dominik Loser[2)8)], Marcel Leist[2)], Karin Grillberger[5)], Gerhard Ecker[5)], Barbara M.A. van Vugt-Lussenburg[6)], Bart van der Burg[6)], Iain Gardner[7)], Anna Forsby[1)]¤, Susanne Hougaard Bennekou[10)]¤.

*Contributed equally

¤Corresponding authors

Affiliation at time of contribution:

1) Department of Biochemistry and Biophysics, Stockholm University, Stokholm Sweden

2) In Vitro Toxicology and Biomedicine, Department Inaugurated by the Doerenkamp-Zbinden Foundation, University of Konstanz, Universitaetsstr. 10, 78457, Konstanz, Germany

3) University of Heidelberg, Centre of Organismal Studies, Im Neuenheimer Feld 504, 69120 Heidelberg, Germany

4) BioTalentum Ltd., H-2100 Gödöllő, Hungary

5) Department of Pharmaceutical Sciences, University of Vienna, Vienna, Austria

6) BioDetection Systems bv Science Park 406, 1098XH Amsterdam, The Netherlands

7) CERTARA UK Limited, Simcyp Division, Level 2-Acero, 1 Concourse Way, Sheffield, S1 2BJ, UK

8) NMI Natural and Medical Sciences Institute at the University of Tübingen, 72770, Reutlingen, Germany

9) University of Aberdeen, School of Biological Sciences, 23 St Machar Drive, Old Aberdeen, AB24 3UU

10) Technical University of Denmark, Kongens Lyngby, Denmark

Table of contents

Foreword 6

Acknowledgements 7

List of abbreviations 11

Executive Summary 12

1 Introduction 13
- 1.1 Background 13
- 1.2 Problem Formulation 13
- 1.3 Purpose 14
- 1.4 Chemical 14
- 1.5 Endpoint 15
- 1.6 Exposure Information 15

2 Hypothesis for performing the IATA 16
- 2.1 Rationale for the IATA and method 16

3 Data gathering and application of the IATA 17

4 Review of existing data from systematic review 19
- 4.1 *In vitro* data 19
- 4.2 *In vivo* data – mammalian 21
- 4.3 *In vivo* data – Zebrafish embryo 23

5 Absorption, distribution, metabolism and excretion 25

6 MoA; nicotinic acetylcholine receptors (nAChR) 26
- 6.2 Altered nAChR expression 28
- 6.3 Signaling effects of prenatal exposure with nicotine 29
- 6.4 Behavior/mental effects after prenatal nicotine exposure 29

7 Putative AOP 30

8 Data generation 31
- 8.1 Test systems 31
- 8.2 Methods to study KEs 37

9 Results (link to publications/BioStudies files) 45
9.1 MIE. Binding to nAChR (docking experiments) 45
9.2 KE1. Activation nAChR 46
9.4 KE3. Altered cellular phenotype 48
9.5 KE4. Altered neurodevelopment (neuronal differentiation, migration, axogenesis, synaptogenesis and brain area organization) 48
9.6 CALUX reporter gene assay results 57
9.7 PBTK models outputs 57
10 Uncertainty analysis 63
11 Integrated Conclusion 66
12 Data Matrix 68
13 References 71
ANNEX I : ZFE method 78
ANNEX II: PBPK report 83
ANNEX III: Existing evidence for IATA on developmental neurotoxicity on Acetamiprid and Imidacloprid 84

FIGURES

Figure 1. The chemical structure of acetamiprid 14
Figure 2. PRISMA chart on the systematic review flow for acetamiprid. 17
Figure 3. Pentameric structure of nAChR. 26
Figure 4. Schematic representation of how neurotransmitter signals control neuronal cell development during specified critical periods. 27
Figure 5. Temporal and regional expression of nicotinic AChR subunit mRNA in developing human and rat brain. 28
Figure 6. A putative adverse outcome pathway describing nAChR binding leads to impaired cognitive function and psychiatric diseases. 30
Figure 7. RNA-seq of cholinergic markers in A) LUHMES cells B) SH-SY5Y cells during differentiation. 33
Figure 8. Common neuronal nAChR subunits are expressed in D42 TDN samples. 34
Figure 9. The zebrafish embryo assays conducted between 0 and 120 hpf. 35
Figure 10. Definition of LOECs for different assays within the CALUX panel. 37
Figure 11. Concentration-dependent effect of nicotine on the [Ca^{2+}]i of LUHMES neurons. 38
Figure 12. Exposure scheme for acute (72 hours) toxicity treatment of TD42 differentiated neurons and astrocytes. 39
Figure 13. The UKN4 neurite outgrowth assay using LUHMES cells. 40
Figure 14. The UKN2 migration assay using neural crest cells 41
Figure 15. Differentiation scheme of the UKN1 test method from hiPSCs into rosette like structures. 42
Figure 16. Binding of nicotine and acetamiprid to nAChR. 46
Figure 17. Acetamiprid activates α7 nAChR in LUHMES and SH-SY5Y cells. 47
Figure 18. Desensitization of nAChRs in LUHMES and SH-SY5Y. 48
Figure 19. Acetamiprid does not affect cell viability after 24 hours of exposure SH-SY5Y cells. 49
Figure 20. Viability of 72 hours nicotine, acetamiprid, treatment in a concentration of 100 to 0.01 µM had no impact on TD42 neuron viability. 49
Figure 21. UKN battery results including endpoint specific and viability measurements. 50
Figure 22. Viability, NEP differentiation and rosette formation in acetamiprid treated hiPSCs. 51

Figure 23. The effects of nicotine on the early behavior of zebrafish embryos during the light/dark cycles of the coiling assay. 53
Figure 24. The effects of acetamiprid on the early behavior of zebrafish embryos during the light/dark cycles of the coiling assay. 54
Figure 25. The effects of nicotine on the later behavior of zebrafish embryos during the light/dark cycles of the basal swimming assay. 55
Figure 26. The effects of acetamiprid on the later behavior of zebrafish (Danio rerio) embryos during the light/dark cycles of the basal swimming assay. 56
Figure 27. Simulated (green line) concentrations of acetamiprid in plasma following an oral dose of 1 mg/kg to male rats. 58
Figure 28. Sensitivity analysis showing the effect of changing clearance on plasma concentrations of Acetamiprid following an oral dose of 1 mg/kg to male rats. 58
Figure 29. Simulated mean plasma concentration of acetamiprid (green) and the desmethylmetabolite (orange) in humans after an oral dose of 5 μg acetamiprid. 59
Figure 30. Simulated cumulative urinary excretion of 59
Figure 31. Simulated mean cumulative urinary excretion of the desmethyl metabolite in humans after an oral dose of 5 μg acetamiprid. 60
Figure 32. Simulated mean plasma concentrations of 61
Figure 33. Simulated plasma (green) and brain (black) concentrations of acetamiprid in rats after multiple oral doses of (A) 1 mg/kg/day and (B) 50 mg/kg/day. 62
Figure 34. Simulated (A) plasma and (B) brain concentrations in human subjects after multiple oral doses of 0.114 mg/kg/day for 10 days. 62

TABLES

Table 1. Criteria for bias scoring 1-4 in Table 2. 19
Table 2. Summary of publications performed *in vitro* identified and reviewed after application of search string. 20
Table 3. Summary of publications performed *in vivo* identified and reviewed after application of search string. 21
Table 4. Summary of publications performed *in vivo* in zebra fish embryos identified and reviewed after application of search string. 23
Table 5. Overview of test methods. 31
Table 6. Input parameters for the PBK model for Acetamiprid (rat and human). 43
Table 7. Input parameters for the PBK model for N-desmethyl metabolite (human only). 43
Table 8. Effect concentrations (EC) of 10 and 50% for nicotine or acetamiprid exposed zebrafish embryos as 96 and 120 hpf. 51
Table 9. All observed endpoints in the FET test, induced by nicotine (N) and acetamiprid (A). 51
Table 10. Uncertainty analysis of the IATA report highlighting the quality of evidence available and generated. 63
Table 11. Summary of data gap filling for Acetamiprid 68
Table 12 (ZFEX1). Parameter-settings in the EthioVision(R)TX software for video recordings, as well as camera settings. 79
Table 13 (ZFEX2). p-values of the coiling assay Kruskal-Wallis and Dunns post hoc test. 81
Table 14 (ZFEX3). p-values of the basal swimming assay Kruskal-Wallis and Dunns post hoc test (n=2). 82
Table 15. Criteria for selecting studies for the sub-questions on the relationship between acetamiprid and imidacloprid and DNT in human studies 84
Table 16. Criteria for selecting studies for the sub-questions on the relationship between acetamiprid and imidacloprid and DNT in *in vivo* studies 84
Table 17. Criteria for selecting studies for the sub-questions on the relationship between acetamiprid and imidacloprid and DNT in *in vitro* studies 85
Table 18. Criteria for selecting studies for the sub-questions on the relationship between acetamiprid and imidacloprid and DNT related to report characteristics and relevant to human, *in vivo* and *in vitro* studies 85

List of abbreviations

AChBP	Acetylcholine binding protein
ADHD	Attention deficit hyperactivity disorder
AO	Adverse outcome
AOP	Adverse outcome pathway
BDNF	Brain derived neurotrophic factor
BIOT	BioTalentum Ltd
DEG	Differentially expressed gene
DNT	Developmental neurotoxicity
EC	Effect concentration
FET	Fish embryo acute toxicity
hiPSC	human induced pluripotent stem cell
hpf	hours post fertilization
IVB	*In vitro* battery
KE	Key event
LOEC	Lowest effect concentration
LOQ	Limit of quantitation
LUHMES	Lund human mesencephalic
MIE	Molecular initiating event
nAChR	Nicotinic acetylcholine receptor
NAM	New approach method
NCCs	Neural crest cells
NEP	Neuroepithelial precursor
NOAEL	No-observed-adverse-effect-level
OECD	Organization for Economic Co-operation and Development
PBTK	Physiologically based toxicokinetic
PRISMA:	Preferred Reporting Items for Systematic Reviews and Meta-Analyses
PND	Postnatal day
SciRAP	Science in Risk Assessment and Policy
VOCC	Voltage-operated-calcium-channels

Executive Summary

The EFSA Scientific Opinion on the developmental neurotoxicity potential of acetamiprid and imidacloprid (2013) concluded that there were uncertainties that prevented a firm conclusion regarding motor activity and learning and memory, whereas decreased auditory startle response was found at 10 and 45 mg/kg/day in an OECD TG426 regulatory study on acetamiprid. The mechanistic data by Kimura-Kuroda (2012) did provide some mechanistic understanding but the study had limitations. Deriving from the uncertainties elaborated in this opinion, the hypothesis for this IATA is that mechanistic understanding of the toxicodynamic properties of acetamiprid contextualized with internal exposure considerations from realistic human exposures can inform the hazard characterization regarding potential DNT effect.

In this case study, further evidence has been collected, appraised, and assessed. The additional *in vivo* DNT data in mice indicated that acetamiprid might affect neurogenesis (Kagawa *et al.* 2018; Nakayama 2018) and reduced anxiety-related behavior in males. However, the available *in viv*o data does not corroborate each other, and no consistent effects have been established. *In vitro* data available shows that acetamiprid exposure induces Ca^{2+} influx via the nAChRs as well as attenuated voltage-operated-calcium-channels (VOCC) function. In addition, several *in vitro* studies have investigated morphological and transcriptional changes due to acetamiprid exposure, but no uniform effects have been observed.

Thus, further *in vitro* and *in silico* data has been generated, characterizing the effects of the compound in a battery of DNT *in vitro* test anchored to a postulated AOP as well as additional screening for nuclear receptor activation. In addition, the *in vitro* toxicodynamic data has been contextualized with internal exposure predictions by PBTK modelling. Although, the MIE and early KEs of the proposed AOP have in this report been firmly established, significant uncertainties remain both related to an adverse outcome and key events adjacent to the adverse outcome.

1 Introduction

1.1 Background

The human brain develops through a series of developmental stages that must occur in a particular sequence and at the right time. The outcome on the human brain is critically dependent upon the physiology of these processes, each of which might be vulnerable to adverse effects from exposures to environmental chemicals or drugs.

Study guideline for rodent developmental neurotoxicity (DNT) has been available for a considerable time (US Environmental Protection Agency (OPPTS 870.630), The Organization for Economic Co-operation and Development (OECD, 20071; OECD, 20182; USEPA, 19983) including guidance for interpreting DNT data (North American Free Trade Agreement (NAFTA) Technical Working Group on Pesticides (TWG), 20174). However, DNT testing is not carried out routinely under any chemical's regulation. DNT testing is only triggered when neurotoxic or endocrine effects is observed in adult rodents. These triggers may not be sufficient (Bal-Price et al., 20185) as some neurodevelopmental processes are not present in the adult brain (Fritsche et al., 20176). Performance of the DNT *in vivo* guideline studies involves the use of large numbers of animals and is therefore cost- and time-intensive (Crofton et al., 20127), they are difficult to interpret, together with the considerable uncertainties related to *in vivo* DNT model (Paparella et al., 20208). Altogether, this has fostered efforts to develop *in vitro* methods that combined in an DNT *in vitro* battery (IVB) reflects the main processes behind the development of the nervous system that can lead to adverse effects (Bal-Price et al., 20185; Masjosthusmann et al.,20209). To support regulatory use of an IVB, the OECD has taken up the activity of developing a guidance for interpretation of data generated from an IVB in the context of an IATA.

1.2 Problem Formulation

This case study aims to develop an IATA that could support hazard identification/characterization based on a problem formulation originating from the EFSA Scientific Opinion on developmental neurotoxicity potential of two neonicotinoid pesticides one being acetamiprid (EFSA, 2013[10]). The scientific opinion was initiated based on *in vitro* data indicating that acetamiprid induced excitation and/or desensitization of nicotinic acetylcholine receptors (nAChRs) in rat neonatal cerebellar neurons and the authors concluded that acetamiprid might have affected the developing brain similarly to nicotine (Kimura-Kuroda *et al.*, 2012[11]).

The scientific opinion outlined the uncertainties for use of some *in vitro* data in the risk assessment of two neonicotinoid pesticides. The uncertainties included:

- the very limited biological 'space' covered by the assay (i.e., only nACh receptors),
- the need for further characterization of the assay in terms of relevance to *in vivo* end points,
- the need for data from positive and negative controls, and
- an assessment of the reliability and reproducibility of the assay.

The scientific opinion concluded that these uncertainties "prevent its current use as a screening tool in the regulatory arena".

On the other hand, the available DNT study on acetamiprid did not allow a full characterization of developmental neurotoxicity since no proper evaluation of important endpoints such as motor activity and learning assessment could be performed due to problems with the control data and high variability (EFSA 2013[12]). Overall, there was residual uncertainty regarding establishing human reference doses (acute and chronic) which was mitigated by proposing additional safety factors.

Hence, in this case study, the problem formulation is derived from these uncertainties and is: Can new approach methods (NAM) data in an IATA context (integrating existing information) on acetamiprid sufficiently characterize DNT hazard?

1.3 Purpose

This IATA case study was developed to provide an example of the use and application of the DNT-IVB for a single substance DNT hazard assessment.

Furthermore, the case study also aims to address the uncertainties identified in EFSA 2013[12] in some of the *in vitro* and *in vivo* data to demonstrate that NAM data in an IATA context (integrating existing information) on acetamiprid. This is pursued by further DNT hazard characterization and a contextualization to exposure and risk by the use of PBK modelling.

The data derive from a case study on neonicotinoid pesticides conducted by the H2020-funded project "EU-ToxRisk". Here acetamiprid, imidacloprid, thiacloprid, thiamethoxam, dinotefuran, clothianidin and nicotine were tested in a range of *in vitro* assays, also assays as such not part of the current "OECD IVB". Testing and results on the other neonicotinoid compounds can be found in Loser *et al*. 2021a[13] and Loser *et al*. 2021b[14] and are not further discussed in the present case.

1.4 Chemical

The target chemical for this case study was the pesticide acetamiprid (CAS number 135410-20-7). The chemical structure is shown in Figure 1.

Figure 1. The chemical structure of acetamiprid

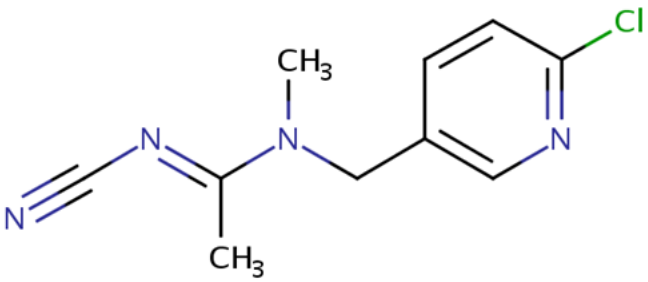

Acetamiprid is a neonicotinoid insecticide that triggers nervous system disturbances by activation of the nAChR(Brown *et al*., 2006[15]; Tan *et al*., 2007[16]). The compounds are widely used in agriculture for pest

control, although recently the use in Europe has been very restricted due to toxicity to pollinators. Neonicotinoids have been designed to display a high species specificity showing a high potency on insect receptors, while having low affinities on mammalian receptors (Casida, 2018[17]). Based on regulatory studies, acetamiprid has been classified according to CLP (EC 1272/2008) as Acute Tox. 4 (LD50 approx. 417 mg/kg bw). The critical effects were liver and kidney effects in rats and NOAELs were 12.4 and 7 mg/kg bw/day, in a 90 day and 2-year chronic toxicity studies, respectively. Neurotoxicity was also observed in an acute and sub chronic neurotoxicity study with a NOAEL of 10 mg/kg bw/dayand 14.8 and 16.3 mg/kg bw per day for males and females respectively (EFSA, 2013[10]).

1.5 Endpoint

The endpoint of interest was DNT induced by exposure to acetamiprid being any adverse effect on the normal development of nervous system structure and/or function, as defined by different specific endpoints measured *in vivo*, *in vitro* and in human observational studies, for example startle response in TG426 protocols, calcium signaling in developing neuronal cells or learning and memory in human observational studies, respectively.

1.6 Exposure Information

Exposure considerations are integrated in this IATA. Dietary and non-dietary exposure to acetamiprid can occur by its use as a pesticide. The case considers dietary exposure information obtained from the European monitoring program to pesticide residues in 2018 (EFSA, 2020[18]).

2 Hypothesis for performing the IATA

The hypothesis is that mechanistic understanding of the toxicodynamic properties of acetamiprid contextualized with internal exposure considerations related to realistic human exposures can inform the hazard characterization in regard to potential DNT effect.

2.1 Rationale for the IATA and method

As outlined above, identified uncertainties both regarding the *in vitro* mechanistic data by Kimura-Kuroda *et al*., 2012[11] and the uncertainties identified from the regulatory TG426 study as analyzed by ESFA in 2013[12], led to the hypothesis, that further mechanistic understanding could reduce the uncertainty on the potential DNT hazard properties of acetamiprid. Mechanistic understanding provided by *in vitro* evidence is expected to contribute to the weight of evidence for the DNT hazard characterization. The IATA workflow contained the following steps.

1) Assembling of evidence (*in vitro, in vivo* and human observational studies) using a systematic literature review approach
2) Screening for relevance
3) Integration of the evidence by an AOP-based approach
4) Generation of additional mechanistic evidence and contextualization
5) Data gap and uncertainty analysis
6) Conclusion

Only *in vivo* and *in vitro* studies from the literature ranked with low risk of bias were considered relevant for further analysis (there was no relevant human observational data). No documented AOP exists for 'Binding to nAChR leading to behavioral effects' and thus a putative AOP was postulated (see Figure 6 in section 7). In the following step the results of testing of acetamiprid in the EU-ToxRisk testing systems were included as mechanistic evidence and were mapped into AOP endpoints network in addition to the evidence retrieved from the systematic literature review.

3 Data gathering and application of the IATA

The literature searches were conducted in PubMed in August 2020 using an information specialist. Search strings are described in the appendix. Terms for the exposure were combined with relevant terms for DNT outcomes (human and *in vivo* studies) or methods (*in vitro* studies). The DNT outcomes were predefined by a series of toxicological *in vivo* and *in vitro* endpoints and measurements in human observational studies and categorized in endpoint categories translated into keywords for the searches (see Annex III). The PRISMA chart below illustrates the flow of the systematic review.

Figure 2. PRISMA chart on the systematic review flow for acetamiprid.

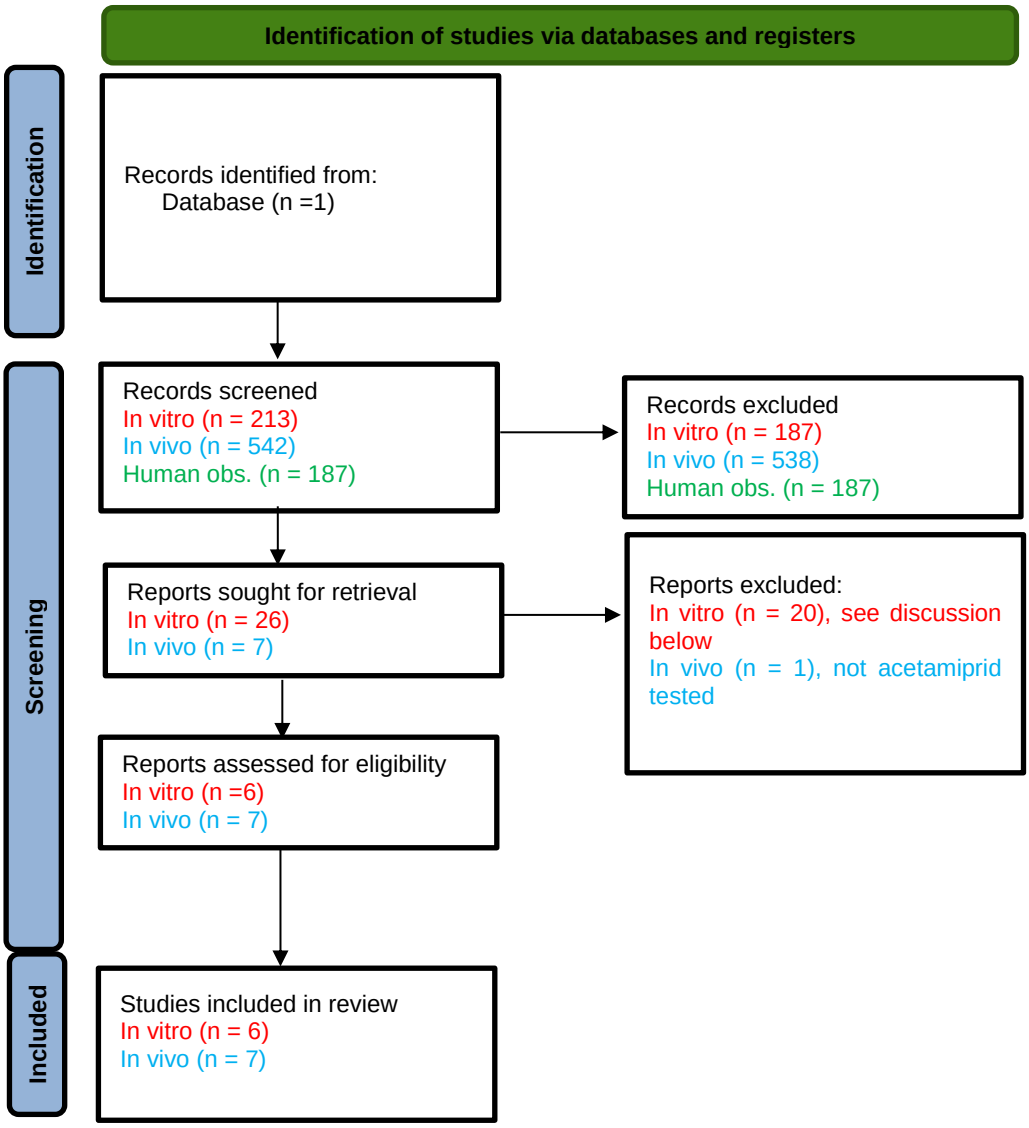

One reviewer screened the literature identified through the searches for the three areas (*in vitro*, *in vivo* and human observational studies).

The retrieved publications were first screened for relevance in terms of study design, test system, endpoint-

The screening resulted in exclusion of a majority of studies:

- For the *in vitro* studies, the main reason was exclusion of studies related to insects, not relevant endpoint studied and/or no investigation of acetamiprid.
- For the *in vivo* studies, the main reason was exclusion of studies was no developmental exposure and/or no investigation of acetamiprid.
- For the human observational studies, no studies were eligible as exposure was not directly measured in the mothers/children but was only inferred by questionnaire or geographical information.

Then the studies were appraised for the risk of bias and relevance using the SciRAP (Science in Risk Assessment and Policy) online tool (www.scirap.org). The SciRAP project was initiated by researchers from Stockholm University and Karolinska Institute with the purpose to increase the use of academic research in regulatory hazard and risk assessment. The online tool developed within the project facilitates structured and detailed criteria for evaluation of relevance and reliability of ecotoxicity and toxicity studies. The criteria developed for *in vivo* and *in vitro* studies are based on OECD test guidelines and guidance documents for such tests. The evaluation of the reliability is divided into “reporting quality” and “methodological quality” with several predefined criteria which can be evaluated as “fulfilled”, “partially fulfilled”, “not fulfilled” or “not determined”. The evaluation is then exported to an excel file, providing a qualitative summary in a color profile, where an overview of the strengths and weaknesses of the study are presented and thus the relevance can be determined.

4 Review of existing data from systematic review

4.1 *In vitro* data

Studies on acetamiprid induced neurotoxicity

While there is a large number of studies published on acetamiprid's effects in insects and insect targets, only a few studies that are relevant for DNT were performed on mammalian cells. Since the primary target for acetamiprid is ionotropic nicotine sensitive acetylcholine receptors and may even be more specific by targeting receptor isoforms differently, it is important that the neuronal models used in the studies are fully characterized in terms of nAChR subtypes. Furthermore, nAChRs are known to become desensitized rapidly, in particular the α7 homomeric nAChR, which also challenge the experimental set-up and instrument sensitivity. A negative result in a study using inadequate cell models, not expressing functional nAChR, or irrelevant endpoints of significance for DNT, may thus be misleading for any conclusion that acetamiprid does not impair neurodevelopment.

Further criteria were used to judge the relevance of the studies in terms of DNT in humans (Table 1). All studies must include relevant endpoints for any of the putative AOP key events (DNT). Studies on insect targets/cells were excluded, but mammalian cell models were included. In addition, 18 assays indicated active hit calls in the ToxCast data for acetamiprid. Of these, two binding studies were relevant as MIEs in the putative AOPs.

Table 1. Criteria for bias scoring 1-4 in Table 2.

Bias/relevance score	Criteria
1	Relevant model of human targets/neurons from early neurodevelopment. Cell culture properties known. Chemical references known. Several, non-cytotoxic, concentrations tested corresponding to realistic human plasma concentrations (micromolar or less). Negative control (exposure medium with solvent at known concentration) tested.
2	Relevant mammalian model of non-human targets/neurons from early neurodevelopment. Cell culture properties known. Chemical references known. Non-cytotoxic, concentration(s) tested corresponding to realistic human plasma concentrations (micromolar or less). Negative control (exposure medium with solvent at known concentration) tested.
3	Less relevant mammalian model of non-human targets/neurons. Several concentrations tested. Cytotoxicity unknown and/or negative control missing

4	Less relevant model of non-human targets/neurons and/or One concentration tested. and/or Cytotoxicity unknown and/or negative control missing

Table 2. Summary of publications performed *in vitro* identified and reviewed after application of search string.

Study design	Endpoints studied	Method	Cytotoxicity	Effects /concentrations	Nicotine included as positive control	Source	Risk of bias
PC12 cells (rat): NGF-induced differentiation 5 days (medium renewed every 48 h)	1. Neurite outgrowth (NO) 2. Transcriptomics	1. Imaging, neurite length (ImageJ) 2. qPCR of 6 target genes	Not determined	1. No sign. altered NO at 1, 10, 100 µM. Weak, but not sign. at 100 µM 2. Log2FC>1 (sign. UP): at 10 µM: camk2a, GAP43	No	Christen *et al.*, 2017 [19]	3
DIV14-16 neonatal rat cerebellar neurons Acute exposure	1. nAChR function 2. Voltage-operated Ca^{2+} channel (VOCC) function	1. Ca^{2+}influx without and with nAChR antagonists by imaging 2. KCl-induced Ca^{2+} influx after acetamiprid exposure	Indirectly	1. Transient Ca^{2+} influx at 1, 10 and 100 µM. Total block of 100 µM ACE by MEC, a-BT and DhI- 2. Attenuated or abolished VOCC function after ACE exposure	Yes, 1, 10, 100 µM	Kimura-Kuroda, *et al.*, 2012 [11]	2
DIV2 neonatal rat cerebellar neurons 14 days exposure (half of the medium was renewed every 2 days)	1. Transcriptomics 2. Morphology	1. Whole genome microarray and RT-qPCR 2. Immunocytochemistry	By morphology (2)	One concentration tested (1 µM) 1. 4557 DEGs of 23012 genes in total Out of 48 selected DEGs: 22 up, 26 down. Slight down-regulation of Chrna7. Common genes in GO and DP: Cacna1h, Cacng1, Hrh2, F2rl2, Dcdc2 2. No cytotoxicity by morphology, reduced dendritic area of purkinje cells observed	Yes, 1 µM	Kimura-Kuroda *et al.*, 2016[20]	3
Primary cortical rat neurons, DIV14-15	Electrical activity	MEA	PI staining	Only one concentration: 40 µM. Neg results	Yes, 40 µM (NEG in MEA)	Valdivia *et al.*, 2014[21]	4 One conc
Membranes from human neuroblastoma cells	Binding study on CHRNA2	displacement of [H^3]-epibatidine	N.A.	AC50: 5.41 µM	N.A.	CompTox.epa.gov (Sipes *et al.,2013* [22])	3 Efficacy not studied
Membranes from primary rat cortical brain tissue	Binding study on Chrna7	displacement of [I^{125}]-a-bungarotoxin	N.A.	AC50: 9.30 µM	N.A.	CompTox.epa.gov (Sipes *et al.,2013*[22])	3 Efficacy not studied

The *in vitro* data reviewed here shows that acetamiprid induces Ca^{2+} influx via the nAChR as well as attenuated VOCC function after exposure at concentrations between 1-100 µM (Kimura-Kuroda *et al.*, 2012[11] ; Valdivia *et al.*, 2014[21]). The Ca^{2+} influx of 100 µM acetamiprid was blocked completely by mecamylamine (non-selective antagonist), α-bungarotoxin (selective α7 nAChR antagonist) and dihydro-

β-erythroidine (selective α4β2 nAChR antagonist), indicating agonist activation of several nAChR subtypes(Kimura-Kuroda *et al*., 2012[11]). In addition, the data on acetamiprid in the Comptox Chemicals dashboard was also assessed. Binding studies show that acetamiprid binds to both the CHRNA2 and CHRNA7 subunits in human neuroblastoma cells and primary rat cortical brain tissue respectively (Sipes *et al*., 2013[22]). Functional endpoints in terms of morphology have been investigated where no statistically significant effect was seen on neurite outgrowth but reduced dendritic area of rat purkinje cells were observed (Christen *et al*., 2017[19]; Kimura-Kuroda *et al*., 2016[20]). Two of the studies reviewed performed transcriptomics after acetamiprid exposure and observed DEGs relevant for neuronal development were identified. Kimura-Kuroda exposed DIV2 neonatal rat cerebellar neurons to 1 µM during 14 days (repeated exposure every 2 days) where 48 DEGs were identified, among these two calcium channel subtypes (*Cacna1h* and *Cacng1)* were downregulated and a slight down-regulation of *Chrna7* (Kimura-Kuroda *et al*., 2016[20]). Christen *et al*. analyzed 6 target genes by qPCR in PC12 cells were exposed for 5 days to 10 and 100 µM acetamiprid. The results showed that 10 µM acetamiprid significantly (log2FC > 1) increased the expression of *camk2a* and *gap43* (Christen *et al*., 2017[19]*). Camk2a* belongs to the calcium/calmodulin-activated protein kinase family, functioning in neural synaptic plasticity and neuronal migration (Kim *et al*., 2015[23]; Nicole *et al*., 2018[24]). *Gap43* (neuromodulin) is associated with axonal growth during development and regeneration (Snipes *et al*., 1987[25]).

Taken into account the importance of nAChRs during neuronal development, the six *in vitro* studies reviewed here indicate that exposure of acetamiprid during pregnancy are of concern. However, some of the studies had high bias scores due to only one concentration studies, less relevant mammalian models used, long exposure time, no efficacy or that cytotoxicity was not studied.

4.2 *In vivo* data – mammalian

The eligible *in vivo* studies were scored for risk of bias and relevance using the SciRAP tool. Four studies were reviewed in total where two of them have a score of 1 or 2.

Bias/relevance score	Criteria
1	OECD TG 426 compliant study or similar
2	Dose-response design Exposure ascertained Full reporting Relevance in terms of the identity of the tested substance, the animal model used, the endpoint studied, the route of administration, the dose levels and resulting tissue levels
3	No dose-response design Otherwise, like "2"

Table 3. Summary of publications performed *in vivo* identified and reviewed after application of search string.

Study design	Endpoints studied	Method	Systemic toxicity Dams/offspring	Effects /doses	Source	Risk of bias
Spague-Dawley rat Oral gavage 0, 2.5, 10, 45 mg/kg bw/day GD6-PND21	TG426 compliant as described in Sheets et al. 2016	TG426 compliant as described in Sheets et al. 2016	Maternal NOAEL 10 mg/kg bw/day Decreased bw and BW gain at 45 mg/kg bw/day/ Decreased bw and bw gain, pre-weaning survival at	Decreased auditory startle response: 10 mg/kg bw/day: 27% at PND 20 and 40% at PND 60 45 mg/kg bw/day: 42% at PND 20 and 53% at PND 60	EFSA 2013[10]	1

			45 mg/kg bw/day	No conclusion on motor activity (control did not have normal behaviour) and learning and memory due to high variability		
ICR mice Oral gavage 0, 5 mg/kg bw/day in 0.5% carboxymethylcellulose sodium GD3-PND14	Neurogenesis, neuronal distribution, microglial activation in dorsal telecephalon GD14 and neocortex PND14	Immunostaining and morphological analysis, quantitative cell cycle kinetics	No effects: Clinically, partuition/ viability, bw, Relative brain weight	Hypoplasia of the cortical plate in the dorsal telecephalon Decreased neurogenesis measure at PND14 Increased migroclia activation	Kagawa 2018[26]	3
ICR mice Oral gavage 0, 5 mg/kg bw/day in 0.5% carboxymethylcellulose sodium PND 12-26	Neurogenesis, microglia activiation in hippocampal dentate gyrus	Immunostaining and morphological analysis, quantitative cell cycle kinetics	No effects: viability body weight, Relative brain weight	Decreased neurogenesis at PND26 Increased migroclia activation .	Nakayama 2019[27]	3
C57BL/6J mice Oral gavage 0. 1, 10 mg/kg/day GD6-LD21 in water GD6-PND21	Social-sexual behaviour, anxiety-related behaviour, behavioural flexibility Vasopressin expressing cells – hypothalamus Serum testosterone	Male sexual behaviour test (n=9-11) Male aggressive behaviour test (n=9-11) Female sexual behaviour test (n=8-10) Light-dark transition (LDT) test (n=8-11) Group behavior in Intellicage (n=5-8) Immunostaining (n=2-6) Testosterone enzyme immunoassay(n=5-11)	No effects: body weight, Brain weight Vasopressin expressing cells Testosterone levels	Male adult at 1 & 10 mg/kg bw/day reduced anxiety in LDT Male adult at 1 mg/kg bw/day increase sexual and aggressive behavior	Sano 2016[28]	2

According to the NAFTA guidance on DNT studies (2016)4, the auditory startle response in rodents is a simple behavior controlled by a simple neural circuit involving sensory, neural, and motor systems. Because of this, treatment-induced changes in the startle response can usually be ascribed to alterations in one or more of these systems and this reflects a treatment-induced disruption in nervous system functioning even if the specific location or nature of the alteration is not clearly identified. For instance, alterations in sensory thresholds or alterations in neuromuscular functions may both impact auditory startle responding. Treatment-induced alterations in habituation can usually be interpreted as treatment-related effects on non-associative learning that is mediated by the central nervous system. In the regulatory DNT TG426 study, decreased startle response were seen at 10 and 45 mg/kg bw/day in rat, according to the EFSA assessment (EFSA, 201310) and effects on bodyweight was seen at the highest dose.

In the Sano et al., the effects on anxiety-related behavior were seen at both tested doses (1 and 10 mg/kg bw/day) showing a dose response relationship (Sano et al., 201628). There have been several reports regarding the effects of nicotine exposure on anxiety- related behaviors during the developmental period (as discussed in Sano et al., 2016). However, there is not a consistent pattern, thus both positive and negative effects was reported, depending on the experimental conditions such as the dose, time of administration, and the behavioral test paradigm. The described effects on male social-sexual behavior and behavioral flexibility, where only observed at the low dose. It is acknowledged in the NAFTA guidance that non-monotonic dose-responses should always be carefully examined, and Sano et al. contextualize their finding with different effects of on vasoprenergic system by nicotine depending on dose, however in their study they could not see effect on number of vasopressin immunoreactive cells in the paraventricular nucleus.

Two studies describe effect on neurogenesis and microglial activation in mice in the dorsal telencephalon and hippocampal dentate gyrus, Nakayama *et al*., 2019[27] and Kagawa *et al*., 2018[26] at 0.5 mg/kg bw/day. However, only one dose was investigated, and it seems to be the same experiment.

Altogether, the available *in vivo* mammalian data show quite some variability across the studies on reported effects, with no consistent specific effects/adverse outcome. Also, the experimental design, exposure methods, the endpoints investigated, and the species are not similar.

4.3 *In vivo* data – Zebrafish embryo

Table 4. Summary of publications performed *in vivo* in zebra fish embryos identified and reviewed after application of search string.

Study design	Endpoints	Method	Systemic toxicity	Effects /doses	Source	Bias
AB type zebrafish embryos (ZFE) Static exposure **Clutch 1: 54, 107, 263, 374, 433, 537, 644, 780, 848, 974 mg/l** **Clutch 2: 107, 53, 760 mg/l** **Clutch 3: 54, 107, 263, 374, 433 mg/l** **Clutch 4 & 5: 107, 537, 760, 974 mg/l**	Lethal and sub-lethal (hatching, development, movement) endpoints between 6 and 120 hpf.	C1: Mortality and malformation 24-120 hpf, hatching success at 72 hpf. FET test. C2: Heart rate (HR) at 48, 60 and 72 hpf; 10 sec videos to calc beats/minute. C3: Body length (BL) measurement at 120 hpf. C4: Coiling assay (STM) 17-25 hpf. C5: Touch response of head (HT) and tail (TT) at 27, 36, 48 hpf.	C1: bent spine, uninflated swim bladder, pericardial oedemata, yolk oedemata. C2: 20-25% HR reduction regardless of exp and time. C3: dose-dependent decrease in BL. C4 & 5: dose-dependent decrease in STM and HT/TT.	C1: 120 hpf EC_{50}: 323 mg/l; 120 hpf LC_{50}: 518 mg/l; 72hpf $EC_{50hatch}$: 554 mg/l. C2: >107 mg/l sign reduced HR at 48+ hpf; =107 mg/l sign reduced HR at 72 hpf. C4: 107 mg/l delayed peak to 24 hpf; 537 mg/l delayed it to 25 hpf; 760 mg/L delayed peak to 25 hpf and reduced nr/movement by 50%; 974 mg/l inhibited movement. C5: HT reduced by 537 mg/l at 36+ hpf and =760 at 27+ hpf; TT reduced by 760 mg/l at 27 hpf only and 974 mg/l at 27+ hpf.	Ma et al., 2019[29]	2
AB type ZFE, juveniles and adults Semi-static exposure **Concentrations: ACE: 0.042, 0.17, 0.67 mg/l** **Also tested other compound not pertaining to the present report.**	FET test (ZFE and larvae (ZFL), 4-day exposure of 1-month old juveniles (ZFJ) and adults (ZFA). PCR for all groups.	ZFE, ZFL: FET endpoints, HR, gene expression. ZFJ, ZFA: mortality, gene expression	Individual tox.: increased Cas8, Tnf, TRß. Reduced ERa	Individual tox LC_{50}.: ZFE: 13,33 mg/l; ZFL: 15.52 mg/l; ZFJ: 36.91 mg/l; ZFA: 10.36 mg/L	Wang et al-2018[30]	2

The data outlined here shows that acetamiprid exposure affects the general development (Ma *et al*., 2019[29]), the cardiovascular system (Ma *et al*., 2019[29]; Wang *et al*., 2018[30]), and the behavioral aspects of the development of the zebrafish, as well as during adult life stages (Ma *et al*., 2019[29]; Crosby *et al*., 2015[31]). As the nAChRs are present and during embryogenesis already, playing a vital role in e.g., early neural plate development (Svoboda *et al*., 2002[32]), thus, altered receptor functioning may induce spinal cord malformation along with the disorganization of craniofacial cartilaginous features. Considering the heart-rate changes observed by Ma *et al*., 2019[29], it has previously been shown, that heart deformation, oedemata, and reduced circulation were linked to the delayed transition of stem cells through the mesoderm (Palpant *et al*., 2015[33]). The behavioral alterations noted in the discussed publications outline

that acetamiprid exposure induces a concentration dependent decrease in early coiling movements, whilst also affecting general development and the touch response later during development (Ma *et al*., 2019[29]). Here, the activation, and subsequent desensitization of muscle-specific nAChRs is thought to induce the observed endpoint (Svoboda *et al*., 2002[32]), which may also lead to muscle degeneration with high concentrations (Leonard *et al*., 1979[34]), based on the myopathy and tissue degeneration noted after prolonged nicotine exposure in 7-day old zebrafish embryos (Welsh et al., 2009[35]) possibly based on the post-excitatory rise in muscle calcium levels (Engel *et al*.,1982[36]; Engel *et al*.,2003[37]; Gomez *et al*., 2002[38]). The observed significant decrease in juvenile swimming behavior (Crosby *et al*., 2015[31]) has been hypothesized to stem from the protection of the chorion, hindering direct contact between the entire amount of compound in the exposure medium and the individual until 72 hours post fertilization (hpf) (Osterauer and Köhler, 2009[39]; Vignet *et al*., 2019[40]).

5 Absorption, distribution, metabolism and excretion

Acetamiprid is a neutral compound with a reported Log P_{ow} of 0.8 (Brunet *et al*., 2008[41]). Acetamiprid has high permeability across the Caco-2 cell monolayer with an apparent permeability (Papp) value of 26 x 10^{-6} cm/s reported (Brunet *et al*., 2008[41]).

There have been relatively few studies that have studied the *in vivo* pharmacokinetics of acetamiprid. Ford and Casida have studied the metabolism and tissue distribution of acetamiprid following intraperitoneal injection in mice (Ford and Casida, 2006[42]). Metabolites identified included the desmethyl metabolite and various cleavage products. Both parent compound and the desmethyl metabolite were detected in the brain, liver, plasma, and urine of the mice. The levels of parent compound in the brain were about half of those in the plasma at equivalent time points. Other studies have also measured brain concentrations of acetamiprid after exposure via drinking water to mice (Terayama *et al*. 2016[43]). Unfortunately, in this study plasma concentrations were not reported to allow a brain:plasma ratio to be calculated.

Studies with radiolabeled acetamiprid in rats show rapid and extensive absorption of radioactivity after single (1 or 50 mg/kg) or multiple (1 mg/kg) doses. With rapid excretion of radioactivity mainly via the urine. In both rats and goats, demethylation of acetamiprid is a major metabolic pathway (EFSA, 2013[10]).

In humans the urinary excretion of deuterated acetamiprid and desmethylacetamiprid following oral dosing of deuterated (D6) acetamiprid (5 μg) has been measured (Harada *et al*., 2016[44]). The urinary excretion of acetamiprid (2.6% of the dose) was lower than that of the desmethyl metabolite (31% of the dose). In an additional part of the study by Harada *et al*. (2016) desmethylacetamiprid was found in the urine of every subject (n=373) where measurement was attempted. Using a pharmacokinetic model it was estimated that for a daily intake of 1.94 μg/d of acetamiprid a total of 1.14 μg/d would be excreted in the urine as desmethylacetamiprid (~63% of the dose once differences in molecular weight are accounted for).

6 MoA; nicotinic acetylcholine receptors (nAChR)

nAChR are ligand gated cation channels. The receptors are assembled of 5 subunits which can form heteromeres or homomeres with ligand-binding extracellular and ion channel transmembrane domains (Figure 3). The most abundant isoforms in brain are the heteropentameric α4β2 nAChR and the homopentameric α7 nAChR (Wada *et al*.,1989[45]; Tribollet *et al*., 2004[46]). The α4β2 nAChR is more permeable for Na^+ ions than for Ca^{2+}, but the α7nAChR is more permeable for Ca^{2+} (Buisson *et al*., 1996[47]; Seguela *et al*., 1993[48]). This receptor is also rapidly desensitized upon ligand binding, and it is debated if receptor activation and Ca^{2+}influx is mediating the desensitization or if the receptor inactivation can take place by a conformational change upon ligand binding, i.e., an allosteric modulation (Williams *et al.,* 2011[49]).

Figure 3. Pentameric structure of nAChR.
A) top view of heteropentameric α4β2 (with stoichiometry 3*α4 (blue ribbon) and 2*β2 (grey ribbon)
B) side view of 2 adjacent full-length subunits that are forming the ligand (e.g., nicotine – green calotte model) binding site
C) ECD of homopentameric α7 isoform (yellow ribon – binding site residues in stick representation and circled: homology model50).

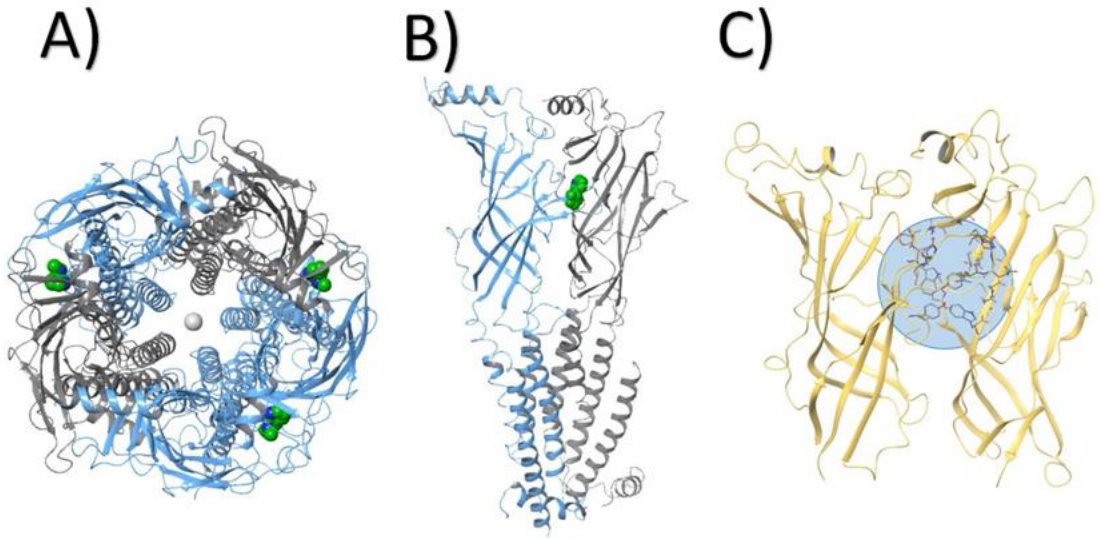

Neurodevelopment is orchestrated by cues such as neurotransmitters, growth and neurotrophic factors giving signals to cell to take actions in a precise timely manner (Figure 4). Hence, altered signaling at specific sensitive windows during neurodevelopment will have impact on proliferation, apoptosis, migration, differentiation and synaptogenesis, i.e., cellular organization and maturation that will have an impact on brain function.

Figure 4. Schematic representation of how neurotransmitter signals control neuronal cell development during specified critical periods.

Depending on the context in which stimulation occurs, the same neurotransmitter, operating through the same receptors and signalling pathways, can promote cell replication, can elicit a switch from replication to differentiation, can promote or arrest cell growth, can evoke apoptosis, or can program the genes that determine the future responsiveness of the cell to external stimulation (cell learning). Figure from Slotkin *et al*.,2008[51].

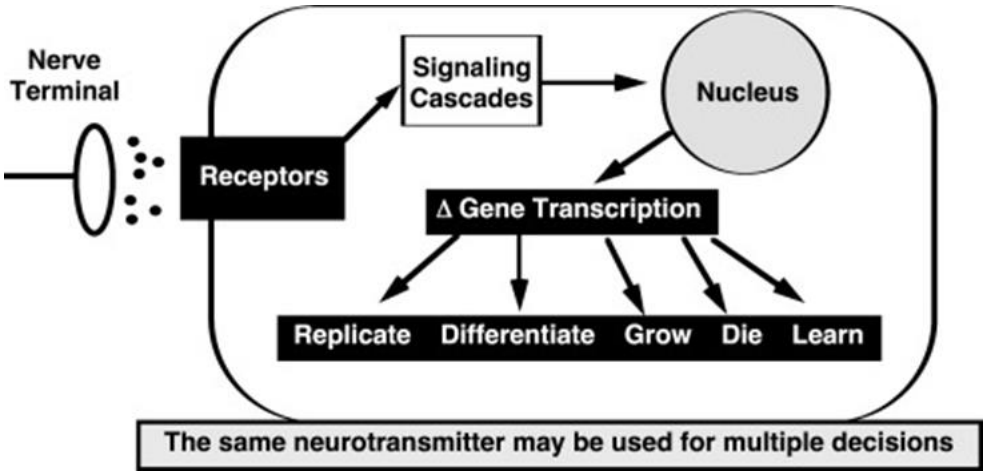

The nAChRs play central roles during neurodevelopment and the transient patterns in nAChR subtype expression during embryogenesis have different impact on each developmental stage (Figure 5). Hence, any alteration in nAChR expression, function or activity may disturb crucial steps in neuronal organization. Furthermore, altered cholinergic signaling has effects on other neurotransmitter systems, including dopamine, noradrenaline and serotonin (Azam *et al*., 2007 [52]; Xu *et al*., 2001[53]; Slotkin *et al*., 1987[54])

Figure 5. Temporal and regional expression of nicotinic AChR subunit mRNA in developing human and rat brain.

Timeline for initial expression of mRNA for different nicotinic AChR subunits is illustrated. Given the diversity of nicotinic AChR subtypes as well as the differences in subunit composition and conformation (i.e., spatial arrangement of the different subunits within the receptor), mRNA expression is most often used to identify the potential for the presence of a specific nicotinic AChR subunit in different brain regions. However, it is important to note that expression of mRNA does not necessarily indicate the presence of functional receptors that incorporate that subunit. Abbreviations: GD, gestational day; PND, postnatal day. Figure from Smith *et al*., 2010[55].

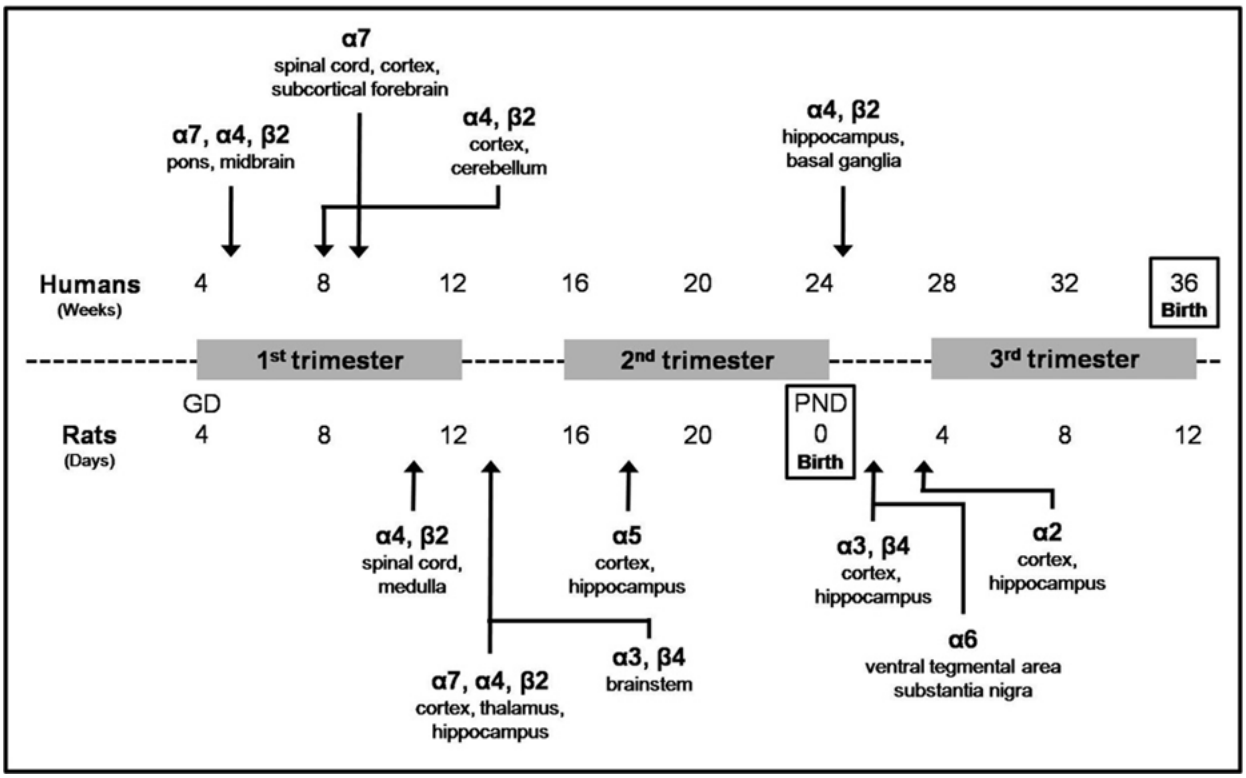

6.2 Altered nAChR expression

The α7 nAChR subtype is essential for normal neurodevelopment. Increased or attenuated activity (eg. by neuroactive compounds) as well as up or down regulation of the expression have can be linked to a number of diseases. The α7 subunit gene is located in 15q13.1 locus, which is very sensitive to alterations, i.e., microdeletions or microduplications. Alterations in 15q13.1 in any direction (increase or decrease in functional receptors) may result in mental dysfunction, late onset of speaking, intellectual disabilities, risk of epilepsy and schizophrenia (Gillentine *et al*., 2017[56]; Ziats *et al*., 2016[57]; Deutsch *et al*., 2016[58]). The α7 nAChR subtype is not the exclusive product of the 15q13.1 locus. Nevertheless, there is a clear connection between impaired α7 nAChR function and schizophrenia (Marcus *et al*., 2016[59]). Association between dysfunctional α7 nAChR signaling and mental illness is further shown in different knockout mouse models that display phenotypes with depression-like symptoms (Zhang *et al*., 2016[60]) and impairments of cognitive and social behavior (Nacer *et al.,* 2021[61]). Studies performed on α7 KO mice (8-14 weeks old) led to temporal processing deficits in the midbrain and auditory brainstem (Felix *et al*., 2019[62]). In 2009, Levin *et al*. studied the effects on learning and memory in a radial maze test in β2 or α7 KO mice. The results

demonstrated that male β2 KO mice had choice accuracy impairment whilst the α7 KO mice also showed a significant impairment for both male and females (Levin *et al*., 2009[63]).

6.3 Signaling effects of prenatal exposure with nicotine

Slotkin (2008) reviewed the literature of nicotine exposure during pregnancy and evidence for abnormal neurodevelopment in animal models and humans (Slotkin, 2008)[51]. Prenatal doses of nicotine that do not affect growth or induce secondary gross effects (most common endpoints in developmental studies), still have adverse effects on neurodevelopment and behavior (Navarro *et al*.,1989[64]; Eppolito and Smith, 2006[65]). Cigarette smoke contains thousands of compounds and reports should therefore be evaluated with some skepsis regarding the impact of nicotine as such. However, specific alterations on cholinergic targets have been reported after exposure to cigarette smoke during pregnancy. Maternal smoking upregulates nAChR expression in brain of infants (Nachmanoff *et al*., 1998[66]). Corresponding nicotine exposure in monkeys and rats give the same upregulation as a consequence of receptor desensitization (Slotkin *et al*., 2002[67]). Disturbed nAChR signaling after prenatal nicotine exposure has also an impact on other neurotransmitter systems. nAChRs act as modulators of presynaptic transmitter release and will thus change the signaling of multiple neurotransmitters at different developmental stages. For example, altered cholinergic signaling affects GABA and glutamate release and thus synaptic connectivity (Frazier *et al*., 1998[68]; Cheng *et al*., 2015[69]).

6.4 Behavior/mental effects after prenatal nicotine exposure

Prenatal nicotine exposure can affect signaling permanently and may alter the mood regulating neurotransmitter serotonin during adolescence (Slotkin *et al*., 2007[70]; Slotkin *et al*., 2006[71]).

Evidence for behavioral/mental effects after nicotine exposure is rich when related to studies on children with smoking mothers during pregnancy. Several studies have shown an association between maternal smoking and developmental disorders such as ADHD and auditory and visual cognitive impairments (Milberger *et al.,* 2010[72]; Mick *et al*., 2002[73]; Jacobsen *et al*., 2007[74]). However, taking into account that cigarette smoke contains more than 4000 compounds (Borgerding and Klus, 2005[75]), co-exposure to multiple other problematic compounds confounds describing findings.

7 Putative AOP

In order to integrate the various data generated for the purpose of the case study with existing mechanistic understanding, a putative AOP is proposed, since there is no adverse outcome pathway (AOP) described in AOP Wiki that explains nAChR binding as a molecular initiating event (MIE) leading to neurodevelopmental dysfunction as the adverse outcome (AO). However, an AOP has been described as chronic binding of antagonist to the glutamatergic ionotropic NMDA receptor during neurodevelopment, leading to attenuated Ca^{2+} influx, decreased release of brain derived neurotrophic factor (BDNF), impaired synaptogenesis and impaired learning and memory formation as AO (AOP:13 in AOPWiki.org and AOP no.5 in the OECD series) (Sachana *et al.,* 2018[76]; Sachana *et al.,* 2016[77]). Based on the evidence of α7nAChR polymorphism and AOs like attention deficit syndrome (ADS), delayed mental development, schizophrenia and epilepsy together with the substantial evidence for nicotine as a neuroteratogenic compound, a putative AOP as a working hypothesis can be proposed. The AOP include binding to nAChRs (MIE), leading to activation of nAChR (KE1), leading to desensitization of nAChRs (KE2), leading to altered cellular phenotype (KE3), leading to altered neurodevelopment (KE4), resulting in delayed mental development, ADS, schizophrenia or epilepsy (AO). However, KE2 may be excluded in the case direct activation of nAChRs has impacts on KE3, KE4 and AO. As a key event relationship (KER), altered gene expression can be a consequence of nAChR activation or desensitization (KE1 and KE2). The AOP include binding to nAChRs (MIE), leading to activation of nAChR (KE1), leading to desensitization of nAChRs (KE2), leading to altered cellular phenotype (KE3), leading to altered neurodevelopment (KE4), resulting in delayed mental development, ADS, schizophrenia or epilepsy (AO). However, KE2 may be excluded in the case direct activation of nAChRs has impacts on KE3, KE4 and AO (Figure 6). In addition, gene expression changes can be considered as a possible KER between KE2 and KE3.

Figure 6. A putative adverse outcome pathway describing nAChR binding leads to impaired cognitive function and psychiatric diseases.

KE1 can lead to KE3 via KE 2 or directly. * Indicates endpoints not measured in this study.

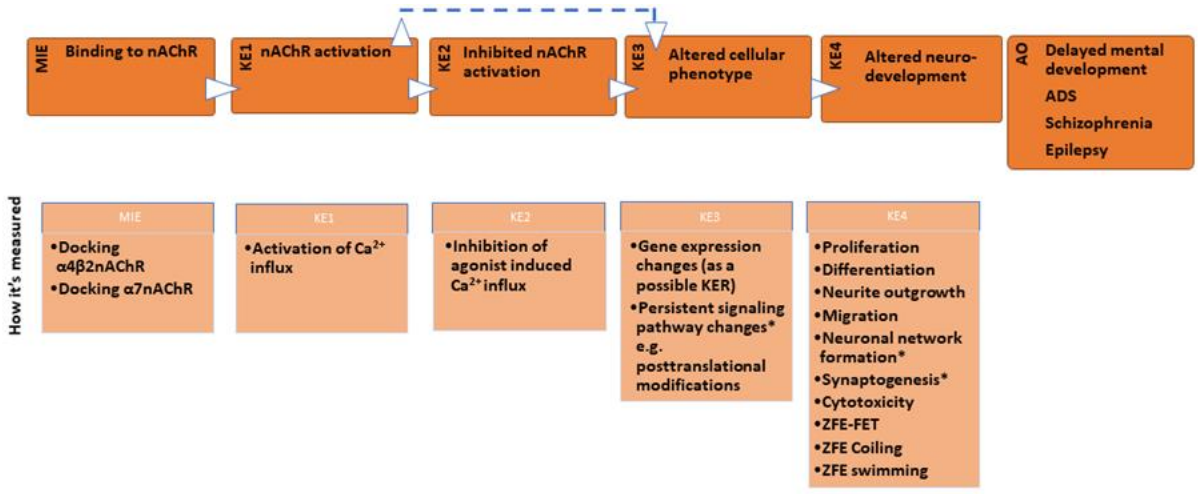

8 Data generation

8.1 Test systems

The MIE can be measured by docking models of acetamiprid on specific subtypes of the nAChRs and the KEs can be measured in cell models that display functional targets, i.e. nAChR subtypes that are relevant for neurodevelopment (Figure 5). Below, we describe the test systems that were used to measure the MIE and the KEs in the putative AOP. An overview of the test methods is provided in Table 5 below.

Table 5. Overview of test methods.

	Key neurodevelopmental processes and cell survival						
Test Method	UKN2	UKN4	UKN5	NPC1-5 *	RoFA	TD42 iPSCs	SHSY5Y cells
Test System	neural crest cells	LUHMES (CNS neurons)	hiPSC neurons (PNS neurons)	**data from EFSA report (Masjosthusman et al.) reviewed and commented in report. Not in particular part of this IATA*	hiPSC differentiation into neuronal rosettes		
Endpoint 1	cytotoxicity	cytotoxicity	cytotoxicity		cytotoxicity	cytotoxicity	cytotoxicity
Endpoint 2	migration	neurite outgrowth	neurite outgrowth		rosette formation	-	-
SOP	attached	attached	attached		in work	attached	attached
publications	10.14573/altex.1605031	10.1007/s00204-013-1072-y	10.5966/sctm.2015-0108		10.1007/s00204-019-02612-5	10.1016/j.diff.2016.06.002	10.1007/s00204-021-03031-1

	Biochemical/Signalling			Transciptomic profiling of:	Zebrafish	In silico	
Test Method	CALUX assays	Calcium measurements			FET (OECD 236)	Docking	PBTK/QIVIVE
Test System	Several (31 human cell based assays in total)	LUHMES	SHSY5Y	neural crest, LUHMES, NEPs, TD42 iPSCs and SHSY5Y	Fish embryos	IFD; Schrödinger Release 2020-2	in silico
Endpoint 1	Cell signalling pathways	Ca whole well and single cell	Ca whole well		Lethality	representative docking poses	Internal exposure
Endpoint 2	Nuclear receptors	patch clamp	-		velopmental alteratio	-	-
SOP	attached	in work	attached		OECD TG 236	Induced Fit Docking protocol; Glide, Schrödinger, LLC, New York, NY, 2021: Prime.	Report attached
publications	https://doi.org/10.1002/9781118538203.ch28	10.1007/s00204-021-03031-1	10.1007/s00204-021-03031-1		https://www.oecd-ilibrary.org/environment/test-no-236-fish-embryo-acute-	https://doi.org/10.1021/jm050540c	Relevant references are described in the report

8.1.1 MIE: Docking models

For the structure-based approach, we focused on the major isoforms of the nAChRs in the human brain, α4β2 and α7. The heteropentameric subtype α4β2 had been resolved using cryo-EM-methodology and was retrieved from the protein data bank (rcsb.org; PDB-ID: 6cnk, 6cnj)[72]. Regarding the homopentameric α7-subtype, we used a homology model which is based on a template of a chimeric structure that previously had been used as binding activity prediction model (Ng *et al.*,2018)[50]. This was needed because there was no experimentally resolved structure when the study was conducted. However, a cryo-EM structure was released this year by Noviello *et al.* 2021[78]. The homology model was compared using superposition of the structures and resulted in a RMSD (root-mean-square deviation) of 2.8 Angstroms which is less than the resolution of the structure (3.6 Angstroms). Both, the ligand Acetamiprid and the protein structures have been prepared for docking accordingly. We conducted molecular docking studies using the induced fit procedure in the software package of Maestro (Schrödinger Release 2020-

2), which integrates receptor flexibility up to a certain degree. The analysis of the docking poses was performed using protein-ligand-interaction fingerprint clustering and also the binding poses have been compared to conformations of other neonicotinoids co-crystallised in model organisms (Lymnaea stagnalis; PDB-ID: 2zju) (Ihara *et al*., 2008[79]). More details about the docking approach can be found in the publication about subgrouping of neonicotinoids (Loser *et al*., 2021[13]).

8.1.2 KE1-4: LUHMES cells

The Lund human mesencephalic (LUHMES) cells were used as a test system to represent neurons with a dopaminergic phenotype. Via tetracycline induction LUHMES cells can be switched from a proliferating into a post-mitotic neuronal status in which cells further differentiate and grow a neuronal network, as described earlier in detail by Scholtz *et al*. 2011[80]. During differentiation cells change receptor composition including the expression of nAChRs (Figure 7A). For example, gene expression of α4 and β2 subunits increase from day of differentiation 0 (D0) to D2. The LUHMES cell system can be used as a developmental system, targeting endpoints such as neurite outgrowth during differentiation as shown before Stiegler, 2011[81]; Krug *et al.*, 2013[82]. Additionally, cells with a functional network can serve as a model to measure functional capacity, such as calcium signaling at present receptor types (Loser *et al*., 2021[13]).

8.1.3 KE1-4: SH-SY5Y cells

The human SH-SY5Y neuroblastoma cells express functional muscarinic and nicotinic acetylcholine receptors (mAChR and nAChR, respectively) and they possess acetylcholine esterase activity (Gustafsson *et al.,* 2010[83]). The expression of both metabotropic (M3) and ionotropic AChRs increases upon differentiation that is induced by all-trans retinoic acid (RA) (Figure 7B). When cultured in defined medium with N2 supplements and RA, the cells display neurochemical, structural and functional features of differentiated neurons as described earlier by Gustafsson, 2010[83]; Attoff *et al.,* 2020[84]; Delp *et al*., 2021[85]. Hence, the cell model is useful for studies from proliferating neuroblasts to differentiated neurons. In the present study, 3 days-differentiated cells were exposed with compounds and direct and inhibitory effects on α7 nAChR induced Ca^{2+} influx, gene expression and cytotoxicity were assessed.

Figure 7. RNA-seq of cholinergic markers in A) LUHMES cells B) SH-SY5Y cells during differentiation.
Figure A and B from Loser *et al*. 2021[13].

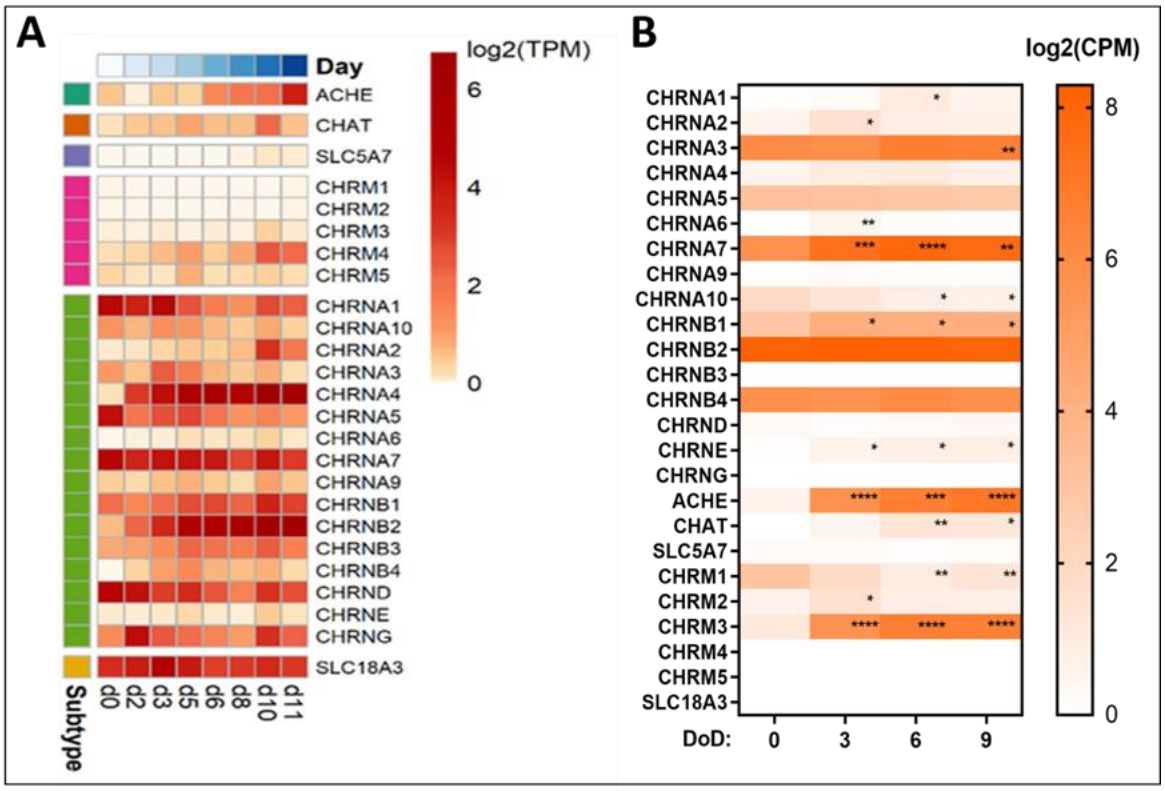

8.1.4 KE3-4: iPSC TD42

The test procedures describe the acute cytotoxicity of test compounds on human induced Pluripotent Stem Cell (hiPSC) -derived TD42 neural cultures using cell viability endpoint [Adenosine triphosphate (ATP) release measurement] (ECVAM, 2019[86]). The neural differentiation based on the differentiation protocol as described before by Chambers *et al*. 2009[87]. iPSC-derived TD42 neural cultures are characterized and validated as previously described by Ochalek, *et al*., 2017[88]; Chandrasekaran *et al*., 2017[89], and Zhou *et al.,*2016[90]. The test method is related to neural progenitor cell differentiation into glial and neuronal cells, mimicking the cytotoxic effect of compounds in early fetal stages (maturing neuro- and astrocytic toxicity at TD42) of neural development (developmental cytotoxicity). In addition, TD42 neuronal culture expresses specific subtypes of nAChRs as seen in Figure 8.

Figure 8. Common neuronal nAChR subunits are expressed in D42 TDN samples.
The expression values were calculated as a relative amount of the mRNA versus the expression value of the Human Cerebral Cortex, which was set to 1. Samples were measured in triplicates.

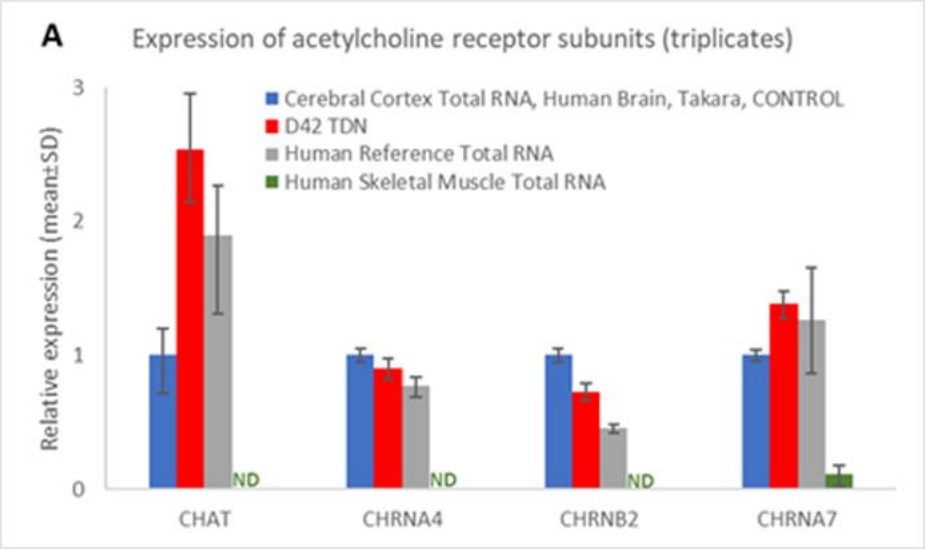

8.1.5 KE3-4: Neural crest cells (NCCs)

Neural crest cells (NCCs) represent a cell type during early neurulation, known for their characteristic to migrate throughout the body and capability to form different cell types. Here, NCCs were differentiated from the hiPSC line IMR90_clone #4 (WiCell, Wisconsin). Differentiation from hiPSC line IMR90 into NCCs was performed according to the modified protocol of Mica *et al.,* 2013[91].

8.1.6 KE3-4: hiPSC-derived neuroepithelial precursors

The hiPSC line iPSC EPITHELIAL-1 (= Sigma 0028) was used and differentiated following the differentiation protocol as described before by Chambers *et al*. 2009[87], with minor adaptations in differentiation factor concentrations as already used previously in Dreser *et al*. 2020[92]. In more detail, hiPSCs were seeded as single cells and differentiated for a period of up to 12 days. The cell system represents an early stage of neurodevelopment, with strong SC marker expression in the beginning and a development to cells expressing markers typical for neuroepithelial precursor cells, like PAX6 or OTX2 (Dreser *et al*. 2020[92]). Deregulated expression of these markers can be used as indicators for disturbed early neurodevelopment.

8.1.7 KE4: Peripheral/Sensory neurons

Sensory neurons for this study were differentiated from the hiPSC line SBAD2. SBAD2 cells were previously derived and characterized at the University of Newcastle from Lonza fibroblasts CC-2511, Lot 293971 with the tissue acquisition number 24245 (Baud *et al*., 2017[93]). Cells were differentiated as described earlier by Hoelting *et al* 2016[94] with the minor adaptations used in a previous compound screen (Masjosthusmann *et al*., 2020[9]).

8.1.8 KE4: Zebrafish embryo

The Fish Embryo Acute Toxicity (FET) test, in accordance with the Organization for Economic Co-operation and Development Test Guideline (OECD, 2013[95]), assesses the general teratogenicity of a compound to the developing zebrafish embryo between ±1.5 and ≤120 hpf. Thus, this assay was conducted to determine the 10 and 50% effect concentration (EC_{10} and EC_{50}, respectively), and endpoints were defined according to von Hellfeld *et al*., (2020) (Figure 9a)[96]. Medium samples at 120 hpf, as well as freshly prepared samples, were collected and frozen in liquid nitrogen, before being sent for compound analysis. 120 hpf embryos for all FET test replicates were collected, washed in control medium, and frozen in liquid nitrogen, before being sent for transcriptome analysis.

Following the FET test, the compounds were tested in two behavioral assays in order to determine the effect of the compounds on the early neuro-developmental stages. The coiling assay was conducted between 24 and 48 hpf (Figure 9b) as described in Zindler *et al*., 2019[97], and examines the phase during which random neuronal firing turns into a distinct side-to-side coiling action within the chorion, considered to being vital for hatching. This assay was followed with the basal swimming assay between 83 and 120 hpf (Figure 9c), as outlined in Zindler *et al.,* 2019[97]. A more detailed description of the methods, along with the statistical analysis of all zebrafish embryo data can be found in the ANNEX I : ZFE method.

Figure 9. The zebrafish embryo assays conducted between 0 and 120 hpf.
a: The FET test in accordance with the OECD TG 236. Semi-static exposure of the embryos for 120h, with full medium renewal every 24h.

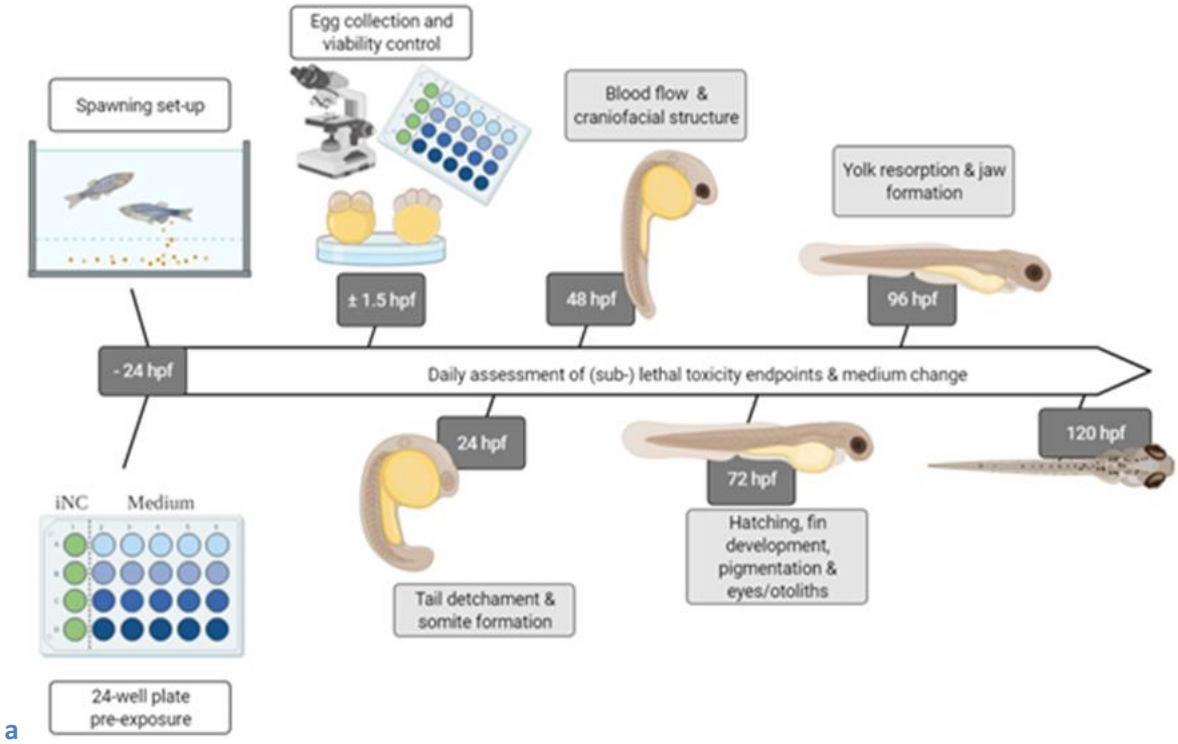

b: The coiling assay, with rearing conditions like the FET test, and video analysis of the burst frequency and duration between 24 and 48 hpf.

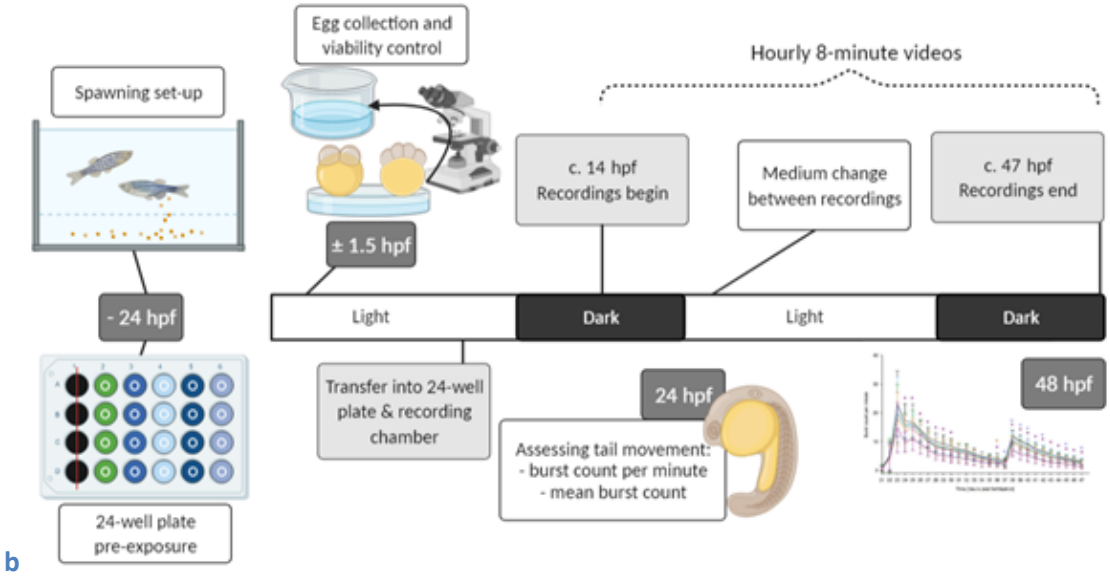

c: The basal swimming assay, with similar rearing conditions to the FET test until 72 hpf, followed by video analysis of the swimming duration and velocity between 82 and 120 hpf. The figure was adapted from von Hellfeld, (unpublished)

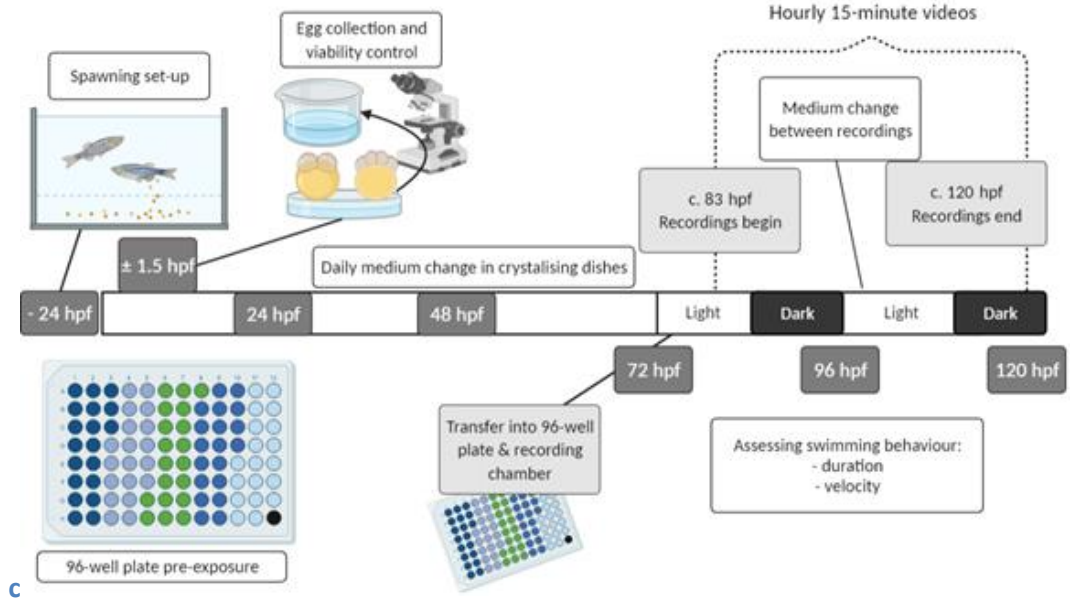

8.1.9 KE3: CALUX reporter gene assays

From the CALUX® (Biodetection Systems) battery of *in vitro* reporter gene assays a panel of 31 human cell-based assays was used, each able to measure chemical interactions between a test chemical and a

specific nuclear receptor or cell signaling pathway (Burg *et al.*, 2013[98]). Exposure to the test compounds, dissolved at 0.1 M in DMSO, was performed for 24 h and at 1% (v/v) according to the assay procedure as described in DB-ALM protocol 197 "Automated CALUX reporter gene assay procedure". The concentration range used was 0.1 nM – 0.1 mM in 0.5 Log unit increments. The analysis consisted of technical triplicates and was performed twice as independent biological replicates. Lowest effect concentrations (LOEC) were derived per assay based on the background responses (Figure 10). For nuclear receptor agonist assays, the LOEC was defined as the PC10 concentration in LogM, which is the concentration where the test compound causes an activation effect equal to 10% of the maximum effect elicited by the test's reference compound. For nuclear receptor antagonist assays, the LOEC was defined as the PC20 concentration, which is the concentration where the test compound causes an antagonist effect equal to 20% of the maximum antagonist effect elicited by the test's reference compound. For the stress pathway related assays which typically do not show sigmoidal dose-response curves, the LOEC was defined as the FI 1.5 concentration, which is the concentration where the test compound elicits pathway activation 1.5-fold above baseline.

Figure 10. Definition of LOECs for different assays within the CALUX panel.

A: nuclear receptor agonist assay; B: nuclear receptor antagonist assay; C: stress pathway assays (no sigmoidal dose-response).

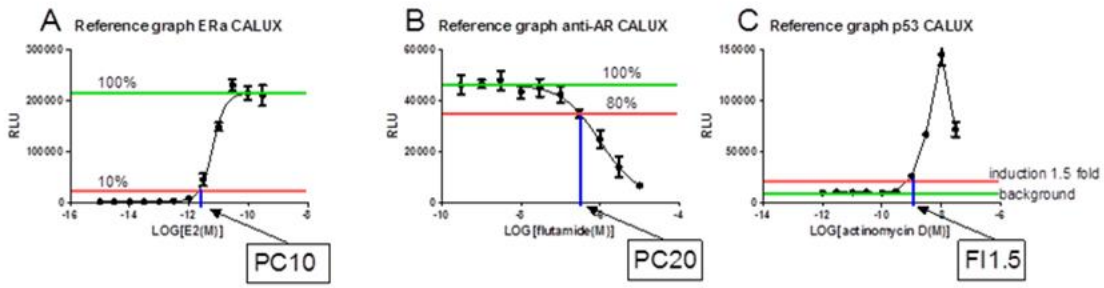

8.2 Methods to study KEs

8.2.1 KE1. Activation of nAChR

Nicotinic AChR activation can be studied by monitoring changes in intracellular free Ca^{2+} concentration $[Ca^{2+}]_i$ using fluorescent dyes that bind Ca^{2+} (see Figure 11).

Figure 11. Concentration-dependent effect of nicotine on the [Ca^{2+}]i of LUHMES neurons.

The exposure to nicotine stimulated fast and transient increases in [Ca^{2+}]i.

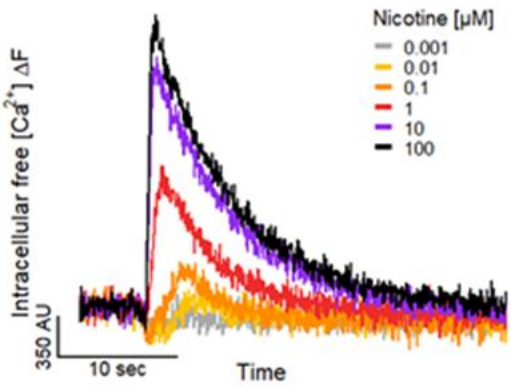

Ca^{2+}-imaging was performed using HT Functional Drug Screening System FDSS/µCELL (Hamamatsu Photonics) at nominal 37 °C. The FDSS/µCell system enables the indirect recording of changes of $[Ca^{2+}]_i$ via a Ca^{2+}-sensitive fluorescent dye. The fluorescence signal of a complete 384-well plate is acquired at once with a high-speed and high-sensitivity digital ImagEM X2 EM-CCD camera (Electron Multiplying Charge-Coupled Device, Hamamatsu Photonics), but with limited spatial resolution. Therefore, the software only determines the mean fluorescence signal of each well rather than of individual cells. Cells were pre-incubated with Cal-520 AM (AAT Bioquest) at a concentration of 1 µM for 1 h at 37 °C. For recording, the medium was exchanged by a buffer solution containing [mM]: 135 NaCl, 5 KCl, 0.2 $MgCl_2$, 2.5 $CaCl_2$, 10 HEPES, and 10 D-glucose, pH 7.4. Test compound application was executed after obtaining a 1.5 min baseline recording. Where applicable, a second application was executed 4.5 min after the first application. The total recording never exceeded 8 min.

Changes in $[Ca^{2+}]_i$ in SH-SY5Y cells were analyzed over time by measuring FURA-2AM fluorescence in a semi-high throughput screening (HTS) plate reader (FlexStation II, MolecularDevices). The area under the curve of the ratio in fluorescence between Ca^{2+}-bound FURA-2 (ex 340 nm, em 510 nm) and free FURA-2 (ex 380 nm, em 510 nm) was monitored during 150 seconds after acute addition of the compounds. In the majority of the experiments, the allosteric α7nAChR modulator PNU-120596 was used to prevent rapid desensitization and to favor measurement of Ca^{2+} influx induced by the same receptor subtype.

8.2.2 KE2. Inhibition nAChR function (desensitization)

The inhibitory effect on nAChR activity (i.e., inhibition of agonist-induced Ca^{2+} influx) was analyzed in LUHMES and SH-SY5Y cells in the presence of receptor specific allosteric modulators as described above after pre-exposure with the target compound and acute addition of receptor agonists.

8.2.3 KE3. Altered cellular phenotype

In order to assess if altered Ca^{2+} signaling results in an altered phenotype as a downstream consequence, which was supposed in the putative AOP, transcriptomic changes were analyzed. For this, iPSC TD42, neural crest cells, neural ectodermal precursors, SH-SY5Y and LUHMES cells were treated with nicotine and acetamiprid and analyzed using an RNA-sequencing method (TempO-Seq assay, by BioSpyder Technologies Inc.) (House *et al*., 2017[99]).

Other phenotypic alterations than gene expression profile was not investigated so far.

8.2.4 KE4. Altered neurodevelopment (neuronal differentiation, migration, axogenesis, synaptogenesis and brain area organization)

Viability – SH-SY5Y cells

The cell viability was determined in SH-SY5Y cells after 24 hours exposure with nicotine or acetamiprid by the conversion of resazurin to resorufin in metabolically active cells (O'Brien *et al,* 2000[100]). Resorufin fluorescence was measured at excitation 540 nm and at emission 590 nm using a FlexStation II fluorometer (Molecular Devices).

Viability - iPSCs TD42

At BIOT acute cytotoxicity assay is a medium throughput assay. Cells were seeded in 96-well plates with cell density 90.000 cells/cm^2. After 42 days, media was changed to 100 µl media containing the appropriate concentration of test compound. This TD42 assay is suitable to detect synaptic toxicity of compounds on mature neurons and neurotoxicity on astrocytes (see exposure scheme in Figure 12). The technical steps were provided in a Standard Operation Procedure (SOP) document (see DB-ALM Protocol No. 207).

Figure 12. Exposure scheme for acute (72 hours) toxicity treatment of TD42 differentiated neurons and astrocytes.

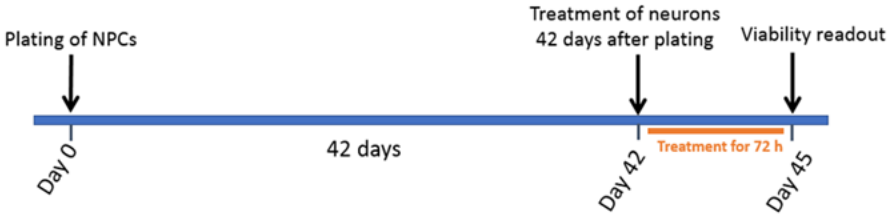

Cell viability is measured after 72 hours incubation time with the tested compounds by **ATP viability assay**. Endpoint values are the luminescent signals determined by the CellTiter-Glo® Luminescent Cell Viability Assay Kit (Promega, Cat. No. G7571).

Neurite outgrowth LUHMES cells (UKN4 assay)

LUHMES cells were differentiated for 2 days. On day 2 cells were reseeded and neurite outgrowth assay was performed as described earlier in detail by Krug *et al*., 2013[82] and Delp *et al.*, 2018[101]. Shortly, cells were treated with compounds for 24h and allowed grow out neurites. After 24h, cells were live stained with H-33342 and calcein-AM and neurite area were measured using a high content imaging microscope (Cellomics ArrayScanVTI). In parallel, viability of cells was measured quantifying amount of double positive in relation to total cell number (single positive cells) (See scheme of assay in Figure 13). Neurite area and viability are normalized vs 0.1% DMSO control. A normalization to cell number is not done as it was found in previous studies that the results do not differ.

Figure 13. The UKN4 neurite outgrowth assay using LUHMES cells.
A) Representative scheme of performance of the UKN4 method.
B) Algorithmic readout of d3 neurites, indicating an image typical for a solvent control (left) and a positive test compound (right) (Figure A from Loser *et al*. 2021[13], Figure B from Masjosthusman *et al,* 2020[9]).

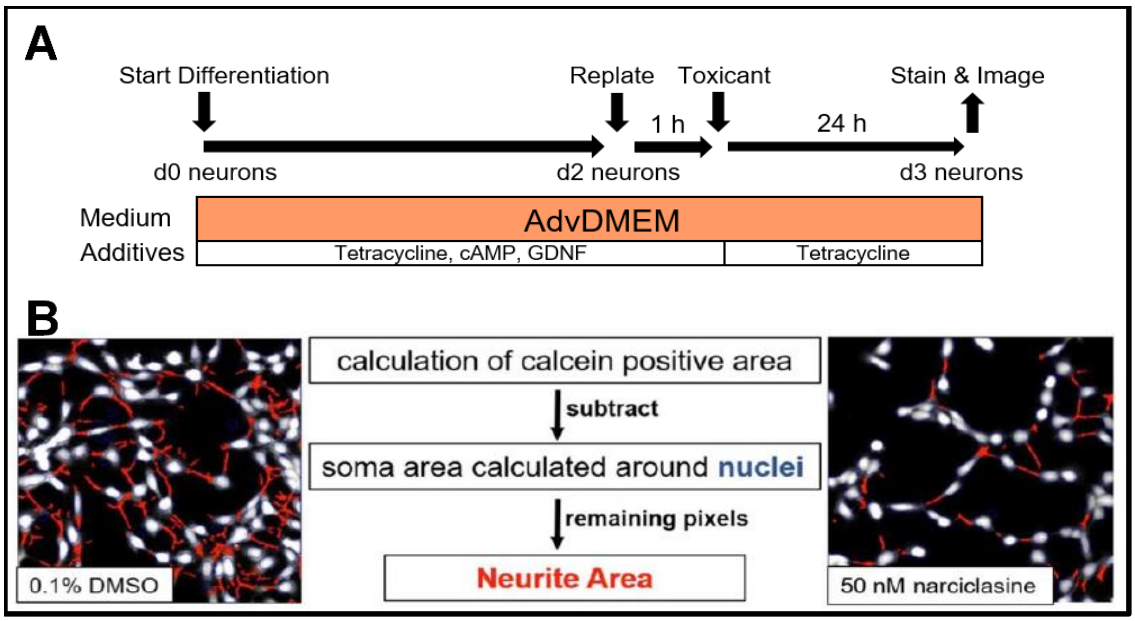

Neural crest cell migration (UKN2 assay)

NCCs were thawed and seeded for 4 days surrounding silicon stoppers in 96 well plates, as described in detail before by Nyffeler *et al.* 2017[102]. During their migration phase, cells were treated from day 3 to day 4 for 24 hours and live stained with H-33342 and calcein-AM and afterwards imaged using a high content imaging microscope (Cellomics ArrayScanVTI). A program designed for this purpose was used to assess the number of cells which successfully migrated into the previously cell free area (http://invitrotox.uni-konstanz.de/RA/) (see Figure 14 below).

Figure 14. The UKN2 migration assay using neural crest cells
A) Representative scheme of performance of the UKN2 method
B) Algorithmic readout of cells migrated into the region of interest (ROI) indicating an image typical for a solvent control (far left), a positive test compound (left) and assessment of viability (right) (from Masjosthusman *et al*., 2020[9])

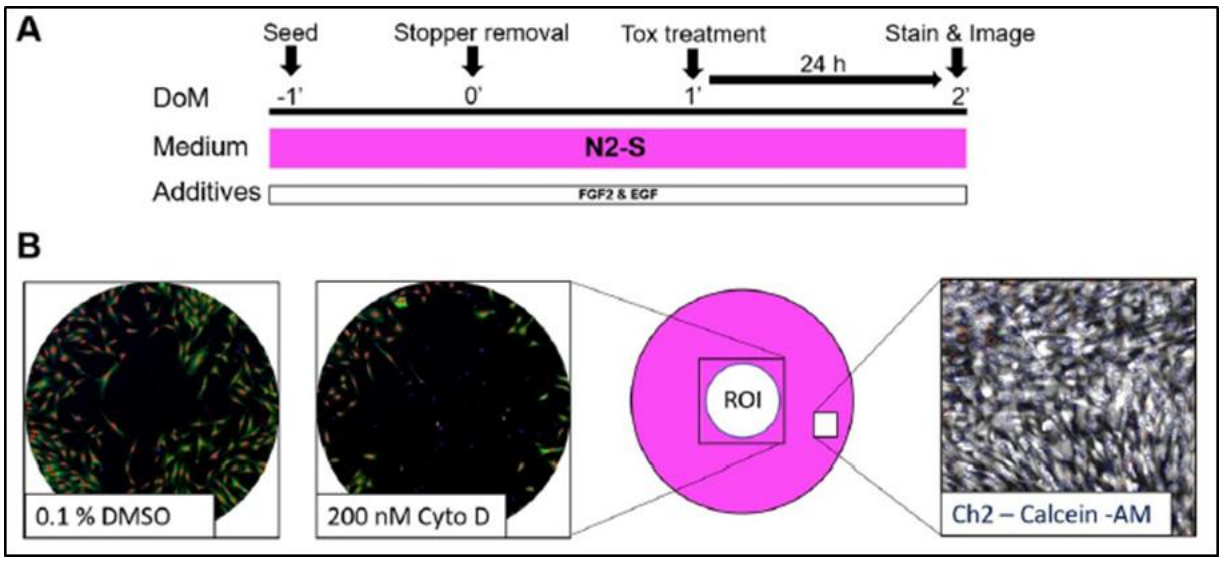

Neurite outgrowth sensory neurons (UKN5 assay)

Sensory neurons were thawed and seeded for 24h and exposed during this time to solvent or test compounds. Similar to the UKN4 test method (see above) cells were stained with H-33342 and calcein-AM to assess neurite area and viability in parallel. For detailed description of assay performance see Masjosthusman 2020[9].

NEP differentiation and rosette formation (UKN1 and RoFA)

Differentiation of hiPSC into NEPs and a rosette like phenotype was performed as described before by Dreser et al. 202092 with a shortened protocol as shown in Figure 15 below. Cells were treated for 96 hours with compounds and qPCR analysis was performed after 144 hours to assess correct differentiation into NEPs as an endpoint using marker genes (PAX6, OTX2). As a phenotypic endpoint, Rosette formation was assessed on day 12 via immunostaining as described earlier by Dreser et al. 202092.

Figure 15. Differentiation scheme of the UKN1 test method from hiPSCs into rosette like structures.

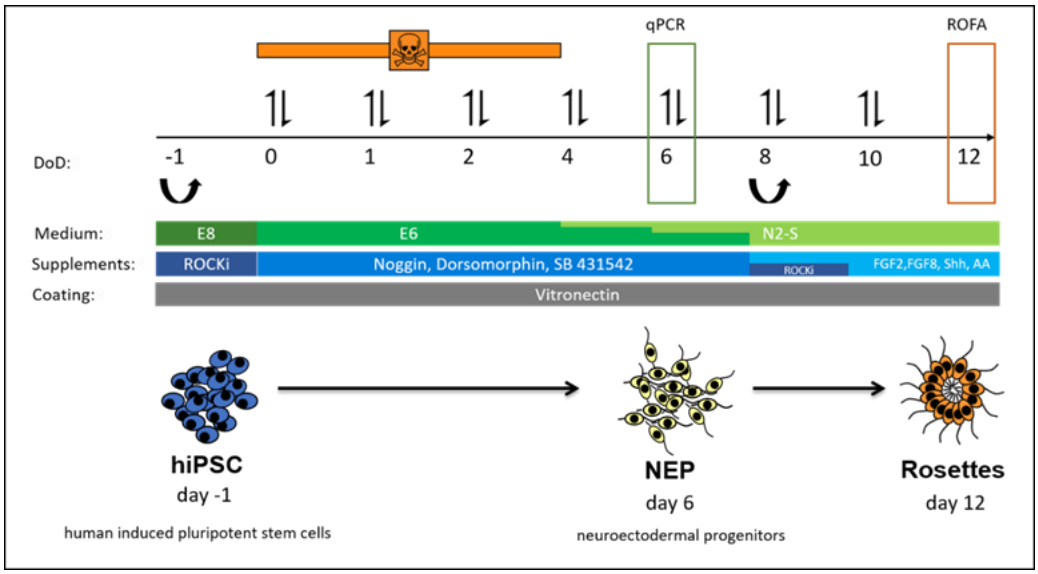

ZFE endpoints

FET test: Validity of a biological replicate was given, when no more than 10% of individuals in the negative control (untreated embryos) showed any developmental alterations, and at least 80% of the control group (and solvent control, where applicable) had hatched by 96 hpf. Moreover, validity was based on a minimum mortality of 30% in the 3,4-dichloroaniline (positive control) group (OECD, 2013).

Behavioral assays: Due to the nature of the assays, only solvent controls were utilized in the coiling and swimming assays. No morphological developmental alterations in the controls were observed, and the data analysis of the treated groups were normalized to the controls.

8.2.5 PBTK models

PBTK models for acetamiprid were constructed in the Simcyp Simulator V19 (Certara UK Ltd, Sheffield). To help with the parameterization of the PBTK models, metabolism of Acetamiprid in human hepatocytes and binding to human plasma and blood was measured *in vitro*. Unfortunately, the metabolism of Acetamiprid was below the limit of quantitation (LOQ) in the standard human hepatocyte suspension stability assay (LOQ ~ 3.86 µl/min/10^6 hepatocytes; Cyprotex unpublished observations) to reliably determine the hepatic intrinsic clearance *in vitro*. In the absence of a measured value for protein binding in the rat a value was calculated assuming the same equilibrium dissociation constant (K_d) for human and rat albumin taking into account differences in the level of serum albumin in rat and human plasma.

PBK models were constructed using full body models in both rat and human where each organ of the body is modelled as a separate compartment. Distribution to tissues was modelled assuming perfusion limited distribution with the tissue:plasma partition coefficients being predicted based on physicochemical data using the method described by (Rodgers and Rowland, 2006)[103]. The Kp scalar was adjusted in the rat to bring the predicted concentrations of acetamiprid in line with the observed concentrations for total radioactivity at early timepoints. The same Kp scalar was applied to simulations in human assuming a consistent underprediction of Kp values. The clearance of acetamiprid has not been determined in the rat after oral or intravenous dosing and so a clearance value was used in the simulations that leads to exposure of acetamiprid in the rat that is lower than the total radioactivity exposure at a dose of 1 mg/kg ^{14}C-acetamiprid. A sensitivity analysis is shown to illustrate the effect of changing the clearance of acetamiprid over a 100-fold range.

Oral absorption of acetamiprid in rat and human models was predicted using a permeability value predicted from an *in vitro* determined Papp value in Caco-2 cells together with the solubility of acetamiprid. Oral absorption was predicted using the advanced, dissolution, absorption and metabolism (ADAM) model within the Simcyp simulator (Jamei *et al*., 2009[104]).

The human clearance of Acetamiprid has not been defined. The clearance used in the human model was calculated using a clearance value in rat (0.7 ml/min) that gave exposure in line with the total radioactivity observed in rat plasma following oral dosing of ^{14}C-acetamiprid. The human clearance was allometrically scaled using a single species approach and an exponent of 0.75 (equation 1). This clearance was then partitioned into metabolic and renal CL with the renal CL defined as ~2.6% of the total CL based on the data in Harada *et al*., 2016[44]. The metabolic CL was arbitrarily split into metabolism by CYP 3A4 (~80%) resulting in formation of desmethyl acetamiprid and metabolism not forming the metabolite (~20%). All input parameters are listed in Table 6 below.

The N-desmethyl metabolite was also simulated in the human PBTK model. As for parent compound Vss and Kp values were predicted using the method described by Rodgers and Rowland. Clearance was calculated based on the half-life of renal excretion of desmethylacetamiprid observed in the study conducted by Harada *et al*., 2016[44] and the predicted volume of distribution. The split between renal and hepatic CL for the metabolite was calculated based on the calculated amount of acetamiprid ingested in the diet and the observed urinary excretion of desmethylacetamiprid in the study reported by Harada *et al*., 2016[44]. All input parameters for demethyl are listed in Table 7 below.

Table 6. Input parameters for the PBK model for Acetamiprid (rat and human).

Parameter	Value	Reference
Molecular Weight	222.7	Pubchem
Log P	0.8	Brunet et al.(2008)[41]
Compound Type	Neutral	
Blood:plasma ratio	0.951	Measured
Fraction unbound in plasma	0.719	Measured
Intestinal permeability		
Caco-2 cell A-B (papp)	26 x 10^{-6} cm/s	
Solubility	4.25 mg/mL	Pubchem
Distribution		
Vss	Predicted Rat 0.80 L/kg Human 0.69 L/kg Kp scalar 1.3	Rodgers and Rowland (2006)[103] Kp scalar use dto ensure that predicted concentrations in the rat were in line with measured concentrations of total radioactivity.
Brain Kp	0.5 rat (predicted 1.07) 1.2 Predicted (human)	Modified in rat to be in line with the measured data in mouse. Ford and Casida (2006)[42].
Clearance	Rat 1.3 ml/min 0.08 ml/min renal CL Human 0.082 L/h renal CL	5-7% excreted as unchanged drug Assumed that metabolism is by CYP 3A4 -allows metabolite formation to occur. Arbitrarily ~80% of the acetamiprid is metabolised to the desmethyl metabolite. Based on 2.6% excretion in human urine 2.6% excreted in urine. Harada et al.(2016)[44]

Table 7. Input parameters for the PBK model for N-desmethyl metabolite (human only).

Parameter	Value	Reference
Molecular Weight	209	Pubchem
Log P	1.3	Pubchem
Compound Type	Neutral	Assumed

Blood:plasma ratio	1	Assumed
Fraction unbound in plasma	0.719	Assumed same as parent
Distribution		
Vss	Predicted Human 1.11 L/kg Kp scalar 1.3	Rodgers and Rowland (2006)[103] Assumed the same as human
Clearance	Hepatic 0.201 µl/min/mg Renal 0.95 L/h	Split between hepatic and renal CL calculated using data from Harada *et al.*(2016)[44]

9 Results (link to publications/BioStudies files)

9.1 MIE. Binding to nAChR (docking experiments)

The main goal of docking and subsequent analyzing-methods such as clustering, in this study, are suggestions for structural explanations for differences in neonicotinoid activity on human nAChRs, that have been observed from cell experiments. Generally, the structures of the proteins and ligands of interest need to be prepared prior to the docking-procedure. Then we applied an induced fit docking protocol with extended sampling which is implemented in the software package of Schrödinger's Maestro (Schrödinger Release 2020-2, 2020). The poses of the ligands have been clustered according to their interaction fingerprints with the protein and have been compared with binding modes from co-crystallized neonicotinoids with homologous structures. Analogous to the acetylcholine binding protein (AChBP) complex from Lymnaea stagnalis (Ihara et al., 2014105), which is an established protein surrogate for mammalian nAChRs, the neonicotinoid Acetamiprid is adopting a binding mode similar to Thiacloprid. Both cyanoiminic molecules show poses in the human nAChR models that are similar to what has been reported for Thiacloprid, which was co-crystallized with AChBP. The electronegative cyano-groups are pointing towards loop C, which is an outstanding structural motif for both, nAChRs and AChBPs. Furthermore, the pyridine ring of co-crystallized nicotine is aligning with the same heteroarylic substructure in representative poses of Acetamiprid (Figure 16).

Figure 16. Binding of nicotine and acetamiprid to nAChR.
Nicotine (green carbon atoms, blue nitrogen atoms) has been co-crystallised in complex with human nAChR α4β2, superimposed with representative pose of Acetamiprid (orange carbon atoms); principal and complementary subunits of the binding site are indicated by blue and grey protein ribbons, respectively.

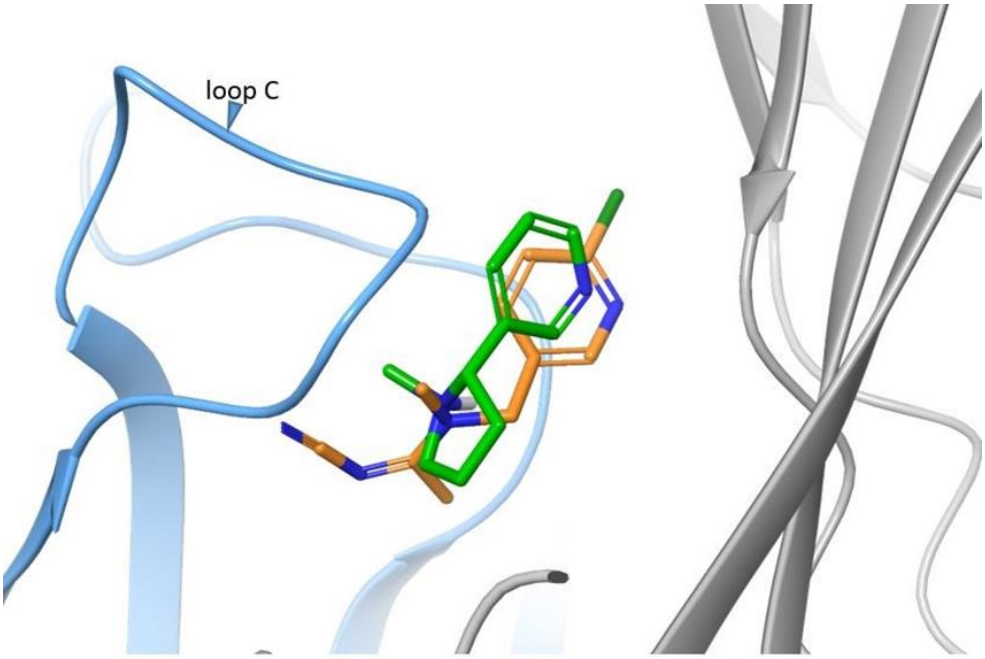

9.2 KE1. Activation nAChR

As previously stated, the α7 nAChRs are widely distributed in the nervous system and play a major role during neuronal development. In order to investigate the effect of acetamiprid on the α7 nAChRs and to avoid rapid desensitization, Ca^{2+} measurements were performed in the presence of the α7 nAChR allosteric modulator PNU-120596. Here we found that PNU significantly enhanced the responses to acetamiprid in both LUHMES and SH-SY5Y cells (Figure 17). These results indicate that acetamiprid activates human α7 nAChRs.

Figure 17. Acetamiprid activates α7 nAChR in LUHMES and SH-SY5Y cells.
A) Potentiation of acetamiprid (100 µM)-evoked $[Ca^{2+}]i$ responses of LUHMES neurons in the presence of 10 µM PNU-120596, a positive allosteric modulator of the α7 nAChR.
B) Acetamiprid and nicotine induces Ca^{2+} influx in the presence of the allosteric modulator PNU-120596 (10 µM) in SH-SY5Y cells
C) acetamiprid induced Ca^{2+} influx in SH-SY5Y neurons in the absence or presence of PNU. The results indicate that acetamiprid activates the α7 nAChR isoforms.

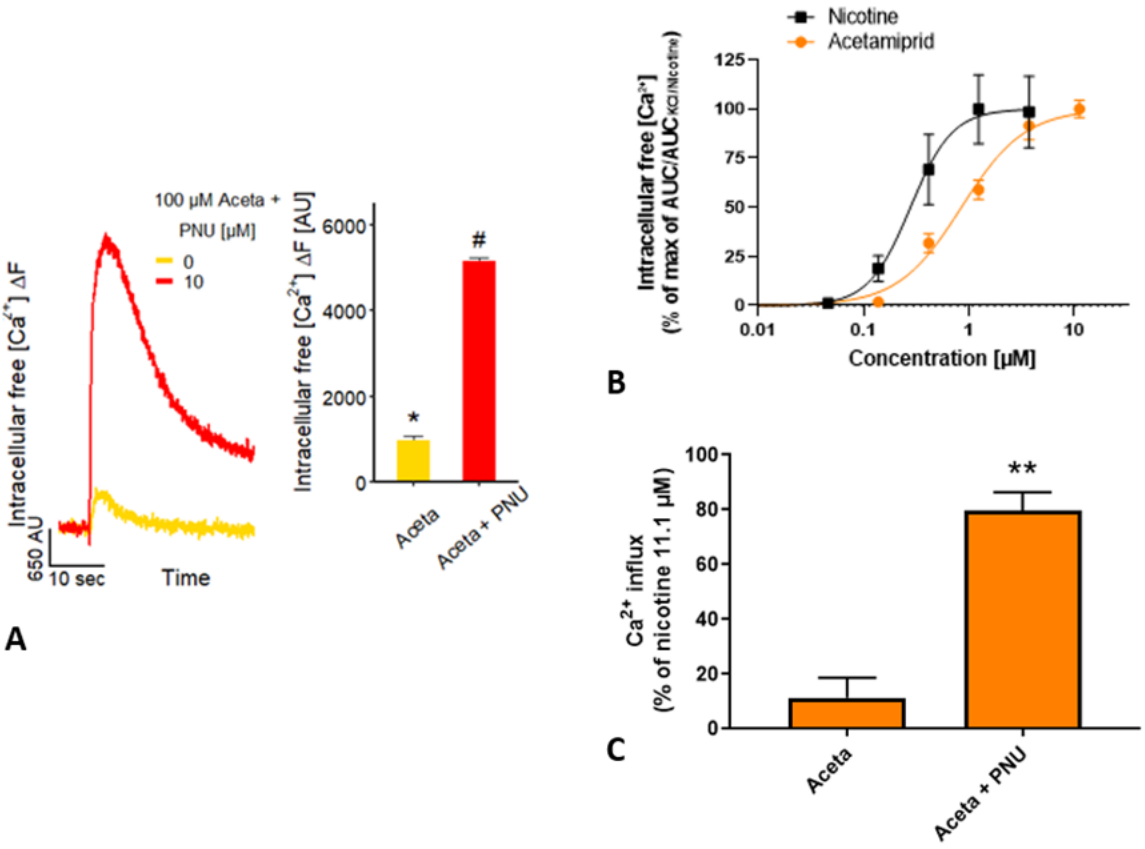

It is known for nAChRs that they can be desensitized, i.e. after a previous stimulus have an attenuated response. Therefore, the capability of acetamiprid to desensitize nAChRs after a successful stimulus as shown in 8.2 above was tested. We found that increasing concentrations of acetamiprid lead to decreasing calcium influx in LUHMES cells treated subsequently with nicotine (Figure 18A) with IC50 values at 5.40 and 10.17 for LUHMES and SH-SY5Y respectively. These effects were confirmed in SH-SY5Y cells as well (Figure 18B).

Figure 18. Desensitization of nAChRs in LUHMES and SH-SY5Y.
The pretreatment with Acetamiprid negatively modulates the $[Ca^{2+}]i$ responses of
A) LUHMES neurons triggered by the subsequent, acute exposure to nicotine (3 µM) or ACh (3 µM) and
B) SH-SY5Y neurons triggered by the subsequent, acute exposure to nicotine (11 µM). Experiments are performed in the presence of PNU.

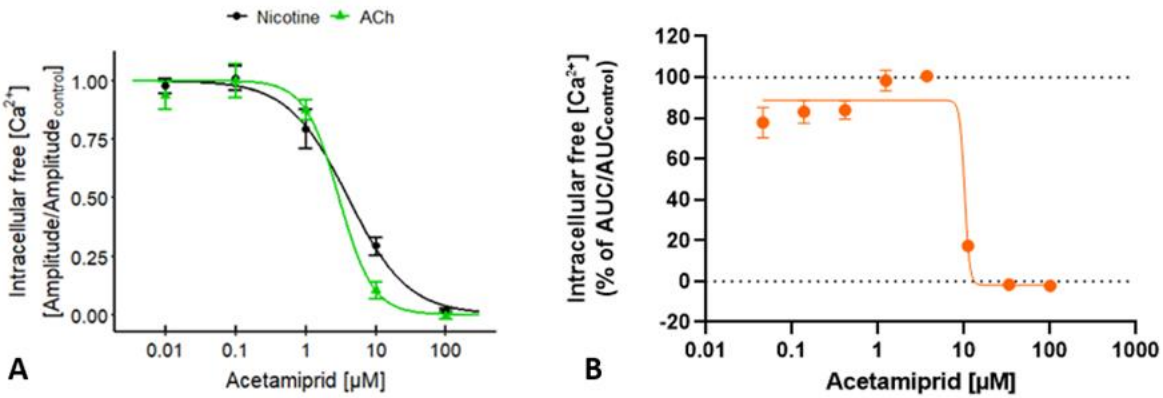

9.4 KE3. Altered cellular phenotype

Intracellular calcium signaling regulates several cellular processes and influences the regulation of gene expression. Therefore, it was of interest to study possible differential gene expression after acetamiprid exposure. After 6 or 24 hours of exposure to non-cytotoxic concentrations of acetamiprid, there were only few or no differentially expressed genes (DEGs) seen. The SH-SY5Y cells indicated few statistically significant DEGs after exposure that were of interest for neuronal development. But from further analysis it could be concluded that this probably was due to the dynamic differential phase the cells were exposed during. Thus, the low effects seen cannot confirm the hypothesis that nAchR activation by acetamiprid causes differential gene expression.

9.5 KE4. Altered neurodevelopment (neuronal differentiation, migration, axogenesis, synaptogenesis and brain area organization)

9.5.1Viability

Viability of SH-SY5Y

Neither acetamiprid (10 and 50 µM), nor nicotine (1, 5 and 10 µM) affected cell viability in SH-SY5Y cells after 24 h of exposure (Figure 19).

Figure 19. Acetamiprid does not affect cell viability after 24 hours of exposure SH-SY5Y cells.

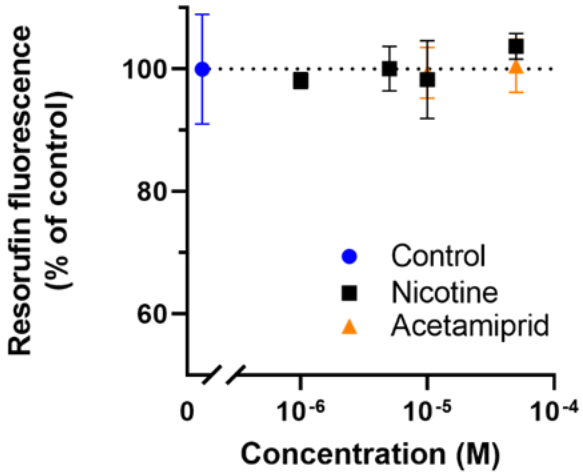

Viability of iPSC TD42

IPSC TD42 cells were exposed to nicotine and acetamiprid, neither of the compounds affected the cell viability after 72 hours (Figure 20).

Figure 20. Viability of 72 hours nicotine, acetamiprid, treatment in a concentration of 100 to 0.01 µM had no impact on TD42 neuron viability.

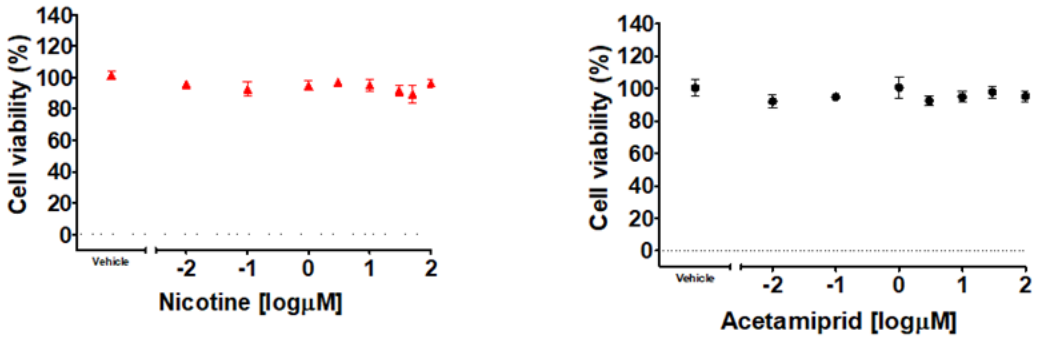

9.5.2 Neurite outgrowth, migration, differentiation and rosette formation

UKN4, UKN5 and UKN2 (Neurite outgrowth LUHMES and sensory neurons, NCC migration)

Cells were treated with concentrations of up to 100 µM. Viability of all 3 cells systems (LUHMES, sensory neurons, NCCs) was not affected with nicotine or acetamiprid (Figure 21 below, Nicotine for UKN2 and UKN5 not shown). The assay specific endpoints i.e., neurite outgrowth in two cell systems and migration of NCCs were also not affected, neither with nicotine nor with acetamiprid.

Figure 21. UKN battery results including endpoint specific and viability measurements.
A) Neurite outgrowth and viability in LUHMES cells for acetamiprid and nicotine
B) NCC migration and viability of cells treated with acetamiprid
C) neurite outgrowth and viability of sensory neurons treated with acetamiprid.

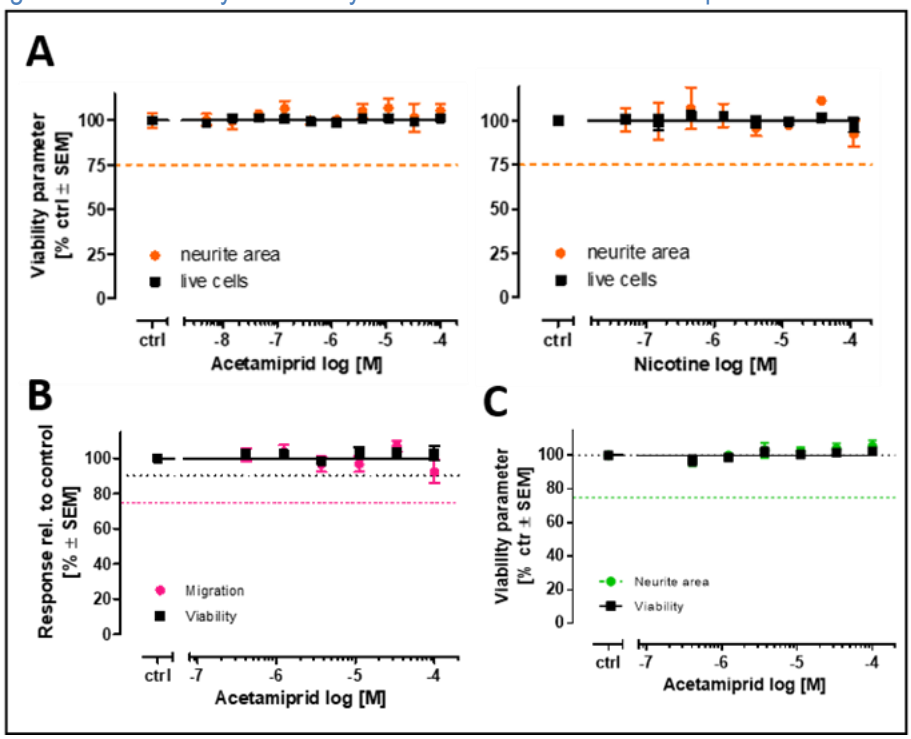

Full DNT *in vitro* battery screen

In addition to the UKN2, 4 and 5 assays, acetamiprid was also part of an extended DNT *in vitro* battery project screen (Masjosthusmann *et al.,* 2020[9]). Additional assays tested in this screening project are NPC1, NPC2, NPC3, NPC4 and NPC 5 (full method descriptions in report). It has to be considered that results from screenings should be handled with caution. Still, in all assays in this battery, acetamiprid showed no significant effect in any of the measured endpoints.

hiPSC differentiation into NEPs and rosette formation (UKN1 & RoFA)

Viability was not affected in day 6 differentiated neuroepithelial precursor (NEP) cells by Nicotine (10 µM) or Acetamiprid (100 µM) as seen in the plot to the left in Figure 22. Expression profile of NEP marker genes was not affected with 100 µM acetamiprid treatment during differentiation process (Figure 22, middle plot). During further differentiation acetamiprid treated NEPs were also capable of forming correct rosette like structures until day 12 of differentiation (Figure 22 right image).

Figure 22. Viability, NEP differentiation and rosette formation in acetamiprid treated hiPSCs.

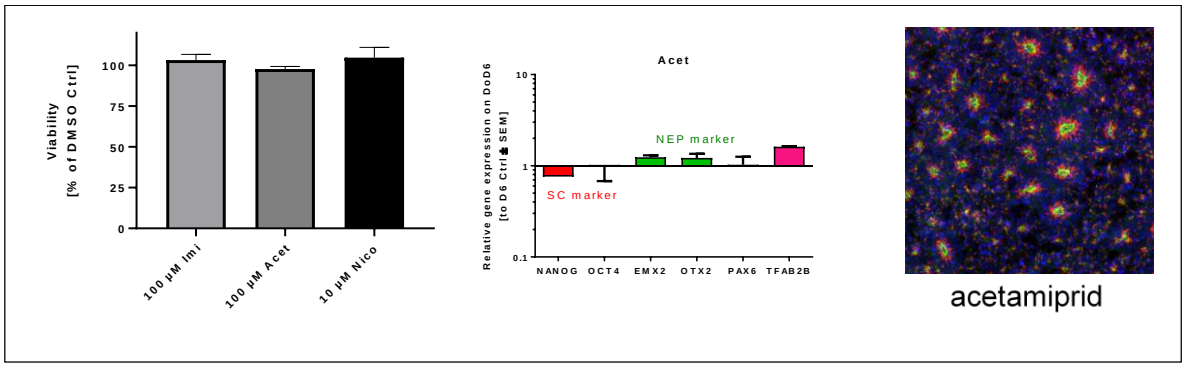

9.5.3 ZFE endpoints

FET test: None of the compounds induced mortality during the FET test duration of 120 hpf. Table 8 outlines the EC_{10} and EC_{50} values obtained at 96 and 120 hpf. At 96 hpf, the EC_{50} value for acetamiprid was based on only two biological replicates, as no effects were observed at this time point in the remaining replicate. Moreover, the 96 hpf EC_{50} value for acetamiprid exposure is greater than the highest nominal concentration of the FET test (100 µM) and is thus only and extrapolated value.

Table 8. Effect concentrations (EC) of 10 and 50% for nicotine or acetamiprid exposed zebrafish embryos as 96 and 120 hpf.
Values computed with ToxRat(R), given as mean (n=3), as outlined in the **ANNEX I : ZFE method**. The table was adapted from von Hellfeld et al., (unpublished)

	96 hpf		120 hpf	
Compound	**EC_{10}**	**EC_{50}**	**EC_{10}**	**EC_{50}**
Acetamiprid	13.7	195 *	0.3	63.8
Nicotine	22.0	44.7	6.1	23.5

*: The computed value is based on two biological replicates (no effects were observed in the remaining replicate)

The observed developmental alterations in the FET test are listed in Table 9. Both compounds reduced the early spontaneous movement at 24 hpf, whilst nicotine was found to increase this parameter at exposure concentrations ≤ 12.5 µM. At 48 hpf, both compounds affected pigmentation, but nicotine failed to induce any further endpoints. An increasing number of endpoints were observed from 72 hpf onwards, with nicotine inducing more adverse effects than acetamiprid. At 96 and 120 hpf, nicotine and acetamiprid affected the overall development (body length, craniofacial formation, and spinal cord), as well affecting the behavior at 120 hpf. Acetamiprid was the only compound to induce an enlarged pericardial area from 72 hpf onwards, whilst nicotine was found to be the only compound to reduce yolk resorption from 96 hpf onwards, as well as inducing tremors at 120 hpf.

Table 9. All observed endpoints in the FET test, induced by nicotine (N) and acetamiprid (A).
The table was adapted from von Hellfeld et al., (unpublished)

Endpoint	**Developmental time-point [hpf]**				
	24	**48**	**72**	**96**	**120**
Spontaneous movement (-, =)	A, N				
Spontaneous movement (+)	N				
Delayed hatching			A, N	N	

Heartbeat (-, =, x)		A		A	N
Blood flow (-, =, x)		A			N
Spinal deformation (K, L)			A, N	A, N	A, N
Reduced body length			N	A, N	A, N
Edema			N	A, N	N
Otolith deformation					N
Pigmentation (-, =, x)		A, N	A, N	A, N	
Enlarged pericardial area		A	A	A	
Craniofacial deformation			N	A, N	A, N
Reduced yolk resorption				N	N
Tremor/Twitching					N
Increased late activity					A, N

Grey box: The respective endpoint cannot be observed at the given time point due to its link to a certain developmental stage.

Coiling assay: Both compounds induced behavioral changes in the coiling assay (Figure 23 and Figure 24). Nicotine exposed embryos showed a delayed coiling onset, with the concentration dependent decrease of the mean burst duration (Figure 24A). Prior to the light cycle change at 37 hpf, all exposure concentrations >1.25 µM induced significant alterations. After the onset of the second dark phase (37.5 hpf), all exposure concentrations induced a significant reduction in mean burst duration. A clear concentration dependent decrease can be seen more clearly in the normalized data (Figure 23B). The burst count per minute was also impaired by nicotine exposure (Figure 23C), where the 25 µM treatment group expressed an immediate lack of burst initiations, whilst the remaining groups showed a concentration-dependent delay in the early burst count peak (±24 hpf), as well as increasing the second peak around 37 hpf. The normalized data further outlines this behavior (Figure 23D).

Figure 23. The effects of nicotine on the early behavior of zebrafish embryos during the light/dark cycles of the coiling assay.
The mean burst duration [seconds]
(A) and normalized burst duration
(B), as well as the mean burst count per minute
(C) and normalized burst count
(D) between 21 and 47 hpf after exposure to various nicotine concentrations (n=3, 20 embryos per concentration/replicate).
Data regimes in A and C given as mean ± standard deviation. Normalized data in B and D was adjusted to the 0.1% DMSO treated solvent control group. Sections in the top bar indicate the phases of the illumination cycle. *: time point and concentration (in corresponding color) of significant difference to solvent control, a table of all significant p-values can be found in **ANNEX I : ZFE method**. The figure was adapted from von Hellfeld *et al*., (unpublished)

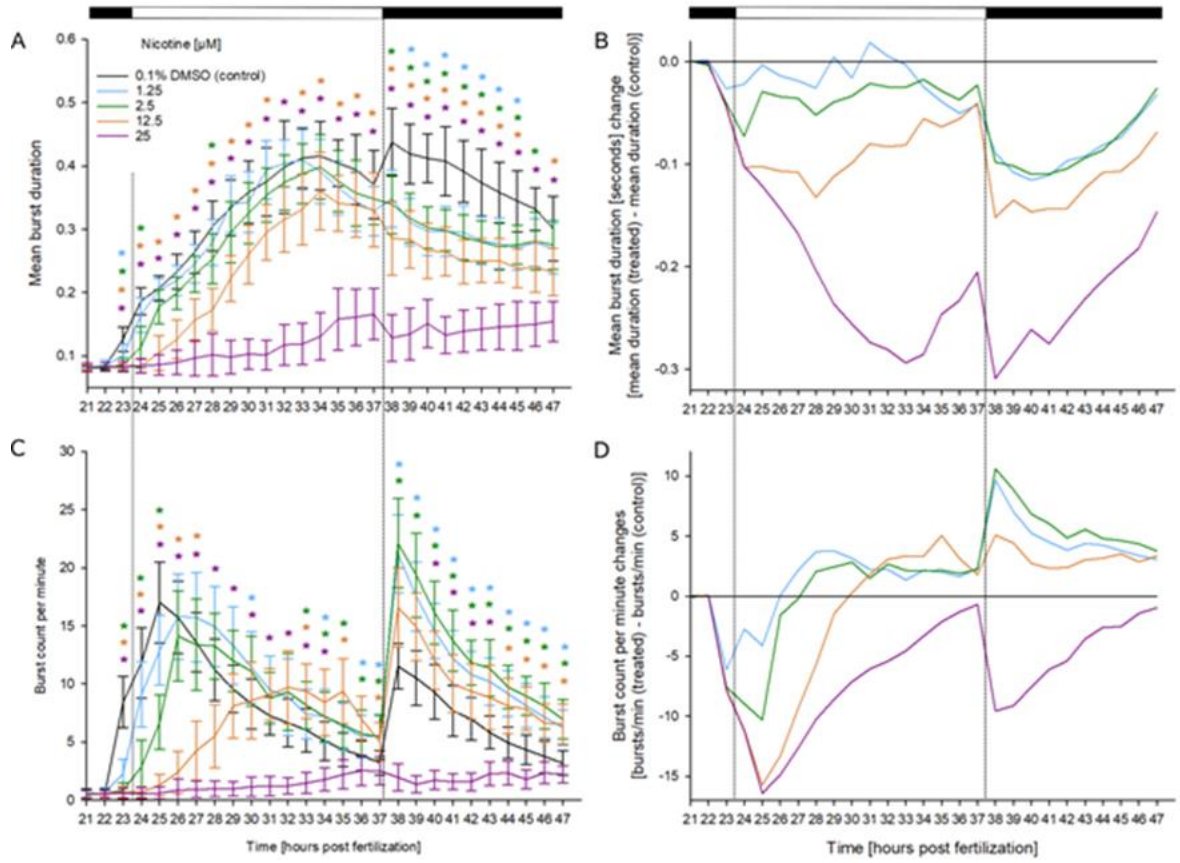

Exposure to 100 µM acetamiprid induced a significant reduction in the mean burst duration observed at 23 and 24 hpf, indicating a mild response to the onset of light (Figure 24A). In the replicate conducted until 47 hpf, a concentration dependent reduction in burst duration was further observed post-37 hpf. The hyperactivity followed by hypoactivity, induced by acetamiprid can further be seen more easily in the normalized representation (Figure 24B). The effect of acetamiprid exposure on the burst count per minute was less continuous, however, the same significance at 23 and 24 hpf could be observed (Figure 24C and D). Furthermore, from 38 hpf onwards (n=1) exposure to 25 and 50 µM induced a significant increase in burst count (hyperactivity).

Figure 24. The effects of acetamiprid on the early behavior of zebrafish embryos during the light/dark cycles of the coiling assay.
The mean burst duration [seconds]
(A) and normalized burst duration
(B), as well as the mean burst count per minute
(C) and normalized burst count
(D) between 21 and 47 hpf after exposure to various acetamiprid concentrations (n=4 until 37 hpf and n=1 post-37 hpf; 20 embryos per concentration/replicate).
Data regimes in A and C given as mean ± standard deviation. Normalized data in B and D was adjusted to the 0.1% DMSO treated solvent control group. Sections in the top bar indicate the phases of the illumination cycle. *: time point and concentration (in corresponding color) of significant difference to solvent control, a table of all significant p-values can be found in the **ANNEX I : ZFE method**. The figure was adapted from von Hellfeld *et al*., (unpublished)

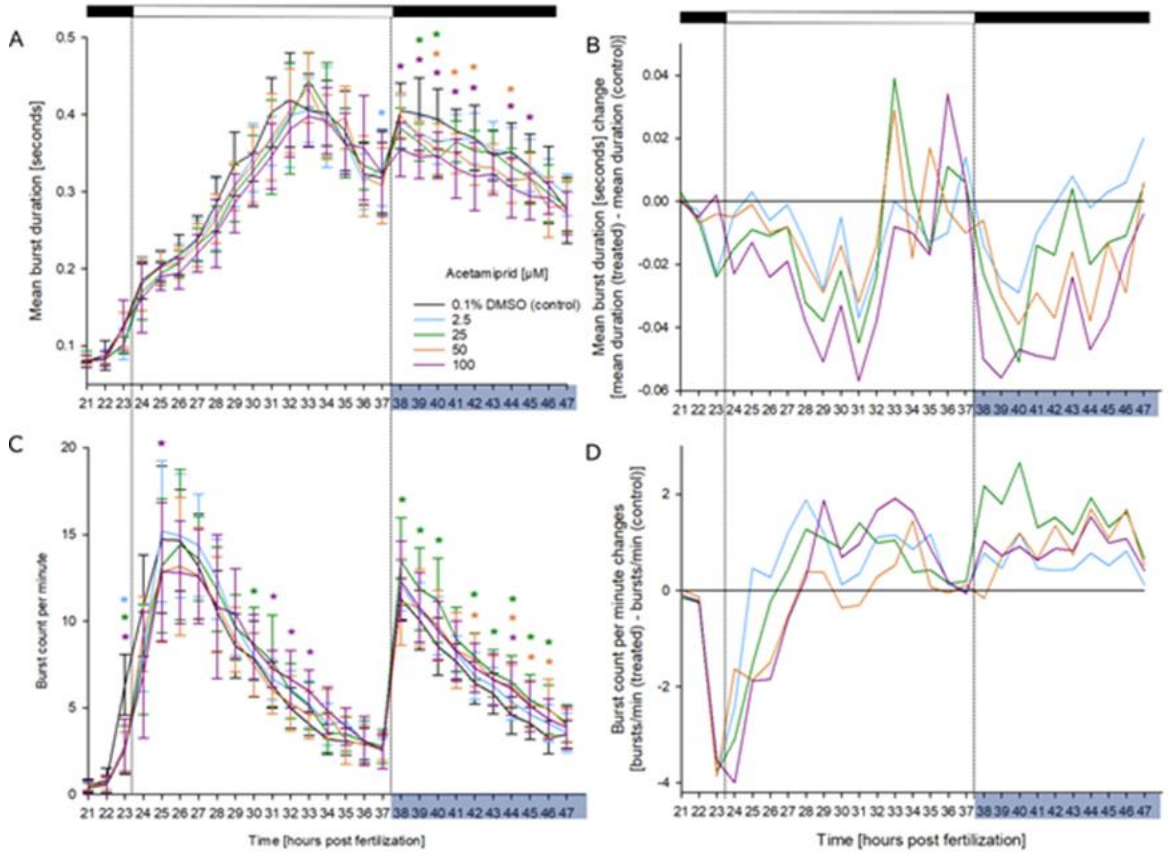

Basal swimming assay: Both compounds were found to have mild effects on the swimming behavior of the 83 to 120 hpf old zebrafish embryos. In the nicotine exposed individuals this effect was found to be non-significant, showing a trend to increase distance moved (Figure 25A and B) whilst initially reducing the movement frequency (Figure 25C and D).

Figure 25. The effects of nicotine on the later behavior of zebrafish embryos during the light/dark cycles of the basal swimming assay.
The grouped total distance moved [mm]
(A) and normalized grouped distance moved
(B), as well as grouped frequency of movement [n/15min]
(C) and normalized grouped frequency moved
(D) between 83 and 120 hpf after exposure to various concentrations of acetamiprid (n=3, 19 embryos per concentration/replicate).
Data regimes in A and C given as mean ± standard deviation. Normalized data in B and D were adjusted to the 0.1% DMSO treated solvent control group. Sections in the top bar indicate the phases of the illumination cycle. The figure was adapted from von Hellfeld *et al*., (unpublished).

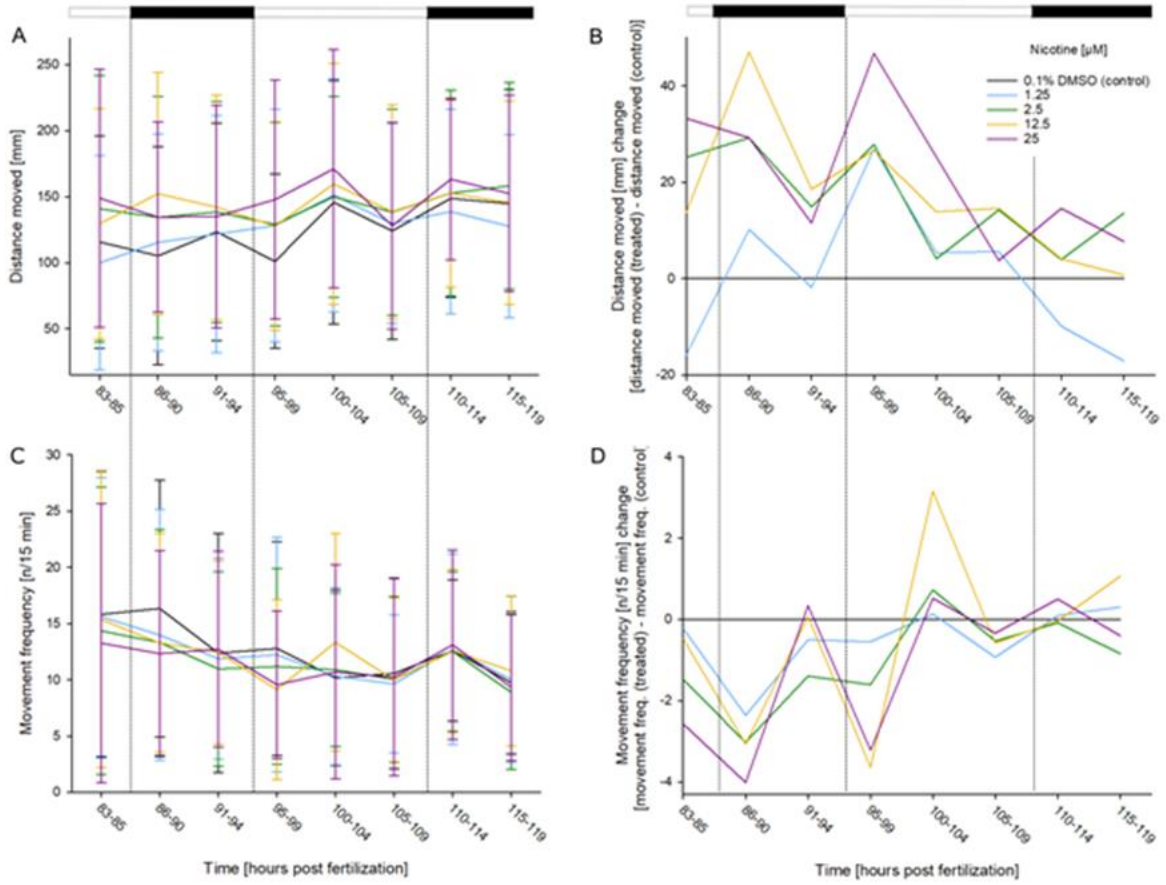

Individuals exposed to ≥50 µM acetamiprid exhibited a reduction in total distance moved compared to the control group, whilst those exposed to ≤25 µM initially exhibited increased distance moved (Figure 26A). The normalized data further outlines this trend, with only the 2.5 µM treatment group exhibiting an increased distance moved throughout the basal swimming assay (Figure 26B). The movement frequency was affected in a similar manner, where the ≤25 µM treatment groups showed decreased movement frequency throughout the basal swimming assay, whilst ≥50 µM treatment induced movement frequencies similar to the control group, or slightly elevated (Figure 26C). This can be seen in greater detail in the normalized data graph (Figure 26D).

Figure 26. The effects of acetamiprid on the later behavior of zebrafish (Danio rerio) embryos during the light/dark cycles of the basal swimming assay.
The grouped total distance moved [mm]
(A) and normalized grouped distance moved
(B), as well as grouped frequency of movement [n/15min]
(C) and normalized grouped frequency moved
(D) between 83 and 120 hpf after exposure to various concentrations of acetamiprid (n=2, 19 embryos per concentration/replicate).
Data regimes in A and C given as mean ± standard deviation. Normalized data in B and D were adjusted to the 0.1% DMSO treated solvent control group. Sections in the top bar indicate the phases of the illumination cycle. *: time point and concentration (in corresponding color) of significant difference to solvent control, a table of all significant p-values can be found in the **ANNEX I : ZFE method**. The figure was adapted from von Hellfeld *et al*., (unpublished)

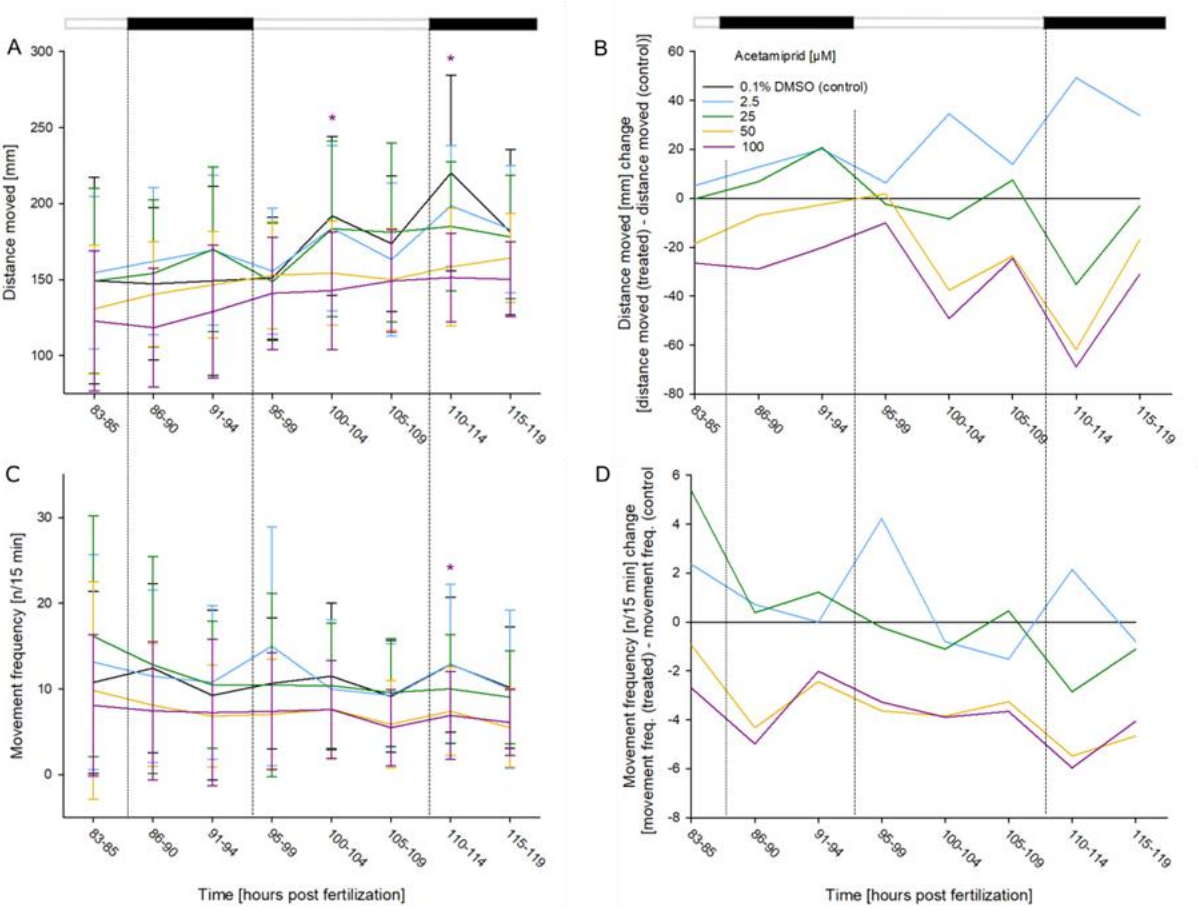

The relevance of these assays to the determination of DNT endpoints have previously been proven. Previous work has shown the strength of the zebrafish embryo as DNT model overall (Bailey *et al*., 2013[106]; De Esch *et al*., 2012[107]; Nishimura *et al*., 2015[108]; Tierney *et al*., 2011[109]) highlighting applicability beyond the FET test. Whilst early locomotor assays, such as the coiling and the swimming assay, have been utilized frequently, the zebrafish has also lent itself to the assessment of other DNT aspects, such as learning and memory (De Esch *et al*., 2012[107]), as identical neurochemicals are involved in the vertebrate learning processes, which includes the zebrafish (Wang *et al*., 2018[30]). Moreover, the assessment of thigmotaxis (wall-hugging behavior) has been used as an indicator for anxiety (Gerlai, 2010[110]; Maximino *et al*., 2010[111]) and has been seen in response to sudden light changes (Schnörr et al., 2012)[112]. Social behavior is another endpoint that can be observed in DNT studies conducted with zebrafish, examining

shoaling patterns (Saverino and Gerlai, 2008[113]; Seibt *et al.,* 2011[114]; Riehl *et al*., 2011[115]; Grossman *et al*., 2010[116] ; Xia *et al.,* 2010[117]) among others.

The locomotor behavior begins with the simple spontaneous coiling behavior around 17 hpf (Saint-Amant and Drapeau, 1998[118]), and is derived from a single neural circuit in the spinal cord (Saint-Amant and Drapeau, 2000[119]). The coiling assay lends itself to the assessment of early DNT, as an effect on the developing neural circuit is directly observable in the coiling behavior. The assay has been accepted as DNT-determining (Zindler *et al*., 2019[97]; Zindler *et al*., 2019[120]; Zindler *et al*., 2020[121]; Selderslaghs *et al.,* 2013[122]; Selderslaghs *et al.,* 2010[123]; Weichert *et al.*, 2017[124]; Velki *et al*., 2017[125]). The swimming assay has been applied in different settings, examining the moved distance or speed, and in some cases turning rates or angle sharpness of the turns, as well as the response the changing light conditions after compound exposure (De Esch *et al*., 2012[107]). This behavior is now based on a fully developed neural system, and with the inflation of the swim bladder, normal “beat and glide” swimming can be observed in healthy zebrafish embryos (Kalueff *et al.,* 2013[126]). A disruption of this behavior through compound exposure, can be seen in response to e.g., light cycle changes, basal swimming patter alterations, or an external stimulus. The assay has been accepted as DNT-determining (Zindler *et al*., 2020[121]; Peng *et al*., 2016[127]; Ganzen *et al*., 2017[128]; Steele *et al*., 2018[129]; Basnet *et al*., 2019[130].

9.6 CALUX reporter gene assay results

Acetamiprid was analyzed on a full CALUX panel, consisting of assays detecting agonism or antagonism on nuclear receptors (ERα, AR, GR, PR, TRβ, LXR, PXR, PPARgamma, PPARdelta, RAR (agonism only), PPARα (agonism only) and AhR (agonism only)). The panel also contained several assays detecting activation of stress pathways (Hif1α, AP-1, ESRE, NFkB, Nrf2, p21, p53, TCF (incl inhibition)) and a cytotoxicity assay. Acetamiprid showed slight cytotoxicity at 0.6 mM, but did not activate any of the nuclear receptors or stress pathways up to the highest tested concentration (not shown).

9.7 PBTK models outputs

Due to the paucity of the data available to construct the PBTK models for acetamiprid and its desmethyl metabolite there is significant uncertainty in many of the parameters used within the PBK model. In the rat available concentration data included data on total radioactive concentrations following dosing of a 1 mg/kg dose to rats. The maximal concentrations of acetamiprid that can be achieved in the rat are the measured radioactivity concentrations but as acetamiprid is extensively metabolized it is likely that the concentrations of acetamiprid are lower than those of total radioactivity particularly at later timepoints. The simulated concentrations of acetamiprid after an oral dose of 1 mg/kg to rats is shown in Figure 27. The predicted absorption (fa=1) of acetamiprid in the rat is in line with experimental data.

Sensitivity analysis showed that decreasing the clearance of acetamiprid by a factor of 2 or increasing it by a factor of 10 both gave results that are consistent with observed data (Figure 28). Further decreasing the clearance of acetamiprid within the model resulted in concentrations that were higher than the observed total radioactivity seen in rat plasma following an oral dose. This is illustrated in Figure 28 with a simulation where the clearance was decreased 10-fold. Using this approach, a lower limit for clearance of acetamiprid in rat can be estimated but it is not possible to say which value higher than this is the correct one.

Figure 27. Simulated (green line) concentrations of acetamiprid in plasma following an oral dose of 1 mg/kg to male rats.

Observed data (orange and grey dots) are for total radioactivity after administration of 1 mg/kg doses of 14C-acetamiprid labelled on the ring (orange) or CN group (grey). Data is taken from the RAR_08 document Table B.6.1.1.1-1, EC 2015[134]. Panel B shows the data with the y-axis on a Logarithmic scale.

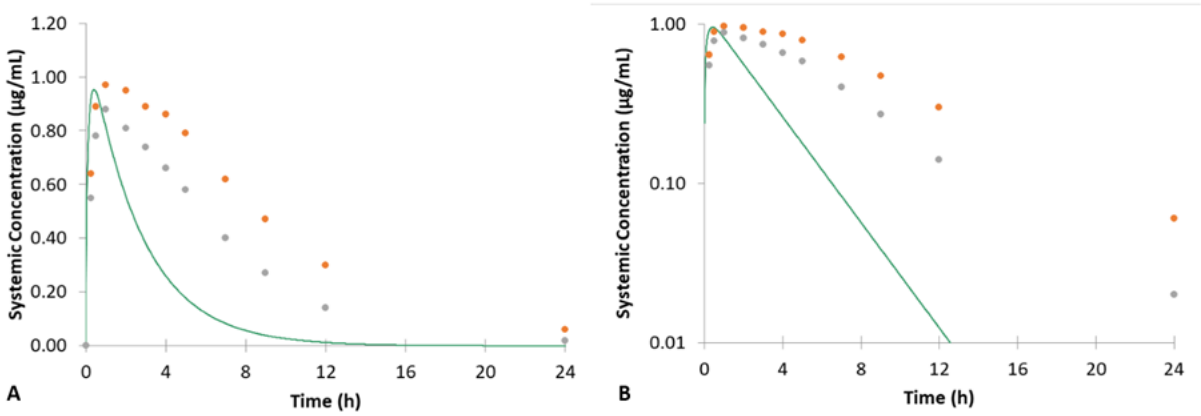

Figure 28. Sensitivity analysis showing the effect of changing clearance on plasma concentrations of Acetamiprid following an oral dose of 1 mg/kg to male rats.

Clearance was the same as in **Figure 27** and **Table 6** (green line) or decreased by a factor of 2 (blue) or 10 (black) or increased by a factor of 10 (red). Observed data (orange and grey dots) are for total radioactivity after administration of 1 mg/kg doses of 14C-acetamiprid labelled on the ring (orange) or CN group (grey). Data is taken from the RAR_08 document Table B.6.1.1.1-1. Panel B shows the data with the y-axis on a Logarithmic scale.

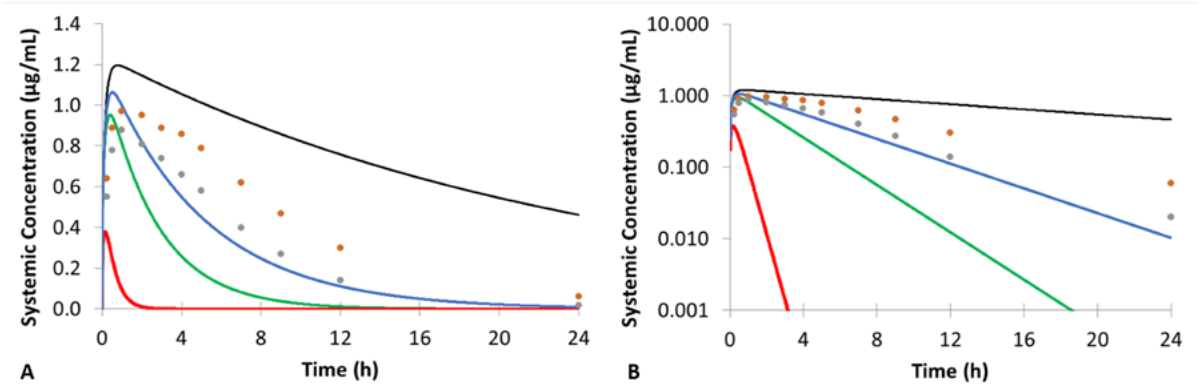

The simulated levels of acetamiprid and the desmethyl metabolite following an oral dose of 5 µg acetamiprid in human plasma (Figure 29) and the cumulative urine excretion (Figure 30 and Figure 31) are shown below. Although part of the metabolism of acetamiprid in the human PBK model was assigned to CYP3A4 an enzyme known to be expressed in the intestine the low rates of metabolism assigned to the enzyme result in 98% of the absorbed drug escaping from first pass metabolism in the gut (Fg = 0.98) and as such the compound is predicted to have high bioavailability >90% after oral dosing in humans.

Figure 29. Simulated mean plasma concentration of acetamiprid (green) and the desmethylmetabolite (orange) in humans after an oral dose of 5 μg acetamiprid.
Simulations were conducted in 100 North European Caucasian subjects (aged 20-50; 50% female).

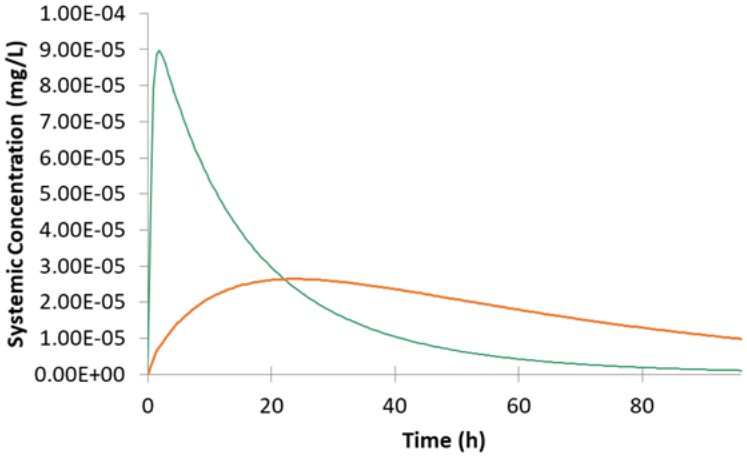

Figure 30. Simulated cumulative urinary excretion of
(A) acetamiprid and
(B) the desmethylmetabolite in humans after an oral dose of 5 μg acetamiprid.
Simulations were conducted in 100 North European Caucasian subjects (aged 20-50; 50% female). The green line represents the mean simulated cumulative renal excretion and the dashed black lines the 5th and 95th percentile of the population. The orange squares in panel B represent the observed data from Harada *et al*.[44].

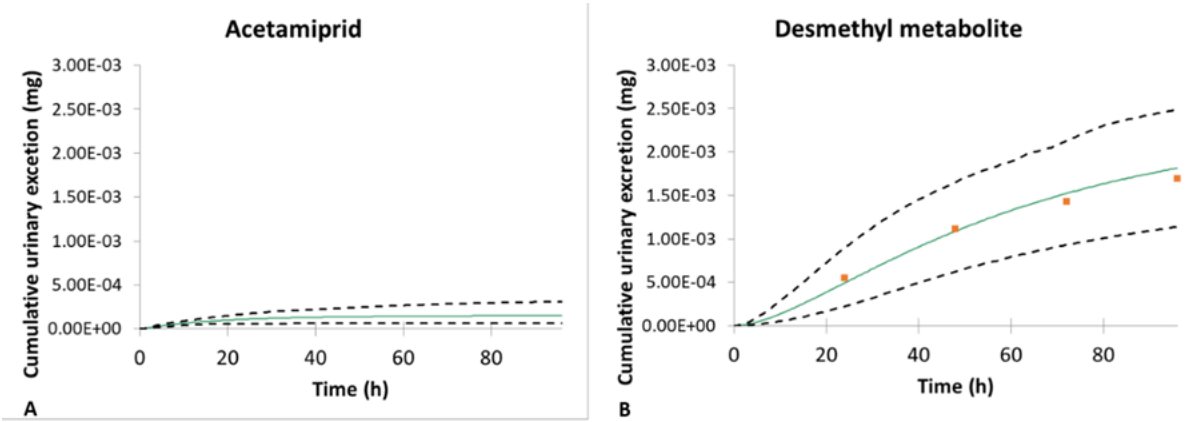

Figure 31. Simulated mean cumulative urinary excretion of the desmethyl metabolite in humans after an oral dose of 5 μg acetamiprid.

Simulations were conducted in 100 North European Caucasian subjects (aged 20-50; 50% female) (green line) and in 100 Japanese subjects (aged 20-50; 50% female) (grey line). The orange squares represent the observed data from Harada *et al.*(2016)[44].

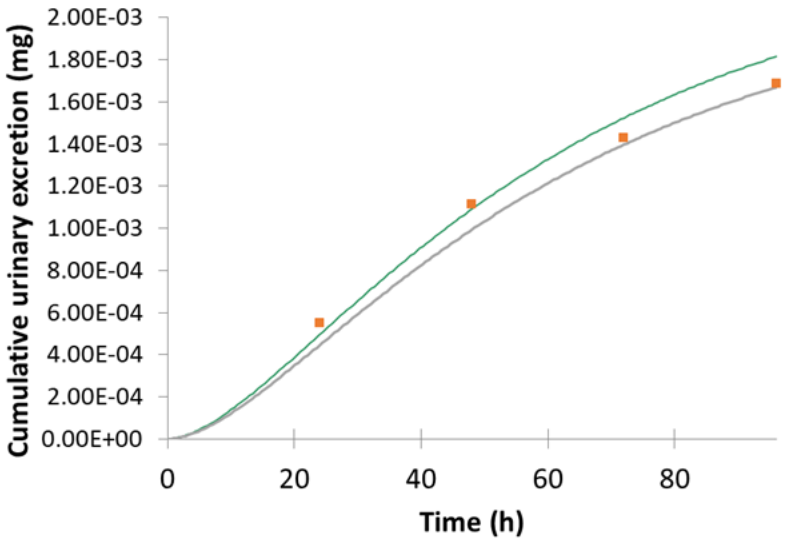

As there is not much data to verify the PBTK model the effect of changing the clearance of acetamiprid on the simulated renal excretion of the desmethyl metabolite was investigated. Simulations were conducted in a population of 100 Japanese subjects (aged 20-50; 50% female) (Figure 32). Changing clearance of acetamiprid over a 100-fold range results in changes in the simulated plasma concentrations of acetamiprid (Figure 32A) with higher concentrations at lower clearances. Increasing the clearance leads to an earlier maximum plasma concentration for the metabolite while decreasing clearance leads to a later time for maximum concentration and lower maximal concentrations of the metabolite. Compared to the observed renal excretion of the metabolite making the clearance of acetamiprid higher has a minimal impact on the time course of metabolite renal excretion as the elimination is mainly controlled by the intrinsic properties within the metabolite PBK model (Figure 32C). Lower clearances of acetamiprid lead to an underprediction of the renal excretion of desmethyl metabolite and suggest that while it is possible that the clearance of acetamiprid is faster than the values used in the base model (Table 7) it is less likely to be significantly slower as this would lead to the renal excretion of the metabolite being inconsistent with the observed data.

Figure 32. Simulated mean plasma concentrations of
(A) acetamiprid and
(B) desmethylacetamiprid and
(C) cumulative renal excretion of desmethylacetamiprid in humans after an oral dose of 5 μg acetamiprid.

Simulations were conducted in 100 Japanese subjects (aged 20-50; 50% female). The green line represents the simulation with the baseline clearance value for acetamiprid and the blue line is a 10-fold decrease in clearance and the black line a 10-fold increase in clearance. No alterations were made to the PBTK model of desmethylacetamiprid. The orange squares represent the observed data from *Harada et al.*[44].

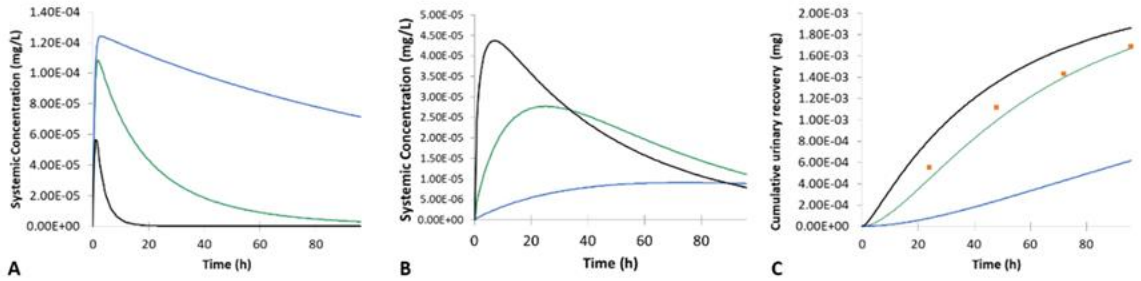

Simulations using the Acetamiprid PBTK model

As the metabolite of acetamiprid is not of toxicological concern simulations in different scenarios only show the data for parent acetamiprid. To make it easier to put the concentrations in context with the *in vitro* data concentrations are reported in μM or nM concentration units.

The simulated exposure in rats doses with 1 or 50 mg/kg/day Acetamiprid is shown in Figure 33. The maximal concentrations are in the low to mid μM range dependent on dose. Besides the effect of solubility there are no non-linear mechanisms eg saturation of clearance accounted for within the PBTK models. The predicted C_{max} is in line with the maximal concentration of total radioactivity seen in blood after dosing male rats with 50 mg/kg of labelled acetamiprid (~180 μM).

The simulated exposure in humans (0.114/mg/kg/day) is shown in Figure 34. To reach a Cmax in plasma of 1μM (where activation of the receptor nAChRs have been observed in the SH-SY5Y cells), it would require an oral dose of 0.1-0.2 mg/kg which is 4-10 times higher than the acute reference dose (0.025 mg/kg/day) (EFSA, 2013[12]). Using the PBTK model to run a simulation in a population of 100 individuals (aged 20-50; 50% female) a dose of 15 mg/kg/day gives a mean unbound maximum acetamiprid concentration in plasma of 84 μM (58-129 μM 5t μ and 95th percentiles). Activation of nAChRs does not affect human neurodevelopment (KE4) up to at least 100 μM. The dose of 15 mg/kg/day is 600 times higher than the acute reference dose (0.025 mg/kg/day).

Figure 33. Simulated plasma (green) and brain (black) concentrations of acetamiprid in rats after multiple oral doses of (A) 1 mg/kg/day and (B) 50 mg/kg/day.

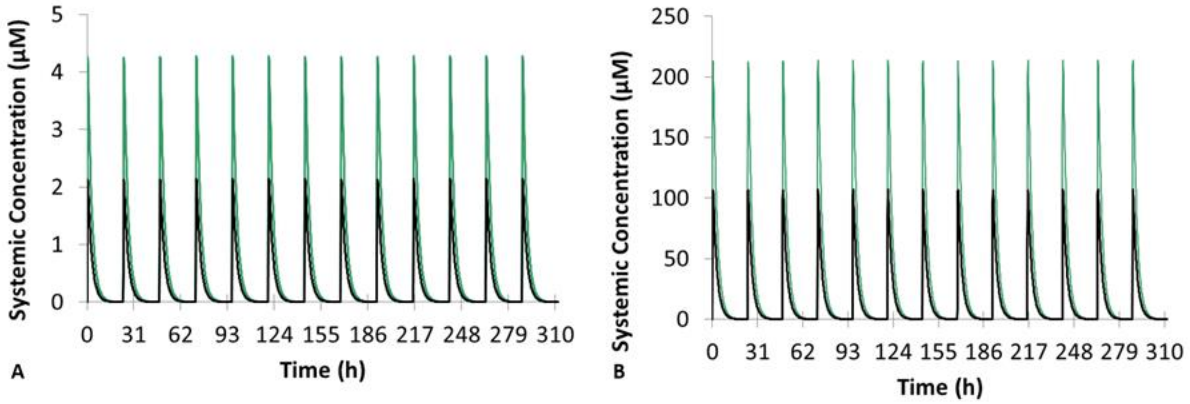

Figure 34. Simulated (A) plasma and (B) brain concentrations in human subjects after multiple oral doses of 0.114 mg/kg/day for 10 days.

The mean concentration is represented by a green line and the 5th and 95th percentiles by dashed black lines. Simulations were conducted in a population of 100 North European Caucasian healthy subjects (age 20-50; 50% female).

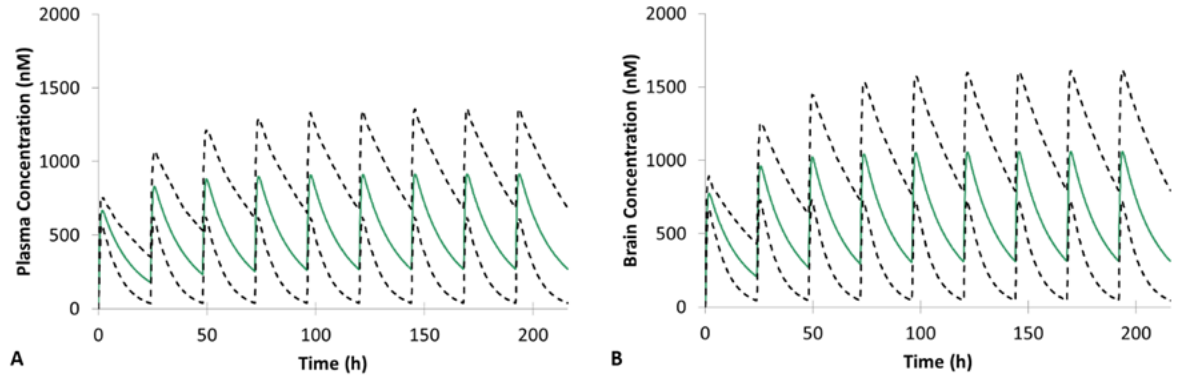

10 Uncertainty analysis

An uncertainty analysis is provided based on categories in an ordinal scale and is presented in Table 10. This is defined referring to the quality of the evidence generated/that was available supporting the assumptions of the case study and the overall weight of evidence and this is again related to the impact of the uncertainty on the hypothesis. For example, limited and poor-quality evidence is likely to lead to larger uncertainty and vice versa.

Table 10. Uncertainty analysis of the IATA report highlighting the quality of evidence available and generated.

Factor	Uncertainty (low, medium, high)	Impact of uncertainty on hypothesis	Comment
Hypothesis	medium	medium	The hypothesis for the hazard characterisation is based on established mode of action regarding the binding to the nAChRs as a pesticidal mode of action, although, the affinity towards the mammalian nAChRs is lower compared to insect nAChRs. However: -the prediction is based only on *in vitro* and *in silico* data, and -AO is an *in vivo* endpoint
Used Approach (e.g. AOP/MOA, Defined Approach, workflow, read-across etc.)	high	high	The approach is based on analyzing and generating data anchored to a putative AOP. Here, the MIE and early KE's are widely recognized as dogma. However, the late KEs and importantly, the AO outcome are not well-characterized/specified. It should be noted that this is a general lack of knowledge for DNT AOPs.
Methods/assays used in the IATA	Medium	medium	Uncertainty of the assays/methods The different *in vitro* NAM methods used for addressing for characterizing the hazard do not have a validated regulatory guideline. However, they all have a consortium-wide reviewed description document according to Krebs et al. 2019. Importantly, the positive reference compound, nicotine has been tested simultaneously. The uncertainty of the individual assays/methods –Docking of a7 and a4◌nAChR. Uncertainty medium. Precise in defining the pockets and placing the molecules and is able to discriminate between neonicotinoid structures which are very similar. It is a well-established method. However, there is a high uncertainty regarding the use of this method as a model for the MIE. -Activation of Ca^{2+} influx. Low, seen in different assays, receptor expression checked -Inhibition of agonist induced Ca^{2+} influx. Uncertainty low since it was shown in two systems -Altered gene expression in responsive assays. Uncertainty low as no effect seen -Proliferation. Uncertainty low; well-established assays at partner institutes and SOP available, Masjostushmann et al

			2020 -Differentiation. Uncertainty low; well-established assays at partner institutes and SOP available, Masjostushmann et al 2020 -Neurite outgrowth. Uncertainty low; well-established assays at partner institutes and SOP available, Masjostushmann et al 2020 -Migration. Uncertainty low; well-established assays at partner institutes and SOP available, Masjostushmann et al 2020 -Cytotoxicity. Uncertainty low; well-established assays at partner institutes and SOP available -hiPCS. Uncertainty low; well-established assay at partner institute. SOP and commercially available -CALUX reporters. Uncertainty low; well-established assay at partner, SOP and commercially available -ZFE FET test: Uncertainty low; well-established assay (in accordance with the OECD TG 236) at partner institute; SOP commercially available. -ZFE coiling assay: Uncertainty low; well-established assay at the partner institute, SOP not developed (assay execution varies between laboratories), programs and material commercially available; the assay has been accepted as DNT-determining -ZFE swimming assay: Uncertainty low; well-established assay at the partner institute, SOP not developed (assay execution varies between laboratories), programs and material commercially available; the assay has been accepted as DNT-determining -TempO-Seq data: Low uncertainty due to no effect seen The overall conclusions regarding the effects and potency of acetamiprid and the reference compound, nicotine, are comparable between the test systems, providing sufficient weight of evidence of low uncertainty for the overall outcome of the different test systems. However, over all the MoA may be dependent on precise developmental stage and neuronal phenotype and can be missed by some test systems. The *in silico* NAM method regarding the molecular docking has been externally reviewed in Loser et al. 2021; but is not well-established in the scientific as well as regulatory research. We consider the uncertainty medium. For the PBTK modelling standard procedures are followed according to OECD guidelines and includes sensitivity analysis to characterize the uncertainty.
Reference chemicals for performance evaluation of the assays/methods	Low	medium	Number of reference chemicals used for the performance evaluation of the assays and models is sufficient. Data has been shown related to nicotine, however, for characterization of the assays relevant well-established specific/general nAChRs agonist/antagonist have also been applied to further characterize the response in assays where activity was found as presented in Loser et al 2021
Quality of the data/information gathered and used in the IATA	medium	medium	Data/information gathered from the open literature was assessed in terms of relevance and reliability (bias) according to the protocol for the systematic review.
Concordance and weight of evidence of all data used for justifying the hypothesis	medium	medium	The gathered mammalian *in vivo* data does not show a consistent pattern regarding possible DNT effects. The available data have not examined similar endpoints between the experiments and also the experiments have done in different species. The ZFE data shows somewhat similar results throughout the assessed data, expressing the overall effect of

			acetamiprid on the organism. However, deviations are found, and experimental procedures were not always the same, hindering the comparison. It is shown that the acetamiprid can bind to mammalian a7 and a4◌̩nAChR and consistently induces CA^{2+}-influx in separate assays. Also, like the reference compound nicotine and also other neonicotinoids (Loser et al 2021) acetamiprid, does not induce detectable functional effects in the assays regarding differentiation, proliferation, neurite outgrowth and migration. No molecular/cellular analyses were conducted with the ZFE, but endpoints correlating with nAChR inhibition were observed.
Overall uncertainty of the IATA	high	high	The main driving uncertainty relates to the lack of an well-established consistent adverse outcome as well as lack of understanding of later key events. However, it is established that acetamiprid inhibit nAChR activation in human cells at concentrations relevant for human exposures.

11 Integrated Conclusion

As described above, this case study presents an IATA with the purpose of characterizing the DNT properties of a neonicotinoid insecticide, acetamiprid. The approach taken was to extract, appraise and assess existing human observational, *in vivo* and *in vitro* evidence related to DNT endpoints. However, no relevant human observational evidence was available, and the available mammalian evidence exhibited that the available data is heterogeneous, and no consistent effect related to DNT have been described. The *in vivo* ZFE data reviewed in the present report outlines the strong effect of nicotine on the development and behavior of ZFE, whilst acetamiprid was found to show lower behavioral and developmental alterations. No lethal effects were observed and at 96 hpf, the EC_{50} value had to be extrapolated. Acetamiprid exposure only induced coiling alterations in later stages of the assay, and with a less clear dose dependent pattern than nicotine. This was the opposite for the swimming assay, in which acetamiprid exposure induced a reduction on swimming distance and frequency. Moreover, discrepancies between the previously conducted work could be found, in terms of observed endpoints and experimental design. However, the overall picture presented does match what was determined in the study conducted for this report.

The *in vitro* data reviewed shows that acetamiprid induces Ca^{2+} influx via the nAChR as well as attenuated VOCC function after exposure at concentrations between 1-100 µM. Functional endpoints in terms of neurite outgrowth have been investigated but no statically significant effects were seen but reduced dendritic area of rat purkinje cells were observed. Two of the studies reviewed performed transcriptomics after exposure and observed DEGs relevant for neuronal development. However, some of the studies had a high risk of bias scores due to only one concentration was studied, less relevant mammalian models were used or that cytotoxicity was not studied.

Therefore, further *in vitro* and *in silico* data have been generated, characterizing the effects of the compound in a battery of DNT *in vitro* tests anchored to a putative AOP and ED endpoints. In addition, the toxicodynamic data *in vitro* data has been contextualized with internal exposure predictions by PBTK modelling.

Although, the further testing in the DNT IVB and additional systems/endpoint firmly establish that neither acetamiprid, nor nicotine affects these endpoints, neither directly affect agonism or antagonism on various nuclear receptors, PPARα and AhR, nor did the compounds activate stress pathways in the CALUX reporter gene assay. However, it is established that acetamiprid has similar, but less potent, activity on nAChR mediated Ca^{2+} influx in neuronal systems from nicotine. There still remains significant uncertainties regarding later KEs, including a specific adverse outcome. We observed no effects on the proposed KE3 and KE4 with the assays used after direct exposure with acetamiprid or nicotine, but the possibility cannot be ignored that the desensitizing effect may alter evoked responses, e.g. voltage operated ion channel function, transmitter release or neural network function. This major uncertainty is currently undergoing further investigations. As a first attempt, analysis of differential expressed genes in systems where acetamiprid and nicotine are active have been generated where no major effects were observed for any of the systems. Thus, KE3 cannot be confirmed using transcriptomics. Another possibility would be investigating activation/inactivation of signaling pathways as exemplified above.

In conclusion, acetamiprid induce Ca^{2+} signaling in neuronal systems mediated by nAChRs at concentrations that are predicted by PBTK modeling to occur at 0.1-0.2 mg/kg which is 4-10 times higher

than the current ARfD set in the EU. This could potentially support a plausible mechanistic link to more firmly established human-relevant adverse outcomes.

12 Data Matrix

In this report, we have presented an IATA and postulated a putative AOP for nAChR binding as a MIE leading to neurodevelopmental dysfunction as the AO caused by the neonicotinoid pesticide acetamiprid. The KEs proposed include activation of the nAChR leading to desensitization/inhibition which in turn results in transcriptional alterations due to increased intracellular calcium levels affecting functional processes such as differentiation and neurite outgrowth. We have generated data to fill data gaps connected to the AOP that are summarized in Table 11.

Table 11. Summary of data gap filling for Acetamiprid

LUHMES = neuron. SH-SY5Y = neuron. iPSC-derived neuronal culture = 42-days differentiated iPSC derived culture with astrocytes and different subtypes of neurons. ZFE = Zebra fish embryo. N/A = could not be determined as no effects were noted in all biological replicates. LCED = Lowest continuous effects dose (with 3 or more conseq. time points showing sign. at this concentration); NEPs = Neuroepithelial precursors; NCCs = Neural crest cells.

Summary of data gap filling					**Case 1**	
Type of chemical					Test compound	Positive control
Chemical					Acetamiprid	Nicotine
	Event	Assay				
in silico	Chemical specific	Similarity 3D		structural modeling a4ß2nAChR-AOP MIE1		
		Similarity 3D		structural modeling a7nAChR-AOP MIE2		
		Absorption				
		Distribution				
		Metabolism				
		Excretion				
	Key event	Tissue/response	Value	Measurement		
in vivo	AO			Neuro/DART		
		Rats. Central nervous system	mg/kg bw/day	Auditory startle response	10	n.d.
		Mice. Central nervous system/dorsal telecephalon	mg/kg bw/day	Histopathological evaluation. Hypoplasia of the cortical plate. Decreased neurogenesis.	0.5	n.d.
		Mice. Central nervous	mg/kg	Decreased	0.5	n.d.

		system/hippocampal dentate gyrus	bw/day	neurogenesis at PND26 Increased migroglia activation		
		Mice. Central nervous system	mg/kg bw/day	Reduced anxiety in light-darkness test Increases sexual and aggressive behavior	1 and 10	n.d.
in vitro	KE1	LUHMES	EC50 (µM) mean± SEM	Ca^{2+} influx, non-a7 nAChR	n.d.	5.93 ± 0.05
		LUHMES	EC50 (µM) mean± SEM	Ca^{2+} influx, a7 nAChR (+PNU)	-	-
		SH-SY5Y	EC50 (µM) mean± SD	Ca^{2+} influx, a7 nAChR (+PNU)	0.82 ± 0.17	0.35 ± 0.10
			EC50 (µM) mean	Ca^{2+} influx, a7 nAChR	-	-
	KE2	LUHMES	IC50 (µM) mean± SEM	Inhibition of Ca^{2+} influx for 10 uM nicotine	5.40 ± 0.08	
		LUHMES	IC50 (µM)	Inhibition of Ca^{2+} influx, a7 nAChR	-	-
		SH-SY5Y	IC50 (µM)	Inhibition of Ca^{2+} influx for 11.1 µM nicotine, a7 nAChR	10,17	-
	KE3	LUHMES	DEGs/BMC	Transcriptomic		
		SH-SY5Y	DEGs/BMC	Transcriptomic		
		iPSC-derived neuronal culture	DEGs/BMC	Transcriptomic		
		ZFE	DEGs/BMC	Transcriptomic		
	KE4	SH-SY5Y	BMC25 (µM)	Cytotoxicity (resazurin)	NE at 50 µM	NE at 10 µM
		iPSC-derived neuronal culture	BMC25 (µM)	Cytotoxicity (CellTiter-Glo® Luminescent Cell Viability Assay)	NE (BMC25>100µM)	NE (BMC25>100µM)
		LUHMES	BMC25 (µM)	Neurite outgrowth (calcein-hoechst stain)	NE (BMC25>100µM)	NE (BMC25>100µM)
		LUHMES	BMC25 (µM)	Cytotoxicity (calcein-hoechst stain)	NE (BMC25>100µM)	NE (BMC25>100µM)
		ZFE	120 hpf EC10 (µM)	FET	0.3	0.6
		ZFE	LCED (µM)	coiling	25	1.25 (induced hyper- and hypoactivity)
		ZFE	LCED (µM)	swimming	N/A	N/A
		Sensory neurons	BMC25 (µM)	Neurite outgrowth (calcein-hoechst stain)	NE (BMC25>100µM)	NE (BMC25>100µM)
		Sensory neurons	BMC25 (µM)	Cytotoxicity (calcein-hoechst stain)	NE (BMC25>100µM)	NE (BMC25>100µM)

		NEPs	Phenotypic	Differentiation and rosette formation	NE (100 µM)	NE (10 µM)
		NCCs	BMC25 (µM)	Migration (calcein-hoechst stain)	NE (BMC25>100µM)	NE (BMC25>100µM)
		NCCs	BMC25 (µM)	Cytotoxicity (calcein-hoechst stain)	NE (BMC25>100µM)	NE (BMC25>100µM)
	Other	Cytotox CALUX	BMC25 (µM) alt. Y/N	Cytotoxicity (U2OS cells)	631 µM	
		anti-AR CALUX	BMC25 (µM) alt. Y/N	anti-androgenicity	100 µM	
		CALUX panel	BMC25 (µM) alt. Y/N	all compounds negative up to 1 mM on all assays unless stated otherwise above		
		Reporters	BMC25 (µM) alt. Y/N	reporter target		
		Reporters	BMC25 (µM) alt. Y/N	reporter target		
		Reporters	BMC25 (µM) alt. Y/N	reporter target		
		Reporters	BMC25 (µM) alt. Y/N	reporter target		

13 References

1. Organisation for Economic Co-operation and Development. *Test No. 426: Developmental Neurotoxicity Study*. (OECD Publishing, 2007).
2. *Test No. 443: Extended One-Generation Reproductive Toxicity Study*. (OECD, 2018). doi:10.1787/9789264185371-en.
3. Agency USEP: USEPA OPPTS 870.6300, Developmental Neurotoxicity Study. *EPA Office of Chemical Safety and Polution Prevention. Washington, U.S.* https://nepis.epa.gov/Exe/ZyNET.exe/P100IRWO.txt?ZyActionD=ZyDocument&Client=EPA&Index=1995 Thru 1999&Docs=&Query=&Time=&EndTime=&SearchMethod=1&TocRestrict=n&Toc=&TocEntry=&QField=&QFieldYear=&QFieldMonth=&QFieldDay=&UseQField=&IntQFieldOp=0&ExtQFieldOp= (1998).
4. Epa Ocspp, U. *NAFTA TECHNICAL WORKING GROUP ON PESTICIDES (TWG) DEVELOPMENTAL NEUROTOXICITY STUDY (DNT) GUIDANCE DOCUMENT*.
5. Bal-Price, A. *et al.* Recommendation on test readiness criteria for new approach methods in toxicology: Exemplified for developmental neurotoxicity. *ALTEX* **35**, 306–352 (2018).
6. Fritsche, E. *et al.* OECD/EFSA workshop on developmental neurotoxicity (DNT): The use of non-animal test methods for regulatory purposes. in *Altex* vol. 34 311–315 (Elsevier GmbH, 2017).
7. Crofton, K. M., Mundy, W. R. & Shafer, T. J. Developmental neurotoxicity testing: A path forward. *Congenital Anomalies* vol. 52 140–146 (2012).
8. Paparella, M., Bennekou, S. H. & Bal-Price, A. An analysis of the limitations and uncertainties of in vivo developmental neurotoxicity testing and assessment to identify the potential for alternative approaches. *Reproductive Toxicology* **96**, 327–336 (2020).
9. Masjosthusmann, S. *et al.* Establishment of an a priori protocol for the implementation and interpretation of an in-vitro testing battery for the assessment of developmental neurotoxicity. *EFSA Supporting Publications* **17**, 1938E (2020).
10. Aagaard, A. *et al.* Scientific Opinion on the developmental neurotoxicity potential of acetamiprid and imidacloprid. *EFSA Journal* **11**, 47 (2013).
11. Kimura-Kuroda, J., Komuta, Y., Kuroda, Y., Hayashi, M. & Kawano, H. Nicotine-like effects of the neonicotinoid insecticides acetamiprid and imidacloprid on cerebellar neurons from neonatal rats. *PLoS ONE* **7**, e32432 (2012).
12. Scientific Opinion on the developmental neurotoxicity potential of acetamiprid and imidacloprid. *EFSA Journal* **11**, (2013).
13. Loser, D. *et al.* Functional alterations by a subgroup of neonicotinoid pesticides in human dopaminergic neurons. *Archives of Toxicology* 1–27 (2021a) doi:10.1007/s00204-021-03031-1.
14. Loser, D. *et al.* Acute effects of the imidacloprid metabolite desnitro-imidacloprid on human nACh receptors relevant for neuronal signaling. *Archives of Toxicology 2021* **1**, 1–22 (2021b).
15. Brown, L. A., Ihara, M., Buckingham, S. D., Matsuda, K. & Sattelle, D. B. Neonicotinoid insecticides display partial and super agonist actions on native insect nicotinic acetylcholine receptors. *Journal of Neurochemistry* **99**, 608–615 (2006).
16. Tan, J., Galligan, J. J. & Hollingworth, R. M. Agonist actions of neonicotinoids on nicotinic acetylcholine receptors expressed by cockroach neurons. *NeuroToxicology* **28**, 829–842 (2007).
17. Casida, J. E. Neonicotinoids and Other Insect Nicotinic Receptor Competitive Modulators: Progress and Prospects. *Annual Review of Entomology* vol. 63 125–144 (2018).
18. National summary reports on pesticide residue analysis performed in 2018. *EFSA Supporting Publications* **17**, 1814E (2020).
19. Christen, V., Rusconi, M., Crettaz, P. & Fent, K. Developmental neurotoxicity of different pesticides

in PC-12 cells in vitro. *Toxicology and Applied Pharmacology* **325**, 25–36 (2017).
20. Kimura-Kuroda, J. *et al.* Neonicotinoid insecticides alter the gene expression profile of neuron-enriched cultures from neonatal rat cerebellum. *International Journal of Environmental Research and Public Health* **13**, 987 (2016).
21. Valdivia, P. *et al.* Multi-well microelectrode array recordings detect neuroactivity of ToxCast compounds. *NeuroToxicology* **44**, 204–217 (2014).
22. Sipes, N. S. *et al.* Profiling 976 ToxCast chemicals across 331 enzymatic and receptor signaling assays. *Chemical Research in Toxicology* **26**, 878–895 (2013).
23. Kim, K. *et al.* A Temporary Gating of Actin Remodeling during Synaptic Plasticity Consists of the Interplay between the Kinase and Structural Functions of CaMKII. *Neuron* **87**, 813–826 (2015).
24. Nicole, O. *et al.* A novel role for CAMKIIβ in the regulation of cortical neuron migration: implications for neurodevelopmental disorders. *Molecular Psychiatry 2018 23:11* **23**, 2209–2226 (2018).
25. GJ, S. *et al.* Evidence for the coidentification of GAP-43, a growth-associated protein, and F1, a plasticity-associated protein. *The Journal of neuroscience : the official journal of the Society for Neuroscience* **7**, 4066–4075 (1987).
26. Kagawa, N. & Nagao, T. Neurodevelopmental toxicity in the mouse neocortex following prenatal exposure to acetamiprid. *Journal of Applied Toxicology* **38**, 1521–1528 (2018).
27. Nakayama, A., Yoshida, M., Kagawa, N. & Nagao, T. The neonicotinoids acetamiprid and imidacloprid impair neurogenesis and alter the microglial profile in the hippocampal dentate gyrus of mouse neonates. *Journal of Applied Toxicology* **39**, 877–887 (2019).
28. Sano, K. *et al.* In utero and lactational exposure to acetamiprid induces abnormalities in socio-sexual and anxiety-related behaviors of male mice. *Frontiers in Neuroscience* **10**, 228 (2016).
29. Ma, X., Li, H., Xiong, J., Mehler, W. T. & You, J. Developmental Toxicity of a Neonicotinoid Insecticide, Acetamiprid to Zebrafish Embryos. *Journal of Agricultural and Food Chemistry* **67**, 2429–2436 (2019).
30. Wang, Y. *et al.* Single and joint toxicity assessment of four currently used pesticides to zebrafish (Danio rerio) using traditional and molecular endpoints. *Chemosphere* **192**, 14–23 (2018).
31. Crosby, E. B., Bailey, J. M., Oliveri, A. N. & Levin, E. D. Neurobehavioral Impairments Caused by Developmental Imidacloprid Exposure in Zebrafish. *Neurotoxicology and teratology* **49**, 81 (2015).
32. KR, S., S, V. & RL, T. Nicotinic receptors mediate changes in spinal motoneuron development and axonal pathfinding in embryonic zebrafish exposed to nicotine. *The Journal of neuroscience : the official journal of the Society for Neuroscience* **22**, 10731–10741 (2002).
33. Palpant, N. J., Hofsteen, P., Pabon, L., Reinecke, H. & Murry, C. E. Cardiac Development in Zebrafish and Human Embryonic Stem Cells Is Inhibited by Exposure to Tobacco Cigarettes and E-Cigarettes. *PLOS ONE* **10**, e0126259 (2015).
34. Leonard, J. P. & Salpeter, M. M. Agonist-induced myopathy at the neuromuscular junction is mediated by calcium. *The Journal of Cell Biology* **82**, 811 (1979).
35. Welsh, L., Tanguay, R. L. & Svoboda, K. R. Uncoupling nicotine mediated motoneuron axonal pathfinding errors and muscle degeneration in zebrafish. *Toxicology and applied pharmacology* **237**, 29 (2009).
36. AG, E., K, O., XM, S. & SM, S. Congenital myasthenic syndromes: multiple molecular targets at the neuromuscular junction. *Annals of the New York Academy of Sciences* **998**, 138–160 (2003).
37. AG, E. *et al.* A newly recognized congenital myasthenic syndrome attributed to a prolonged open time of the acetylcholine-induced ion channel. *Annals of neurology* **11**, 553–569 (1982).
38. Gomez, C. M. *et al.* Active Calcium Accumulation Underlies Severe Weakness in a Panel of Mice with Slow-Channel Syndrome. *The Journal of Neuroscience* **22**, 6447 (2002).
39. R, O. & HR, K. Temperature-dependent effects of the pesticides thiacloprid and diazinon on the embryonic development of zebrafish (Danio rerio). *Aquatic toxicology (Amsterdam, Netherlands)* **86**, 485–494 (2008).
40. C, V. *et al.* Imidacloprid induces adverse effects on fish early life stages that are more severe in Japanese medaka (Oryzias latipes) than in zebrafish (Danio rerio). *Chemosphere* **225**, 470–478 (2019).
41. Brunet, J. L., Maresca, M., Fantini, J. & Belzunces, L. P. Intestinal absorption of the acetamiprid neonicotinoid by Caco-2 cells: Transepithelial transport, cellular uptake and efflux. *Journal of Environmental Science and Health - Part B Pesticides, Food Contaminants, and Agricultural Wastes* **43**, 261–270 (2008).
42. Ford, K. A. & Casida, J. E. Chloropyridinyl neonicotinoid insecticides: Diverse molecular

substituents contribute to facile metabolism in mice. *Chemical Research in Toxicology* **19**, 944–951 (2006).
43. Terayama, H. *et al.* Acetamiprid Accumulates in Different Amounts in Murine Brain Regions. *International Journal of Environmental Research and Public Health Article* doi:10.3390/ijerph13100937 (2016).
44. Harada, K. H. *et al.* Biological Monitoring of human exposure to neonicotinoids using urine samples, and neonicotinoid excretion kinetics. *PLoS ONE* **11**, e0146335 (2016).
45. Wada, E. *et al.* Distribution of alpha2, alpha3, alpha4, and beta2 neuronal nicotinic receptor subunit mRNAs in the central nervous system: A hybridization histochemical study in the rat. *Journal of Comparative Neurology* **284**, 314–335 (1989).
46. Tribollet, E., Bertrand, D., Marguerat, A. & Raggenbass, M. Comparative distribution of nicotinic receptor subtypes during development, adulthood and aging: An autoradiographic study in the rat brain. *Neuroscience* **124**, 405–420 (2004).
47. Buisson, B., Gopalakrishnan, M., Arneric, S. P., Sullivan, J. P. & Bertrand, D. Human α4β2 neuronal nicotinic acetylcholine receptor in HEK 293 cells: A patch-clamp study. *Journal of Neuroscience* **16**, 7880–7891 (1996).
48. Seguela, P., Wadiche, J., Dineley-Miller, K., Dani, J. A. & Patrick, J. W. Molecular cloning, functional properties, and distribution of rat brain α7: A nicotinic cation channel highly permeable to calcium. *Journal of Neuroscience* **13**, 596–604 (1993).
49. Williams, D. K., Wang, J. & Papke, R. L. Investigation of the molecular mechanism of the α7 nicotinic acetylcholine receptor positive allosteric modulator PNU-120596 provides evidence for two distinct desensitized states. *Molecular Pharmacology* **80**, 1013–1032 (2011).
50. Ng, H. W. *et al.* Competitive docking model for prediction of the human nicotinic acetylcholine receptor α7 binding of tobacco constituents. *Oncotarget* **9**, 16899–16916 (2018).
51. Slotkin, T. A. If nicotine is a developmental neurotoxicant in animal studies, dare we recommend nicotine replacement therapy in pregnant women and adolescents? *Neurotoxicology and Teratology* vol. 30 1–19 (2008).
52. Azam, L., Chen, Y. & Leslie, F. M. Developmental regulation of nicotinic acetylcholine receptors within midbrain dopamine neurons. *Neuroscience* **144**, 1347–1360 (2007).
53. Xu, Z., Seidler, F. J., Ali, S. F., Slikker, J. & Slotkin, T. A. Fetal and adolescent nicotine administration: Effects on CNS serotonergic systems. *Brain Research* **914**, 166–178 (2001).
54. Slotkin, T. A., Cho, H. & Whitmore, W. L. Effects of prenatal nicotine exposure on neuronal development: Selective actions on central and peripheral catecholaminergic pathways. *Brain Research Bulletin* **18**, 601–611 (1987).
55. Smith, A. M., Dwoskin, L. P. & Pauly, J. R. Early exposure to nicotine during critical periods of brain development: Mechanisms and consequences. *Journal of Pediatric Biochemistry* **1**, 125–141 (2010).
56. Gillentine, M. A. *et al.* The Cognitive and Behavioral Phenotypes of Individuals with CHRNA7 Duplications. *Journal of Autism and Developmental Disorders* **47**, 549–562 (2017).
57. Ziats, M. N. *et al.* The complex behavioral phenotype of 15q13.3 microdeletion syndrome. *Genetics in Medicine* **18**, 1111–1118 (2016).
58. Deutsch, S. I., Burket, J. A., Benson, A. D. & Urbano, M. R. The 15q13.3 deletion syndrome: Deficient α7-containing nicotinic acetylcholine receptor-mediated neurotransmission in the pathogenesis of neurodevelopmental disorders. *Progress in Neuro-Psychopharmacology and Biological Psychiatry* vol. 64 109–117 (2016).
59. Marcus, M. M. *et al.* Alpha7 nicotinic acetylcholine receptor agonists and PAMs as adjunctive treatment in schizophrenia. An experimental study. *European Neuropsychopharmacology* **26**, 1401–1411 (2016).
60. Zhang, J.-C. *et al.* Depression-like phenotype by deletion of α7 nicotinic acetylcholine receptor: Role of BDNF-TrkB in nucleus accumbens OPEN. *Nature Publishing Group* (2016) doi:10.1038/srep36705.
61. Nacer, S. A. *et al.* Loss of α7 nicotinic acetylcholine receptors in GABAergic neurons causes sex-dependent decreases in radial glia-like cell quantity and impairments in cognitive and social behavior. *Brain Structure and Function* **226**, 365–379 (2021).
62. Felix, R. A. *et al.* Sensory Processing: Nicotinic acetylcholine receptor subunit α7-knockout mice exhibit degraded auditory temporal processing. *Journal of Neurophysiology* **122**, 451 (2019).
63. Levin, E. D. *et al.* Nicotinic α7- or β2-containing receptor knockout: Effects on radial-arm maze

learning and long-term nicotine consumption in mice. *Behavioural Brain Research* **196**, 207–213 (2009).
64. Navarro, H. A. *et al.* Prenatal exposure to nicotine impairs nervous system development at a dose which does not affect viability or growth. *Brain Research Bulletin* **23**, 187–192 (1989).
65. Eppolito, A. K. & Smith, R. F. Long-term behavioral and developmental consequences of pre- and perinatal nicotine. *Pharmacology Biochemistry and Behavior* **85**, 835–841 (2006).
66. Nachmanoff, D. B. *et al.* Brainstem 3H-nicotine receptor binding in the sudden infant death syndrome. *Journal of neuropathology and experimental neurology* **57**, 1018–1025 (1998).
67. Slotkin, T. A., Pinkerton, K. E., Auman, J. T., Qiao, D. & Seidler, F. J. Perinatal exposure to environmental tobacco smoke upregulates nicotinic cholinergic receptors in monkey brain. *Developmental Brain Research* **133**, 175–179 (2002).
68. Frazier, C. J. *et al. Acetylcholine Activates an-Bungarotoxin-Sensitive Nicotinic Current in Rat Hippocampal Interneurons, But Not Pyramidal Cells*. (1998).
69. Cheng, Q. & Yakel, J. L. The effect of α7 nicotinic receptor activation on glutamatergic transmission in the hippocampus. *Biochemical Pharmacology* vol. 97 439–444 (2015).
70. Slotkin, T. A., Ryde, I. T., Tate, C. A. & Seidler, F. J. Lasting effects of nicotine treatment and withdrawal on serotonergic systems and cell signaling in rat brain regions: Separate or sequential exposure during fetal development and adulthood. *Brain Research Bulletin* **73**, 259–272 (2007).
71. Slotkin, T. A., Tate, C. A., Cousins, M. M. & Seidler, F. J. Prenatal nicotine exposure alters the responses to subsequent nicotine administration and withdrawal in adolescence: Serotonin receptors and cell signaling. *Neuropsychopharmacology* **31**, 2462–2475 (2006).
72. Walsh, R.M., Roh, S.H., Gharpure, A., Morales-Perez, C.L., Teng, J., Hibbs, R.E. Structural principles of distinct assemblies of the human α4β2 nicotinic receptor. Nature 557, 261–265 (2018). https://doi.org/10.1038/s41586-018-0081-7).
73. Mick, E., Biederman, J., Faraone, S. V., Sayer, J. & Kleinman, S. Case-Control Study of Attention-Deficit Hyperactivity Disorder and Maternal Smoking, Alcohol Use, and Drug Use During Pregnancy. *Journal of the American Academy of Child & Adolescent Psychiatry* **41**, 378–385 (2002).
74. Jacobsen, L. K., Slotkin, T. A., Mencl, W. E., Frost, S. J. & Pugh, K. R. Gender-Specific Effects of Prenatal and Adolescent Exposure to Tobacco Smoke on Auditory and Visual Attention. *Neuropsychopharmacology 2007 32:12* **32**, 2453–2464 (2007).
75. Borgerding, M. & Klus, H. Analysis of complex mixtures – Cigarette smoke. *Experimental and Toxicologic Pathology* **57**, 43–73 (2005).
76. Sachana, M., Rolaki, A. & Bal-Price, A. Development of the Adverse Outcome Pathway (AOP): Chronic binding of antagonist to N-methyl-D-aspartate receptors (NMDARs) during brain development induces impairment of learning and memory abilities of children. *Toxicology and Applied Pharmacology* **354**, 153–175 (2018).
77. Sachana, M., Munn, S. & Bal-Price, A. OECD Series on Adverse Outcome Pathways No. 5 Adverse Outcome Pathway on chronic binding of antagonist to N-methyl-D-aspartate receptors (NMDARs) during brain development induces impairment of learning and memory abilities. doi:10.1787/5jlsqs5hcrmq-en.
78. Noviello, C. M. *et al.* Structure and gating mechanism of the α7 nicotinic acetylcholine receptor. *Cell* **184**, 2121-2134.e13 (2021).
79. Ihara, M. *et al.* Crystal structures of Lymnaea stagnalis AChBP in complex with neonicotinoid insecticides imidacloprid and clothianidin. *Invertebrate Neuroscience* **8**, 71–81 (2008).
80. Scholz, D. *et al.* Rapid, complete and large-scale generation of post-mitotic neurons from the human LUHMES cell line. *Journal of Neurochemistry* **119**, 957–971 (2011).
81. Stiegler, N. V., Krug, A. K., Matt, F. & Leist, M. Assessment of chemical-induced impairment of human neurite outgrowth by multiparametric live cell imaging in high-density cultures. *Toxicological Sciences* **121**, 73–87 (2011).
82. Krug, A. K. *et al.* Evaluation of a human neurite growth assay as specific screen for developmental neurotoxicants. *Arch Toxicol* **3**, 2215–2231 (2013).
83. H, G. *et al.* Neurofunctional endpoints assessed in human neuroblastoma SH-SY5Y cells for estimation of acute systemic toxicity. *Toxicology and applied pharmacology* **245**, 191–202 (2010).
84. Attoff, K. *et al.* Acrylamide alters CREB and retinoic acid signalling pathways during differentiation of the human neuroblastoma SH-SY5Y cell line. *Scientific Reports* **10**, 16714 (2020).
85. J, D. *et al.* Neurotoxicity and underlying cellular changes of 21 mitochondrial respiratory chain

inhibitors. *Archives of toxicology* **95**, 591–615 (2021).
86. Cytotoxicity, B. DB-ALM Protocol n° 208 : ATP viability assay for measuring acute toxicity (72 hours exposure) on hiPSC derived TD21 neuronal cultures in 96-well plates.
87. Chambers, S. M. *et al.* Highly efficient neural conversion of human ES and iPS cells by dual inhibition of SMAD signaling. *Nature Biotechnology* **27**, 275–280 (2009).
88. Ochalek, A. *et al.* Neurons derived from sporadic Alzheimer's disease iPSCs reveal elevated TAU hyperphosphorylation, increased amyloid levels, and GSK3B activation. *Alzheimer's Research & Therapy 2017 9:1* **9**, 1–19 (2017).
89. A, C. *et al.* Comparison of 2D and 3D neural induction methods for the generation of neural progenitor cells from human induced pluripotent stem cells. *Stem cell research* **25**, 139–151 (2017).
90. S, Z. *et al.* Neurosphere Based Differentiation of Human iPSC Improves Astrocyte Differentiation. *Stem cells international* **2016**, (2016).
91. Mica, Y., Lee, G., Chambers, S. M., Tomishima, M. J. & Studer, L. Modeling Neural Crest Induction, Melanocyte Specification, and Disease-Related Pigmentation Defects in hESCs and Patient-Specific iPSCs. *Cell Reports* **3**, 1140–1152 (2013).
92. Dreser, N. *et al.* Development of a neural rosette formation assay (RoFA) to identify neurodevelopmental toxicants and to characterize their transcriptome disturbances. *Archives of Toxicology* **94**, 151–171 (2020).
93. Baud, A. *et al.* Multiplex High-Throughput Targeted Proteomic Assay to Identify Induced Pluripotent Stem Cells. *Analytical Chemistry* **89**, 2440–2448 (2017).
94. Hoelting, L. *et al.* Stem Cell-Derived Immature Human Dorsal Root Ganglia Neurons to Identify Peripheral Neurotoxicants. *STEM CELLS Translational Medicine* **5**, 476–487 (2016).
95. *Test No. 236: Fish Embryo Acute Toxicity (FET) Test*. (OECD, 2013). doi:10.1787/9789264203709-en.
96. von Hellfeld, R., Brotzmann, K., Baumann, L., Strecker, R. & Braunbeck, T. Adverse effects in the fish embryo acute toxicity (FET) test: a catalogue of unspecific morphological changes versus more specific effects in zebrafish (Danio rerio) embryos. *Environmental Sciences Europe* **32**, 122 (2020).
97. Zindler, F. *et al.* Analysis of tail coiling activity of zebrafish (Danio rerio) embryos allows for the differentiation of neurotoxicants with different modes of action. *Ecotoxicology and Environmental Safety* **186**, (2019).
98. Burg, B. van der *et al.* A Panel of Quantitative Calux® Reporter Gene Assays for Reliable High-Throughput Toxicity Screening of Chemicals and Complex Mixtures. *High-Throughput Screening Methods in Toxicity Testing* 519–532 (2013) doi:10.1002/9781118538203.CH28.
99. House, J. S. *et al.* A Pipeline for High-Throughput Concentration Response Modeling of Gene Expression for Toxicogenomics. *Frontiers in Genetics* **8**, 168 (2017).
100. O'Brien, J., Wilson, I., Orton, T. & Pognan, F. Investigation of the Alamar Blue (resazurin) fluorescent dye for the assessment of mammalian cell cytotoxicity. *European Journal of Biochemistry* **267**, 5421–5426 (2000).
101. Delp, J. *et al.* A high-throughput approach to identify specific neurotoxicants/ developmental toxicants in human neuronal cell function assays. *ALTEX* **35**, 235–253 (2018).
102. Nyffeler, J. *et al.* Design of a high-Throughput human neural crest cell migration assay to indicate potential developmental toxicants. *Altex* **34**, 75–94 (2017).
103. Rodgers, T. & Rowland, M. Physiologically based pharmacokinetic modelling 2: Predicting the tissue distribution of acids, very weak bases, neutrals and zwitterions. *Journal of Pharmaceutical Sciences* **95**, 1238–1257 (2006).
104. Jamei, M. *et al.* The Simcyp® population-based ADME simulator. *Expert Opinion on Drug Metabolism and Toxicology* vol. 5 211–223 (2009).
105. Ihara, M. *et al.* Studies on an acetylcholine binding protein identify a basic residue in loop G on the β1 strand as a new structural determinant of neonicotinoid actions. *Molecular Pharmacology* **86**, 736–746 (2014).
106. Bailey, J., Oliveri, A. & Levin, E. D. Zebrafish model systems for developmental neurobehavioral toxicology. *Birth Defects Research Part C: Embryo Today: Reviews* **99**, 14–23 (2013).
107. De Esch, C., Slieker, R., Wolterbeek, A., Woutersen, R. & de Groot, D. Zebrafish as potential model for developmental neurotoxicity testing: A mini review. *Neurotoxicology and Teratology* **34**, 545–553 (2012).
108. Nishimura, Y. *et al.* Zebrafish as a systems toxicology model for developmental neurotoxicity testing. *Congenital Anomalies* **55**, 1–16 (2015).

109. Tierney, K. B. Behavioural assessments of neurotoxic effects and neurodegeneration in zebrafish. *Biochimica et Biophysica Acta (BBA) - Molecular Basis of Disease* **1812**, 381–389 (2011).
110. Gerlai, R. Zebrafish antipredatory responses: A future for translational research? *Behavioural Brain Research* **207**, 223–231 (2010).
111. Maximino, C. *et al.* Measuring anxiety in zebrafish: A critical review. *Behavioural Brain Research* **214**, 157–171 (2010).
112. Schnörr, S. J., Steenbergen, P. J., Richardson, M. K. & Champagne, D. L. Measuring thigmotaxis in larval zebrafish. *Behavioural Brain Research* **228**, 367–374 (2012).
113. Saverino, C. & Gerlai, R. The social zebrafish: Behavioral responses to conspecific, heterospecific, and computer animated fish. *Behavioural Brain Research* **191**, 77–87 (2008).
114. Seibt, K. J. *et al.* Antipsychotic drugs reverse MK-801-induced cognitive and social interaction deficits in zebrafish (Danio rerio). *Behavioural Brain Research* **224**, 135–139 (2011).
115. Riehl, R. *et al.* Behavioral and physiological effects of acute ketamine exposure in adult zebrafish. *Neurotoxicology and Teratology* **33**, 658–667 (2011).
116. Grossman, L. *et al.* Characterization of behavioral and endocrine effects of LSD on zebrafish. *Behavioural Brain Research* **214**, 277–284 (2010).
117. Xia, J., Niu, C. & Pei, X. Effects of chronic exposure to nonylphenol on locomotor activity and social behavior in zebrafish (Danio rerio). *Journal of Environmental Sciences* **22**, 1435–1440 (2010).
118. Saint-Amant, L. & Drapeau, P. Time Course of the Development of Motor Behaviors in the Zebrafish Embryo. *J Neurobiol* **37**, 622–632 (1998).
119. Saint-Amant, L. & Drapeau, P. Motoneuron Activity Patterns Related to the Earliest Behavior of the Zebrafish Embryo. *Journal of Neuroscience* **20**, 3964–3972 (2000).
120. Zindler, F., Beedgen, F. & Braunbeck, T. Time-course of coiling activity in zebrafish (Danio rerio) embryos exposed to ethanol as an endpoint for developmental neurotoxicity (DNT) – Hidden potential and underestimated challenges. *Chemosphere* **235**, 12–20 (2019).
121. Zindler, F. *et al.* Do environmentally relevant concentrations of fluoxetine and citalopram impair stress-related behavior in zebrafish (Danio rerio) embryos? *Chemosphere* **261**, 127753 (2020).
122. IW, S., J, H., R, B. & HE, W. Assessment of the developmental neurotoxicity of compounds by measuring locomotor activity in zebrafish embryos and larvae. *Neurotoxicology and teratology* **37**, 44–56 (2013).
123. Selderslaghs, I. W. T., Hooyberghs, J., De Coen, W. & Witters, H. E. Locomotor activity in zebrafish embryos: A new method to assess developmental neurotoxicity. *Neurotoxicology and Teratology* **32**, 460–471 (2010).
124. Weichert, F. G., Floeter, C., Meza Artmann, A. S. & Kammann, U. Assessing the ecotoxicity of potentially neurotoxic substances – Evaluation of a behavioural parameter in the embryogenesis of Danio rerio. *Chemosphere* **186**, 43–50 (2017).
125. Velki, M., Di Paolo, C., Nelles, J., Seiler, T. B. & Hollert, H. Diuron and diazinon alter the behavior of zebrafish embryos and larvae in the absence of acute toxicity. *Chemosphere* **180**, 65–76 (2017).
126. Kalueff, A. V. *et al.* Towards a Comprehensive Catalog of Zebrafish Behavior 1.0 and Beyond. *https://home.liebertpub.com/zeb* **10**, 70–86 (2013).
127. Peng, X. *et al.* Anxiety-related behavioral responses of pentylenetetrazole-treated zebrafish larvae to light-dark transitions. *Pharmacology Biochemistry and Behavior* **145**, 55–65 (2016).
128. Ganzen, L., Venkatraman, P., Pang, C. P., Leung, Y. F. & Zhang, M. Utilizing Zebrafish Visual Behaviors in Drug Screening for Retinal Degeneration. *International Journal of Molecular Sciences 2017, Vol. 18, Page 1185* **18**, 1185 (2017).
129. Steele, W. B. *et al.* Comparative behavioral toxicology with two common larval fish models: Exploring relationships among modes of action and locomotor responses. *Science of The Total Environment* **640**–**641**, 1587–1600 (2018).
130. Basnet, R. M., Zizioli, D., Taweedet, S., Finazzi, D. & Memo, M. Zebrafish Larvae as a Behavioral Model in Neuropharmacology. *Biomedicines 2019, Vol. 7, Page 23* **7**, 23 (2019).
131. Sheets, L. P. et al. A critical review of neonicotinoid insecticides for developmental neurotoxicity. Critical Reviews in Toxicology 46, 153–190 (2016).
132. E.Lammera, G.J.Carrb, K.Wendlera, J.M.Rawlingsb, S.E.Belangerb, Th.Braunbecka (2008), Is the fish embryo toxicity test (FET) with the zebrafish (Danio rerio) a potential alternative for the fish acute toxicity test?, Comparative Biochemistry and Physiology Part C: Toxicology & Pharmacology Volume 149, Issue 2, March 2009, Pages 196-209
133. Thomas Braunbeck, Britta Kais, Eva Lammer, Jens Otte, Katharina Schneider, Daniel Stengel &

Ruben Strecker (2015). The fish embryo test (FET): origin, applications, and future, Environmental Science and Pollution Research volume 22, pages16247–16261 (2015)

134, European Commission. Draft Re-Assessment Report and Proposed decision of the Netherlands prepared in the context of the possible renewal of acetamiprid under Regulation (EC) 1107/2009. Volume 3 - Annex B (AS) Acetamiprid. November 2015

ANNEX I : ZFE method

ZFEX1: Methods of the FET test, coiling assay and basal swimming assay, conducted with the zebrafish (Danio rerio) embryo. The following method descriptions and statistical analysis protocols can be found in von Hellfeld et al., (unpublished).

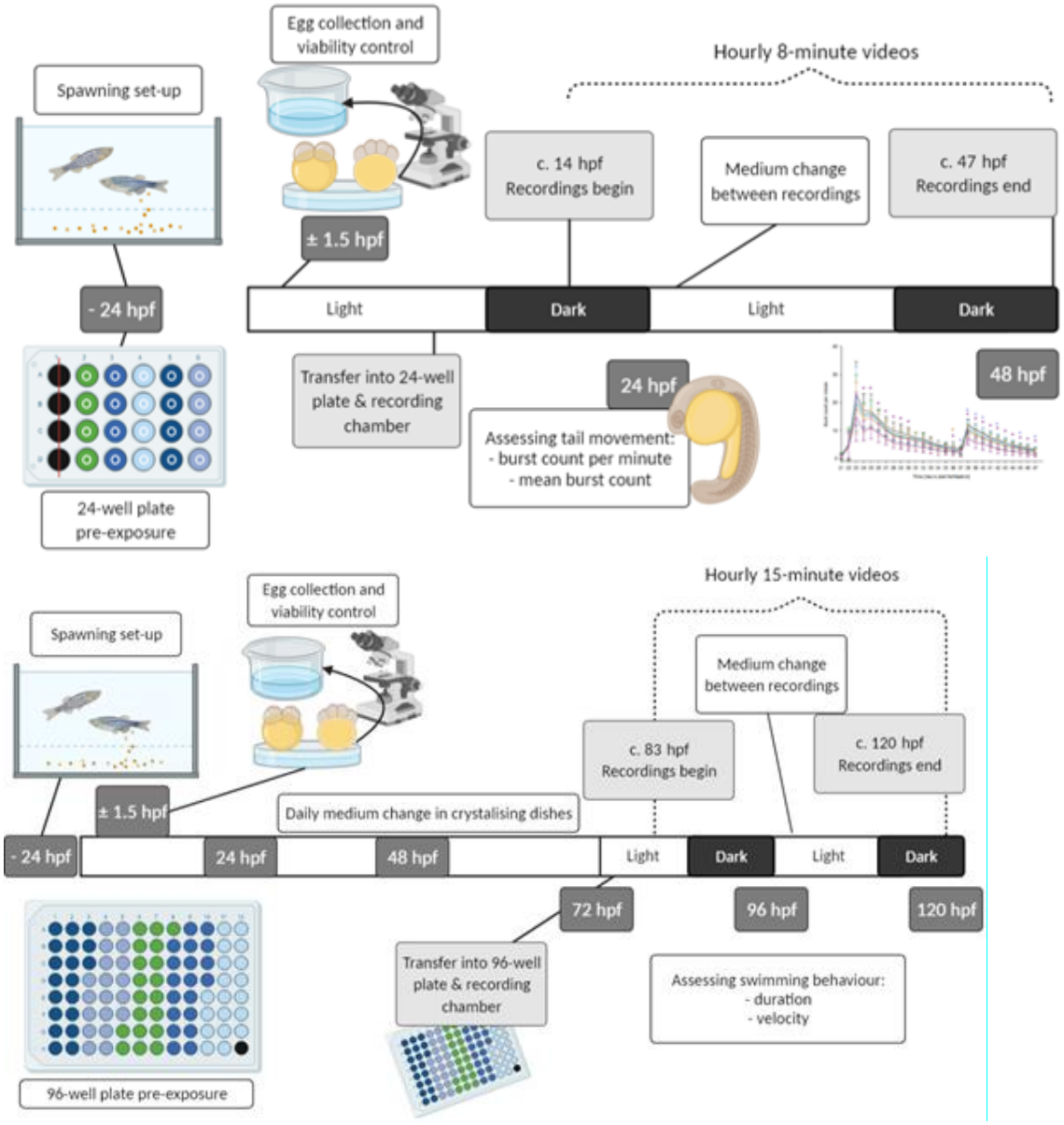

Zebrafish handling and maintenance: Adult 'Westaquarium' strain zebrafish are kept and reared in the breeding facilities at the Aquatic Ecology and Toxicology Group (Centre for Organismal Studies; University of Heidelberg; Heidelberg; Germany; license no. 35-9185.64/BH). In accordance with the OECD TG 236, the maintenance, breeding conditions and egg production was conducted based on internationally accepted standards (Lammer *et al*., 2009). For all assays, the OECD TG 236 standardized water was prepared freshly in-house and the egg collection and handling process of the guideline was followed (OECD, 2013): Freshly laid eggs (<1 hpf) were transferred to 50 ml crystallizing dishes filled with the respective test solutions. For the behavioral assays, the embryos were reared in crystallizing dishes. Total medium renewal was done daily (semi-static exposure) and where recordings were part of the protocol, renewal was conducted between recordings, replacing the well plate at least 20 minutes prior to the next recording for re-acclimatization.

Coiling assay: For each biological replicate (n=3), five 7 hpf embryos were transferred into each well of a 24-well plate (TPP, Trasadingen, Switzerland) containing 2 ml fresh test solution (n=20 technical replicates per biological replicate). The well plates had previously been pre-exposed to the respective concentration medium to account for compound adsorption to the plastic. The embryos were centered with a 5.3 mm diameter polytetrafluoroethylene ring (ESSKA, Hamburg, Germany). The concentration order in the 24-well plate was randomized, containing four test concentrations, as well as a solvent control (0.1% DMSO) utilized here as the "untreated control group". The plate was placed on an acrylic glass covered light box (twelve infrared lights, 880 nm 40° 5 mm, Knightbright, Taiwan) in an incubator (HettCube 600R, Hettich, Tuttlingen,Germany) at 26 ± 1 °C set to a 14/10 h light/dark cycle. The incubator further contained a large water reservoir to prevent medium evaporation from the un-covered well plate. 8-minute long (mpeg-4, 25 frames/s) videos were filmed between 21 and 47 hpf (Camera: Basler acA1920-155µm, Ahrensburg, Germany; Lens: M7528-MP F2.8 f75mm, Computar®, Basler, Ahrensburg, Germany; Germany; Filter: heliopan, RG850, Gräfelfing, Germany) utilizing the Ethovision® Software (Noldus, Wageningen, Netherlands). To avoid unnecessary movement of the recording set-up through the vibrations of the capacitor, the incubator was switched off for 15 minutes every hour, 3 minutes prior to the onset of recording (as outlined by Zindler *et al*., 2019). The lights were not affected by the hourly incubator switch-off. Details of parameter settings can be found in Table 12 below.

Basal swimming assay: At 72 hpf, 1 embryo per well was transferred into 96-well plates (TPP, Trasadingen, Switzerland), containing 360 µl fresh test solution per well (n=19 technical replicates per biological replicate (n=3) for nicotine, and n=2 biological replicates for acetamiprid). The well plates had previously been pre-exposed to the respective concentration medium to account for compound adsorption. The plate was then placed in the DanioVision Observation Chamber (Noldus, Wageningen, Netherlands) and thermostatically controlled through flow (DanioVision external Temperature Control Unit) ensured a constant water temperature of 26 ± 1 °C and a 14/10 h light/dark cycle. 15-Minute videos were recorded every hour between 83 and 120 hpf, using EthoVision Software (Noldus, Wageningen, Netherlands) (Zindler *et al*., 2019). The videos were then analyzed with Danioscope® Software (Version 1.1). Details of parameter settings can be found in Table 12 below.

Table 12 (ZFEX1). Parameter-settings in the EthioVision(R)TX software for video recordings, as well as camera settings.

The table was adapted from von Hellfeld et al., (unpublished)

	Setting	Parameter
Coil	**Video settings**	
	Basler acA1920-155um	1600x1200
	Gain Auto	Off
	Gain Selector	All
	Gain	1,00000

	Black Level Selector	All
	Black Level	0,00000
	Gamma	1,00000
	Digital shift	4
	Detection settings	
	Activity onset	2%
	Activity offset	0.5%
	Minimum inter peak interval	100 ms
	Minimum peak duration	0 ms
Swim	**Video settings**	
	Basler acA1300-60gm	1280x960
	Gain Auto	Off
	Gain Selector	Analog All
	Gain (Raw)	0
	Black Level Selector	All
	Black Level (Raw)	50
	Gamma Enable	Disabled
	Gamma Selector	User
	Gamma	1
	Digital Shift	1
	Detection Settings	
	Method	DanioVision
	Detection Sensitivity	160
	Activity Threshold	100
	Activity Background noise filter	5
	Compression artifacts filter	On

Statistical analysis: For all assays, the biological replicates were initially evaluated individually and compared to the respective controls. ToxRat® (version 2.10.03; ToxRat™ Solutions, Alsdorf, Germany), GraphPad Prism version 7.03 for Windows (GraphPad, La Jolla, California, USA), and the open-source statistical software RStudio (Version 1.3.959) interface running R software (Version 4.0.2 for Windows; R Developmental Core Team, 2020), were used for statistical computing and SigmaPlot Version 14.0 (Systat Software Inc., San Jose, California, USA) for visual data representation. Additionally, the free software Inkscape (Software 0.92.4, 5da689c313, 2019-01-14) was used for post-editing of vector graphs. Differences are declared to be statistically significant at $p < 0.05$.

FET test: Effect concentrations (EC) were calculated at effect levels of 10 and 50% based on probit analysis using linear maximum likelihood regression with ToxRat® (Braunbeck *et al.*, 2015). Due to the overall low frequency of observed sub-lethal effects, however, all three replicates were assessed simultaneously with ToxRat®.

Coiling assay: The videos were analyzed with the Danioscope Software (Version 1.1) and the read-out data for mean burst duration [seconds] and burst count per minute were obtained as excel spread sheets. ANOVA on ranks (Kruskal Wallis test) was utilized to analyze the differences in means of the behavior parameters compared to the untreated control group, followed by the Dunn's *post hoc* test against controls; carried out separately for each replicate, using GraphPad Prism. Time points at which at least two of three replicates were found to be statistically significant ($p \leq 0.05$) were considered as an effect caused by the exposure.

Basal swimming assay: Swimming distance in the basal swimming assay was evaluated by summarizing the data into bins of 3 to 5 hours. Outlier screening was conducted with the R function 'identify_outliers' (rstatix package, Version 0.5.0) for each biological replicate. The distance moved parameter was handled as follows: 1) the raw data was examined, and estimates scored >1.0% (the cut-off threshold) in 'missed

samples' were removed and the remaining data pooled into 3-5 h bins. An outlier check with R was implemented, followed by non-parametric analysis and the Dunn's *post hoc* test. 2) The total distance moved over the recorded 25 h was estimated by summing up the distance moved per individual over all time points. This data was assessed parametric one-way analysis of variance (ANOVA), and multiple comparisons of means from treatment groups against a control group (Dunnett's test, package 'multcomp', Version 1.4.13). Effect size was estimated in terms of eta-squared (η^2) and can be interpreted as follows: 0-0.010: no effect, 0.010-0.060: small effect, 0.060-0.140: intermediate effect, and 0.140-0.200: large effect. To determine swimming frequency, raw data was assessed in time steps of 0.4 s and considered as a movement in events where activity was registered after a period of at least 5 seconds without movement, allowing to distinguish between actual movement and background noise.

Table 13 (ZFEX2). p-values of the coiling assay Kruskal-Wallis and Dunns post hoc test.
At least 2 biological replicates must have indicated a significant difference between the control group and a treatment group to classify as significant. Nicotine (NIC) was tested in 3 biological replicates, whilst acetamiprid (ACE) was tested in 4 biological replicates until 37 hpf, and in 1 biological replicate until 47 hpf. Where only one value is noted, this p-value threshold was observed in both biological replicates. Table adapted from von Hellfeld et al., (unpublished)

	Mean burst duration			Mean burst count per minute		
	Conc. [µM]	hpf	*p*-value(s)	Conc. [µM]	hpf	*p*-value(s)
NIC	1.25	39, 40	≤0.001, ≤0.01, ≤0.05	1.25	30, 34	≤0.01, ≤0.05
		41–45	≤0.001, ≤0.01		36	≤0.01
	2.5	23	≤0.001, ≤0.01		37, 38, 40-42, 47	≤0.001
		24	≤0.001, ≤0.05		39, 43, 46	≤0.001, ≤0.05
		28, 38, 39, 41, 46	≤0.01, ≤0.05		44, 45	≤0.001, ≤0.01
		40, 45	≤0.01	2.5	23, 25, 40-47	≤0.001
		42-44	≤0.001, ≤0.01, ≤0.05		24, 38, 39	≤0.001, ≤0.01
	12.5	23, 30, 38, 45, 46	≤0.001, ≤0.01		33	≤0.01, ≤0.05
		24-29, 31, 39-44, 47	≤0.001		35	≤0.05
	25	23-47	≤0.001		37	≤0.001, ≤0.01, ≤0.05
				12.5	23-26	≤0.001
					27, 34, 45-47	≤0.001, ≤0.01
					33	≤0.01
					35, 44	≤0.001, ≤0.05
					36	≤0.001, ≤0.01, ≤0.05
					37	≤0.05
				25	23, 40	≤0.001, ≤0.05
					24-28	≤0.001
					29-33	≤0.001, ≤0.01
					34	≤0.001, ≤0.01, ≤0.05
					40-42	≤0.01, ≤0.05
					43, 44	≤0.05
ACE*	25	31	≤0.05	2.5	23	≤0.001
		39	≤0.05	25	23	≤0.001

		40	≤0.001		24	≤0.01, ≤0.001
	50	40 - 42	≤0.05		33	≤0.05
		44	≤0.01		38, 39, 43, 45	≤0.05
	100	38	≤0.001		40, 42	≤0.01
		39 - 41	≤0.001		44, 46	0.001
		42, 44	≤0.01	50	23	≤0.01, ≤0.001
		45	≤0.05		24	≤0.001
					42, 45	≤0.05
					44, 46	≤0.001
				100	23	≤0.001, ≤0.05
					24	≤0.001, ≤0.01, ≤0.05
					25	≤0.01
					33, 34	≤0.001, ≤0,05
					44	≤0.01

Blue box: The respective value is based on one biological replicate (n=20 technical replicates)

Table 14 (ZFEX3). p-values of the basal swimming assay Kruskal-Wallis and Dunns post hoc test (n=2).

Where only one value is noted, this p-value threshold was observed in both biological replicates. Table adapted from von Hellfeld et al., (unpublished)

Distance moved [mm]			Mean burst count per minute		
Concentration	hpf	*p*-value(s)	Concentration	hpf	*p*-value(s)
100 µM	100-104	='0.01,' =0.05	100 µM	110-114	=0.05
	110-114	='0.001,' =0.05			

ANNEX II: PBPK report

Please refer to the separate publication for full Annex I.

ENV/CBC/MONO(2022)27/ANN1

ANNEX III: Existing evidence for IATA on developmental neurotoxicity on Acetamiprid and Imidacloprid

Literature search

Database: medline

Table 15. Criteria for selecting studies for the sub-questions on the relationship between acetamiprid and imidacloprid and DNT in human studies

Study design	**IN**	Cohort Case control Cross sectional
	OUT	Ecological studies (studies comparing different populations) Studies with no biomarker
Population	**IN**	All population groups and ages
Exposure	**IN**	acetamiprid (assessment 1) imidacloprid (assessment 2) All types of exposure [specify] When exposure is measured by specific and non specific biomarkers for acetamiprid and imidacloprid
Endpoints	**IN**	Developmental neurotoxicity

Table 16. Criteria for selecting studies for the sub-questions on the relationship between acetamiprid and imidacloprid and DNT in *in vivo* studies

Study design	**IN**	*In vivo* studies in animals
Population	**IN**	Mammals,
	OUT	Studies assessing efficacy on e.g. insects etc.
Exposure	**IN**	acetamiprid imidacloprid All routes of exposure Only studies where the mixture is represented by protocols that are including multiple substances but administered individually to the test system
	OUT	Mixtures
Endpoints	**IN**	Developmental neurotoxicity

Table 17. Criteria for selecting studies for the sub-questions on the relationship between acetamiprid and imidacloprid and DNT in *in vitro* studies

Study design	**IN**	*In vitro*
Population	**IN**	Only cells of nervous origin or complex system replicating part of the nervous system (i.e. neurosphere, brain on a chip) or human pluripotent stem cell differentiated in nervous cells.
	OUT	Studies assessing efficacy on e.g. insects cells lines and frog cells
Exposure	**IN**	acetamiprid and imidacloprid. For zebrafish studies: exposure and assessment of endpoint before 120 hours post fertilisation Only studies where the mixture is represented by protocols that are including multiple substances but administered individually to the test system
	Out	Mixtures For zebrafish studies: exposure after 120 hours post fertilisation
Endpoints	**IN**	Developmental neurotoxicity

Table 18. Criteria for selecting studies for the sub-questions on the relationship between acetamiprid and imidacloprid and DNT related to report characteristics and relevant to human, *in vivo* and *in vitro* studies

Time	**IN**	No time limits
Language	**IN**	English
Publication type	**IN**	Primary research studies (i.e. studies generating new data) Reviews will be used as sources of further references and to assess the appropriateness of the search strategy applied
	OUT	Expert opinions, editorials, letters to the editor, conference proceedings and posters, PhD theses

Search strings – exemplified with acetamiprid (should be similar with imidacloprid) These have been copied from EFSA.

Human studies

Search	Query
#7	Search #5 NOT #6
#6	Search(rat[ti] OR rats[ti] OR mouse[ti] OR mice[ti] OR anopheles[ti] OR mosquito[ti] OR mosquitoes[ti] OR mosquitos[ti] OR rodent[ti] OR rodents[ti] OR fish[tiab] OR zebrafish[ti]) NOT medline[sb])
#5	Search#3 NOT #4
#4	Search("animals"[MeSH Terms]) NOT ("animals"[mesh] AND "humans"[Mesh])
#3	Search #1 AND #2
#2	Search "Attention"[Mesh] OR "Aptitude Tests"[Mesh] OR "Behavior"[Mesh:NoExp] OR "Behavioral Symptoms"[Mesh] OR "Adolescent Behavior"[Mesh:NoExp] OR "Child Behavior"[Mesh] OR "Cognition"[Mesh] OR "Cognition Disorders"[Mesh] OR "Cognitive Dysfunction"[Mesh] OR "Executive Function"[Mesh] OR "Growth and Development"[Mesh:noExp] OR "Human development"[Mesh:noExp] OR "Intelligence"[Mesh:NoExp] OR "Learning"[Mesh] OR "Memory"[Mesh] OR "Neurobehavioral Manifestations"[Mesh] OR "Neurocognitive Disorders"[Mesh] OR "Neurodevelopmental Disorders"[Mesh] OR "Neurologic Manifestations"[Mesh] OR "Neuropsychological Tests"[Mesh] OR "Psychomotor Disorders"[Mesh] OR "Psychomotor Performance"[Mesh] OR "Motor Activity"[Mesh] OR Attention[tiab] OR Attentiv*[tiab] OR ADDH[tiab] OR ADHD[tiab] OR ADHS[tiab] OR AD/HD[tiab] OR Aptitude*[tiab] OR Hkd[tiab] OR Hyperactiv*[tiab] OR Hyper activ*[tiab] OR Hyperkin*[tiab] OR Hyper kin*[tiab] OR Distractib*[tiab] OR Inattention[tiab] OR Inattentiv*[tiab] OR Behavi*[tiab] OR brain disorder*[tiab] OR brain damage*[tiab] OR brain dysfunct*[tiab] OR Cognition[tiab] OR Cognitiv*[tiab] OR Metacognit*[tiab] OR Metamemory[tiab] OR Volition[tiab] OR Executive control[tiab] OR Executive function*[tiab] OR executive dysfunction*[tiab] OR executive impairment*[tiab] OR DNT[tiab] OR (Development*[tiab] AND (disabilit*[tiab]

	OR disorder*[tiab] OR deviation*[tiab] OR "Neurotoxicity Syndromes"[Mesh] OR neurotoxic*[tiab] OR toxic*[tiab] OR abnormal*[tiab] OR activit*[tiab])) OR Defiance disorder* [tiab] OR Defiant disorder*[tiab] OR Disruptive disorder* [tiab] OR Disruption disorder*[tiab] OR Abnormal development*[tiab] OR Intelligence[tiab] OR Comprehension*[tiab] OR Intellectual*[tiab] OR IQ[tiab] OR Memory[tiab] OR Item recall[tiab] OR Remembering[tiab] OR Learning*[tiab] OR Neurobehav* [tiab] OR Neurocogniti*[tiab] OR Neurodevelopment*[tiab] OR Autism[tiab] OR Autistic[tiab] OR Neurologic*[tiab] OR Nervous disease*[tiab] OR Nervous disorder*[tiab] OR Nervous dysfunction*[tiab] OR Nervous manifestation*[tiab] OR Nervous system*[tiab] OR Neuropsychologic*[tiab] OR Psycholog*[tiab] OR Psychomot*[tiab] OR Motor*[tiab] OR Locomot*[tiab] OR Processing speed[tiab] OR Processing velocity[tiab] OR Maze test[tiab] OR Maze tests[tiab] OR Maze testing[tiab] OR reaction time[tiab] OR response inhibition[tiab] OR Stanford Binet[tiab] OR Binet Test*[tiab] OR Bender Gestalt Test[tiab] OR Aphasia Test*[tiab] OR Bayley* [tiab] OR Wechsler[tiab] OR WISC[tiab] OR McCarthy Scale* [tiab] OR Continuous Performance Test[tiab] OR Continuous Performance Tests[tiab] OR Continuous Performance Task[tiab] OR Continuous Performance Tasks[tiab] OR Conners*[tiab] OR CRS-T[tiab] OR CRS-P[tiab] OR academic achievement*[tiab] OR scholastic achievement*[tiab]
#1	Searchacetamiprid[tiab] OR "135410-20-7"[tiab] OR 135410207 [tiab] OR neonicotinoid*[tiab]

In vivo studies

Search	Query
#3	Search #1 AND #2
#2	Searchacetamiprid[tiab] OR "135410-20-7"[tiab] OR 135410207 [tiab] OR neonicotinoid*[tiab]
#1	Search"Attention"[Mesh] OR Attention[tiab] OR (("Behavior"[Mesh:noExp] OR "Behavior, Animal"[Mesh] OR Behavi*[tiab]) AND ("Growth and Development"[Mesh:NoExp] OR development*[tiab] OR exposure*[tiab] OR ontogen*[tiab] OR neurotoxic*[tiab] OR "Neurotoxicity Syndromes"[Mesh] OR toxic*[tiab])) OR "Cognition"[Mesh] OR "Cognition Disorders"[Mesh] OR "Cognitive Dysfunction"[Mesh] OR cognition[tiab] OR cognitiv*[tiab] OR "Learning"[Mesh] OR learning[tiab] OR "Memory"[Mesh] OR memor*[tiab] OR "Embryonic and Fetal Development"[Mesh] OR "Prenatal Exposure Delayed Effects"[Mesh] OR (("Embryonic Structures"[Mesh] OR Embryo*[tiab] OR fetal*[tiab] OR foetal*[tiab] OR fetus*[tiab] OR foetus[tiab] OR gestational[tiab] OR "neonatal"[tiab] OR "neo natal"[tiab] OR postnatal[tiab] OR "post natal"[tiab] OR prenatal[tiab] OR "pre natal" OR perinatal[tiab] OR "peri natal"[tiab] OR "in utero"[tiab] OR immature[tiab]) AND ("Brain"[Mesh] OR brain*[tiab] OR "cerebral cortex"[tiab] OR cerebellum[tiab] OR development*[tiab] OR exposure*[tiab] OR "Motor Skills"[Mesh] OR locomot*[tiab] OR motor*[tiab] OR "Nervous System"[Mesh] OR " Nervous System Diseases"[Mesh] OR Nervous system*[tiab] OR "Neuroanatomy"[Mesh] OR neuroanatom*[tiab] OR neurobehav*[tiab] OR neurocognit*[tiab] OR neurolog*[tiab] OR neuropath*[tiab] OR neurotoxic*[tiab] OR "Neurotoxicity Syndromes"[Mesh] OR toxic*[tiab])) OR DNT[tiab] OR (("Growth and Development"[Mesh:NoExp] OR development*[tiab]) AND ("Brain"[Mesh] OR brain*[tiab] OR cerebellum[tiab] OR "cerebral cortex"[tiab] OR exposure*[tiab] OR "Motor Skills"[Mesh] OR locomot*[tiab] OR motor*[tiab] OR "Morphogenesis"[Mesh] OR morphogen*[tiab] OR morphometr*[tiab] OR nervous system*[tiab] OR "Nervous System"[Mesh] OR "Nervous System Diseases"[Mesh] OR "Neuroanatomy"[Mesh] OR neuroanatom*[tiab] OR neurobehav*[tiab] OR neurocognit*[tiab] OR neurolog*[tiab] OR neurotoxic*[tiab] OR "Neurotoxicity Syndromes"[Mesh] OR ontogen*[tiab] OR startle*[tiab])) OR (("Growth"[Mesh] OR grow*[tiab]) AND ("Brain"[Mesh] OR brain*[tiab] OR "Nervous System"[Mesh] OR nervous system*[tiab])) OR developmental activity[tiab] OR developmental activities[tiab] OR developmental toxic*[tiab] OR (development*[ti] AND (activit*[ti] AND toxic*[ti])) OR Neurodevelopment*[tiab] OR neurohistopatholog*[tiab] OR Neuropatholog*[tiab] OR "Neuropathology"[Mesh] OR "Neurobehavioral Manifestations"[Mesh] OR "Neurocognitive Disorders"[Mesh] OR "Neurodevelopmental Disorders"[Mesh] OR "Neurologic Manifestations"[Mesh]

In vitro

Search	Query
#3	**Search** #1 AND #2
#2	Searchacetamiprid[tiab] OR "135410-20-7"[tiab] OR 135410207 [tiab] OR neonicotinoid*[tiab]
#1	**Search**"Cells, Cultured"[MeSH] OR "Cell Physiological Phenomena"[Mesh] OR "In Vitro Techniques"[MeSH] OR Astrocyte*[tiab] OR brain slice*[tiab] OR calcium channel*[tiab] OR calcium signal*[tiab] OR cell based[tiab] OR cell line*[tiab] OR cell migrat*[tiab] OR cell model*[tiab] OR cell proliferat*[tiab] OR cell system*[tiab] OR cellular assay*[tiab] OR cellular endpoint*[tiab] OR cellular exposure*[tiab] OR cellular migrat*[tiab] OR cellular method*[tiab] OR cellular model*[tiab] OR cellular proliferat*[tiab] OR cellular system*[tiab] OR cellular technique*[tiab] OR electrical activit*[tiab] OR electrode arra*[tiab] OR ESC[tiab]

	OR glial[tiab] OR immortalised[tiab] OR immortalized[tiab] OR "in vitro"[tiab] OR intercellular communicat*[tiab] OR IPS cell*[tiab] OR iPSC[tiab] OR LUHMES[tiab] OR microglia*[tiab] OR myelinogenes*[tiab] OR myelin formation*[tiab] OR network formation*[tiab] OR nerve cell*[tiab] OR neural cell*[tiab] OR neuronal cell*[tiab] OR neural connect*[tiab] OR neuronal connect*[tiab] OR neural crest[tiab] OR neural differentiat*[tiab] OR neuronal differentiat*[tiab] OR neural network*[tiab] OR neuronal network*[tiab] OR neural plastic*[tiab] OR neuronal plastic*[tiab] OR neural precursor*[tiab] OR neuronal precursor*[tiab] OR neural progenitor*[tiab] OR neural prun*[tiab] OR neuronal prun*[tiab] OR neuroblastoma*[tiab] OR neuroinflammation*[tiab] OR neurosphere[tiab] OR neuroprogenitor*[tiab] OR neurotransmitter release*[tiab] OR oligodendrocyte*[tiab] OR pheochromocytoma*[tiab] OR pluripotent cell*[tiab] OR primary cell*[tiab] OR schwann cell*[tiab] OR stem cell*[tiab] OR neurite outgrowth[tiab] OR synaptogenes*[tiab] OR synapse formation*[tiab] OR synapse plastic*[tiab] OR synaptic prun*[tiab]